OULU 2009
C 344

ACTA UNIVERSITATIS OULUENSIS

Wan-Young Chung

UBIQUITOUS HEALTHCARE SYSTEM BASED ON A WIRELESS SENSOR NETWORK

FACULTY OF TECHNOLOGY,
DEPARTMENT OF ELECTRICAL AND INFORMATION ENGINEERING,
UNIVERSITY OF OULU;
INFOTECH OULU,
UNIVERSITY OF OULU

ACTA UNIVERSITATIS OULUENSIS
C Technica 344

WAN-YOUNG CHUNG

UBIQUITOUS HEALTHCARE SYSTEM BASED ON A WIRELESS SENSOR NETWORK

Academic dissertation to be presented with the assent of the Faculty of Technology of the University of Oulu for public defence in Kuusamonsali (Auditorium YB210), Linnanmaa, on 27 November 2009, at 12 noon

OULUN YLIOPISTO, OULU 2009

Acta Univ. Oul. C 344, 2009

Supervised by
Professor Risto Myllylä

Reviewed by
Doctor Heikki Ailisto
Professor Jerker Delsing

ISBN 978-951-42-9289-7 (Paperback)
ISBN 978-951-42-92890-3 (PDF)
http://herkules.oulu.fi/isbn9789514292903/
ISSN 0355-3213 (Printed)
ISSN 1796-2226 (Online)
http://herkules.oulu.fi/issn03553213/

Cover design
Raimo Ahonen

OULU UNIVERSITY PRESS
OULU 2009

Chung, Wan-Young, Ubiquitous healthcare system based on a wireless sensor network.
Faculty of Technology, Department of Electrical and Information Engineering, University of Oulu, P.O.Box 4500, FI-90014 University of Oulu, Finland; Infotech Oulu, University of Oulu, P.O.Box 4500, FI-90014 University of Oulu, Finland
Acta Univ. Oul. C 344, 2009
Oulu, Finland

Abstract

This dissertation aimed at developing a multi-modal sensing u-healthcare system (MSUS), which reflects the unique properties of a healthcare application in a wireless sensor network. Together with health parameters, such as ECG, SpO_2 and blood pressure, the system also transfers context-aware data, including activity, position and tracking data, in a wireless sensor network environment at home or in a hospital.

Since packet loss may have fatal consequences for patients, health-related data are more critical than most other types of monitoring data. Thus, compared to environmental, agricultural or industrial monitoring, healthcare monitoring in a wireless environment imposes different requirements and priorities. These include heavy data traffic with wavelike parameters in wireless sensor network and fatal data loss due to the traffic. To ensure reliable data transfer in a wireless sensor network, this research placed special emphasis on the optimization of sampling rate, packet length and transmission rate, and on the traffic reduction method.

To improve the reliability and accuracy of diagnosis, the u-healthcare system also collects context-aware information on the user’s activity and location and provides real-time tracking.

Waveform health parameters, such as ECG, are normally sampled in the 100 to 400 Hz range according to the monitoring purpose. This type of waveform data may incur a heavy burden in wireless communication. To reduce wireless traffic between the sensor nodes and the gateway node, the system utilizes on-site ECG analysis implemented on the sensor nodes as well as query architecture. A 3D VRML viewer was also developed for the realistic monitoring of the user’s moving path and location.

Two communication methods, an 802.15.4-based wireless sensor network and a CDMA cellular network are used by sensors placed on the users’ bodies to gather medical data, which is then transmitted to a server PC at home or in the hospital, depending on whether the sensor is within or outside the range of the wireless sensor network.

Keywords: accelerometer, CDMA cellular network, ECG, homecare, mobile healthcare, Query, ubiquitous computing, u-healthcare, wireless sensor network

Acknowledgements

A few lines of thanks cannot compensate the contributions given by several persons to this thesis. But allow me to thank them anyway.

First of all, I would like to thank Prof. Risto Myllylä, who initially encouraged me to write a Ph.D. thesis at the University of Oulu, for his generous support and technical and scientific advice. This work would not have been possible without the encouragement and mentoring from him. His academic achievement has served as a model for my work.

Special thanks have to go to my good tutor, and friend, Prof. Esko Alasaarela. He was the first to suggest that I undertake research on ubiquitous healthcare. His simple proposal consisted of a few short sentences, but nowadays around 20 researchers study ubiquitous healthcare in the USN laboratory in Korea. I have been particularly amazed and inspired by Esko’s knowledge and enthusiasm in both academic and business areas.

This work would not have been possible without good co-workers and without my students to help, encourage and trust me. I feel lucky to have had such great people around me in the OEM laboratory of the University of Oulu and in the USN laboratory at Dongseo University and Pukyong National University. I am very grateful to Dr. Hannu Sorvoja, Young-Dong Lee and would also like to extend my warmest thanks to all my Finnish and Korean friends who have not been mentioned. Thank you all.

I would also like to express my gratitude to my wife, Yong-Hee, my daughter, Ye-Sol, and my son, Sang-Hoon, for their encouragement, patience and trust in me.

Oulu, October 2009 Wan-Young Chung

List of terms, symbols and abbreviations

WSN	Wireless Sensor Network
USN	Ubiquitous Sensor Network
RF	Radio Frequency
MSUS	Multi-model Sensing U-healthcare System
ECG	Electrocardiogram
PPG	Photoplethysmography
USB	Universal Serial Bus
HPF	High Pass Filter
LPF	Low Pass Filter
PC	Personnel Computer
DSDV	Destination Sequence Distance Vector
BMAC	Berkley Medium Access Control
MAC	Medium Access Control
GUI	Graphical User Interface
RAM	Random Access Memory
B	Byte
kB	Kilo Byte
MB	Mega Byte
I/O	Input/Output
PHY	Physical
A/D	Analog/Digital
U-IT	Ubiquitous Intelligent Town
IEEE	Institute of Electrical and Electronics Engineering
CPU	Central Processing Unit
mV/s	millivolt/second
SlopeTwave	Slope of T-wave
t	time
ms	millisecond
ISM	Industrial, Scientific and Medical Band
NesC	Network Embedded System C
TinyOS	Tiny Micro Threading Operating System
TOSSIM	Tiny Micro Threading Operating System Simulator
RTOS	Real Time Operating System
g	Force of gravity on Earth
UART	Universal Asynchronous Receive and Transmit

V.L.	Voltage Level
MIT/ BIH	Massachusetts Institute of Technology/Beth Israel Hospital
PDA	Personnel Digital Assistant
HR	Heart Rate
bpm	beat per minute
TDOA	Time Difference of Arrival
TDMA	Time Division Multiple Access
ID	Identification
TCP/IP	Transmission Control Protocol/Internet Protocol
D	Dimensional
VRML	Virtual
CAD	Computer Aided Design
MVM	Microsoft Virtual Machine
JVM	Java Virtual Machine
EAI	External Authoring Interface
DEF	Define (in VRML)
LAN	Local Area Network
CDMA	Code Division Multiple Access
WLAN	Wireless Local Area Network
AP	Access Point
ADC	Analogue to Digital Converter
DAC	Digital to Analogue Converter
USART	Universal Synchronous Asynchronous Receiver Transmitter
H/W MULT	Hardware Multiplier
DMA	Direct Memory Access
SPI	Serial Peripheral Interface
KWISF	Korea Wireless Internet Standardization Forum
WIPI	Wireless Internet platform for Interoperability

List of original papers

I Chung W-Y & Myllylä R (2006) Ubiquitous Sensor Network for Chemical Sensors. Rare metal materials and engineering 35(S3): 400–404.

II Lee Y-D, Lee D-S, Chung W-Y & Myllylä R (2006) A Wireless Sensor Network Platform for Elderly Persons at Home. Rare metal materials and engineering 35(S3): 95–99.

III Lee Y-D, Lee D-S, Walia G, Myllylä R & Chung W-Y (2006) Query Based Duplex Vital Signal Monitoring System Using Wireless Sensor Network for Ubiquitous Healthcare. IFMBE Proceedings, World Congress on Medical Physics and Biomedical Engineering 2006. August 27-September 1, Coex, Seoul: 388–391.

IV Chung W-Y, Walia G, Lee Y-D & Myllylä R (2007) Design issues and implementation of query-driven healthcare system using wireless sensor Ad-hoc network. IFMBE Proceedings, International Workshop on Wearable and Implantable Body Sensor Networks (BSN 2007). March 26-28, RWTH Achen University, Germany: 99–104.

V Chung W-Y, Bhardwaj S, Purwar A & Lee D-S (2007) A Fusion Health Monitoring using ECG and Accelerometer Sensors for Elderly Persons at Home. Proceedings of EMBC 2007(29th Annual International Conference of the IEEE Engineering in Medicine and Biology Society), Lyon, France, August 23–26: 3818–3821.

VI Lee D-S, Bhardwaj S, Alasaarela E & Chung W-Y (2007) An ECG Analysis on Sensor Node for Reducing Traffic Overload in u-Healthcare with Wireless Sensor Network. Proceedings of IEEE Sensors Conference, Georgia, USA, October 28–31: 256–259.

VII Singh VK, Lim H, Myllylä R & Chung W-Y (2006) Passive and Cost effective People Location Tracking System for Indoor Environments Using Distributed Wireless Sensor Network. IFMBE Proceedings, World Congress on Medical Physics and Biomedical Engineering. August 27–September 1, Coex, Seoul: 384–387.

VIII Chung W-Y, Singh VK, Myllylä R & Lim H (2006) Security Enhanced Indoor Tracking System for Ubiquitous Home Healthcare. Proceeding of IEEE Sensors Conference, B1L-B2, October 22-25, Daegu, Korea.

IX Purwar A, Myllylä R & Chung W-Y (2008) A Wireless Sensor Network Compatible Triaxial Accelerometer: Application for Detection of Falls in the Elderly. Sensor Letters 6(2): 319–325.

X Chung W-Y & Yang C-S (2008) Dynamic VRML-Based Navigable 3D Map for Indoor Location-Aware Systems. In: Mukhopadhyay SC & Huang RY-M (eds) Sensors: Advancement in Modeling, Design Issues, Fabrication and Practical Applications. LNEE Series. Berlin Heidelberg, Springer-Verlag: 269–284.

XI Chung W-Y, Yau C-L, Shin K-S & Myllylä R (2007) A Cell Phone Based Health Monitoring System with Self Analysis Processor using Wireless Sensor Network Technology. Proceedings of EMBC 2007(29th Annual International Conference of the IEEE Engineering in Medicine and Biology Society), Lyon, France, August 23–26: 3705–3708.

In the following text, these papers will be referred to by the Roman numbers I–XI.

Paper I provides a review of ubiquitous sensor network technology with a focus on using chemical sensors to monitor the environment, particularly under dangerous circumstances. The paper also summarizes emerging wireless sensor network technologies for the benefit of researchers interested in sensor devices. Sensor nodes, an elementary component in wireless sensor networks, are introduced and their development history is outlined. Finally, the paper reviews some common application areas of wireless sensor networks.

Paper II concentrates on a wireless sensor network platform designed for elderly persons at home. Developed for the continuous monitoring of ECG signals, the system comprises wireless sensor network nodes, a base-station and a server computer. It allows real-time ECG data of elderly persons or patients, as well as stored previous data, to be retrieved and played back to assist diagnosis. For this paper, Chung gave research motivation and ideas for this research.

Wireless data communication allows bidirectional radio frequency communication with ad-hoc routing. As a result, motes attached to patients are able to send data to the base-station, even if they are not within its direct radio range. To enhance the system's power efficiency for long-term operation, the system incorporates an on-command 'sleep' and 'wake' feature, which enables the motes to transfer data only when desired and sleep for the rest of the time. To ensure that abnormal changes in data are not being missed in the sleep mode, the sensors are kept active. A query-based duplex vital signal monitoring system using a wireless ad-hoc sensor network for ubiquitous healthcare is presented in papers III and IV.

Paper V studies an ECG and triaxial accelerometer signal analysis algorithm and monitoring method for the homecare of elderly persons or patients based on wireless sensor technology. For ECG analysis, a variant of the Pan-Tompkins algorithm is developed for signal processing. This algorithm proposes real-time QRS detection based on analyzing the slope, amplitude and width of QRS complexes and then automatically adjusting the thresholds. Activities such as walking, running and accidental falling are determined on the basis of body acceleration data recorded by an accelerometer. These data are then used to make a high accuracy diagnosis of the patient's health status. Coupled with ECG signal analysis, this information is used to set off an emergency alarm, if the monitored person falls abruptly. Paper VI develops a new approach for reducing traffic overload in a u-healthcare system based on a wireless sensor network. A robust, real-time monitoring platform with an ECG analysis function is implemented on sensor nodes, and ECG signals obtained from the patient's body are first analysed by the sensor node itself, and only abnormal ECG signals are transferred via the network to the server, where they are further analyzed.

Paper VII describes an indoor location system for mobile, location-dependent in-building healthcare applications. Ceiling-mounted beacons are spread throughout the building, publishing location information using RF and ultrasonic signals, thereby allowing applications running on mobile and static nodes to learn their physical location. The target to be tracked carries a listener node, which listens to the beacons and forwards the information to the base-station. Paper VIII presents a security-enhanced indoor-tracking system for ubiquitous home healthcare. This system combines tracking data with activity data to monitor the health status of elderly persons. Activities such as resting, working and running are monitored by an accelerometer attached on the body. In paper IX, a MEMS accelerometer is used to measure the acceleration of a person wearing a sensor unit on the chest during different activities.

A three-dimensional navigation viewer (3DNV), representing the convergence of a location-aware application and three-dimensional (3D) graphics technology are developed for the 3D visualization of location-aware information in paper X. The system allows visualization of situational information in a complete, 3D model of indoor environments. Moreover, it is equipped with instantly updated route results, which are synchronized with the physical world. The viewer provides valuable insights into a novel integration approach between the 3D graphics standard, virtual reality modelling language (VRML) and indoor location-aware systems.

The last paper (XI) describes an integrated wireless CDMA-based ubiquitous healthcare monitoring system for chronic disease management and high quality patient care in the hospital, home or travel environments using an extended standalone simple electrocardiogram (ECG) diagnosis algorithm in a cell phone. Utilizing a wireless dongle prototype as an intermediate device for internetworking between the IEEE 802.15.4 wireless network and CDMA mobile network communication infrastructures, the system provides a mobile healthcare solution with the capability to roam continuously within and outside the hospital environment.

Most of above papers were written in USN Laboratory in Dongseo University and OEM laboratory by Chung and his graduate students by the aid of Prof. Myllyla. Chung has done the planning and management of the research however some experimental practice were done by the laboratory members.

Contents

1 Introduction

1.1 Overview and motivation

Population aging has become one of the most significant demographic processes of modern times. Decreasing fertility along with lengthening life expectancy has reshaped the age structure of the population in most regions of the world by shifting relative weight from younger to older groups. In much of the world, populations are aging at an extremely rapid pace. The elderly population, that is, those aged 65 years and over, currently comprises around 10 percent of the world's population, and this figure is projected to increase to 22 percent by the year 2050 [1]. Together with a concomitant socio-economic transition, this demographic shift has been forcing policy makers to prepare for the challenges of a rapidly aging society.

Providing patients with convenient health facilities at a low cost has always been a great challenge for health service providers. Moreover, the fast changing life style of the modern world and the problem of aging society pose an urgent need to modernize such facilities. This involves devising cheaper and smarter ways of providing healthcare to sufferers of age-related diseases. In addition, emphasis has to be paid on providing health monitoring in out-of-hospital conditions for elderly people and patients who require regular supervision, particularly in remote areas. Future trends in national healthcare services are expected to include shorter hospital stays and better community care.

This dissertation presents a ubiquitous monitoring system for the continuous monitoring of patients under their natural physiological states or elderly persons with chronic diseases. Especially our system is designed for homecare or the monitoring of the elderly who live in country side or small rest home without enough support from caregivers or doctors, instead of patient monitoring in big hospital environment. Further insights into the natural cause and progression of diseases are afforded by context-aware sensing, which includes the use of accelerometers to monitor patient activities, or by location-aware indoor tracking based on ultrasonic and RF sensing. Moreover, indoor location tracking provides information about the location of patients in their physical environment and helps the caregiver in the provision of appropriate support.

1.2 Contribution of the dissertation

Although it is a difficult undertaking to provide a healthcare monitoring and assistance service without any inconvenience and interference caused by the measuring apparatus, elderly persons and patients can be continuously monitored both at home and in the hospital environment by wireless ad-hoc network technology. This technology could also satisfy the requirements of 'ubiquitous' wireless health state monitoring, including minimum intervention by medical caregivers. An environment of this type can be constructed using wireless sensor network (WSN) technology, which allows the coverage area of single wireless network to be expanded by ad-hoc network technology, capable of handing over wireless data to neighbouring wireless networks.

Thanks to the efforts of researchers working in the fields of computer science, network technology and medicine, a number of wireless healthcare applications already utilize sensor network technology, and others are in the pipeline. Some of these systems use Wi-Fi and other LAN technologies. A case in point is the European Community's MobiHealth System (2002-2004), which employs a Body Area Network (BAN) [2]. In addition, CodeBlue [3], developed at Harvard, is a wireless infrastructure that uses a WSN for deployment in emergency situations or disaster medical care. Another health monitoring system is Coach's Companion [4], which allows the monitoring of physical activities, while CardioNet employs a PDA to collect data from an ECG monitor and to send it to a service center over a cellular network [5]. As a final example, Medtronic uses a dedicated monitor connected to the internet to send pacemaker information to a medical professional.

Although all the systems described above demonstrate moderate performance in a limited wireless environment, I feel that research in the area tends to focus on device development and on testing the feasibility of the developed technology. Little attention has been paid to reliability problems which affect data transfer in network environments. And yet the reliability of data transfer is a critical factor for healthcare applications.

To increase the reliability of health data transfer in wireless sensor networks, we need to know that healthcare data (i.e., data collected from different sensors) consists of wavelike data and linear data. Wavelike healthcare data (such as ECG or EKG) require a higher sampling rate and are more dependent on monitoring reliability than linear signals (including body temperature, blood pressure and oxygen content). ECG signals, for example, necessitate a high sampling rate, usually between 100 and 400 Hz, depending on the monitoring purpose. Loss of

ECG signals, that is, EEG data that arrive late or are lost altogether, may have dire consequences to the patient. As a result, such factors as sampling rate, packet length, transmission rate and reliability must be considered very carefully for different types of data.

This dissertation can be thought to make five special contributions:

1. A WSN-based ubiquitous healthcare platform will be studied. The developed u-healthcare platform includes most of the possible WSN-compatible applications, including health parameter monitoring, activity monitoring, patient tracking, mobile monitoring and 3-dimensional realistic viewing.
2. The reliability of wireless data propagation in a wireless sensor network environment can be considered to reflect special features of the monitored health parameters. Therefore, the effect that the sampling rate and packet size of various medical data have on transmittance performance in a wireless sensor network will be surveyed here.
3. To reduce traffic overload caused by the need to minimize the power consumption of the deployed sensor nodes and to reduce data loss in the wireless sensor network, a noble sensor node platform with portable real-time analysis of ECG signals will be developed.
4. Fusion health data, combining more than two signals, such as ECG and activity data, will be analysed to determine their accuracy and usefulness for diagnosis. Context information, such as activity and tracking data, will be provided to offer further insight into the natural cause and progression of diseases and to enhance the accuracy of early symptom detection.
5. A WSN-compatible mobile healthcare system will be developed. This cellular phone-based u-healthcare monitoring system for disease management and better patient care in the hospital, home or travel environment has a simple, standalone ECG diagnosis algorithm implemented in a cell phone. Employing a wireless sensor network environment based on the IEEE 802.15.4 wireless communication standard, the system collects physiological signs from patients to a wireless dongle and then relays the information to the cell phone.

1.3 Outline of the dissertation

An overview of the ubiquitous healthcare system based on a wireless sensor network will be introduced in Section 2. Design constraints that emerged from the application's requirements posed several challenges, because a sensor network for wireless healthcare monitoring has different requirements and priorities than a network used for environmental, agricultural or industrial monitoring. This section seeks to explain why WSN technology has to be applied to the u-healthcare system. In addition, the sector introduces the system architecture of the “Multi-Modal Sensing u-Healthcare System” (MSUS), and discusses some major design issues that had to be solved during its development.

Section 3 discusses imbedded software design issues that must be addressed in query-driven healthcare monitoring. It also deals with the effects that the varying sampling rates and packet sizes utilized by different medical sensors have on network performance.

Real-time fusion monitoring of multiple sensors, combining ECG data with activity data of patients at home or in a hospital setting, is attempted in Section 4. Moreover, an ECG analysis algorithm is developed and a new method of reducing communication traffic between sensor nodes to improve the data transmission reliability in wireless sensor network will be introduced. Patient activities, including posture changes, working, running or falling, are tested using a tri-axial accelerometer attached on a chest belt or on the wrist.

Section 5 deals with the development of a wearable wireless sensor node, its implementation in a shirt and testing on a treadmill at different speeds. Motion artefacts are a major problem when measuring ECG signals with conductive fabric electrodes. However, these motion artefacts can be removed by adaptive filtering and other techniques.

Indoor location tracking can serve as a complementary measurement for continuous health parameter monitoring. Sometimes the recorded moving patterns of elderly persons or the recorded moving distance per day provides valuable data, enabling an exact diagnosis by a remote specialist. Section 6 examines the RF-based indoor tracking method which utilizes an ultrasonic transceiver and 3-D visualization of the patient’s position. Finally, Section 7 describes experiments conducted on the personal mobile healthcare diagnosis system based on the IEEE 802.15.4 standard and provides a summary of the findings.

2 Wireless sensor network in a healthcare application

Advances relating to the integration of low-power electronic devices with wireless communication capabilities and sensors have opened up an exciting new field in computer science. The emerging field of wireless sensor networks seeks to combine sensing, computation and communication into a single tiny device [6,7]. The power of these networks lies in their ability to deploy large numbers of tiny nodes that assemble and configure themselves. One important application area of WSN is remote healthcare monitoring.

2.1 Wireless sensor network for u-healthcare

Recent advances in WSN technology enable envisaging novel ubiquitous healthcare systems [8,9] that simplify the monitoring and treatment of patients, although much of the research effort in the area only regards the use of such technology in the context of personal and local area networks. As summarized in original paper I, WSN technology plays a key role in enabling communication capabilities everywhere. It will improve the quality of life of patients, provide early detection for certain ailments and improve doctor-patient efficiency. Consequently, it will serve to reduce the health-related budget burden that governments in aging societies face. Nonetheless, WSNs also pose several challenges to ubiquitous healthcare applications, as indicated in original paper II. They comprise numerous energy and resource-constrained devices, which have to be self-configuring, self-monitoring, self-healing and robust in often unpredictable environments with noise, signal loss and failures [10–12]. In addition, the devices can be mobile, such as emergency devices, or fixed, such as temperature sensors, etc. Some of the main characteristics of a networked sensor are: (1) small physical size, (2) low power consumption, (3) limited processing power, (4) short-range communication capability and (5) small storage capacity.

As healthcare applications commonly handle several types of waveform data, the application of wireless sensor network technology to ubiquitous healthcare is rather more demanding than its application to other real-time systems monitoring such factors as temperature, humidity, acoustics, light and pollution [13,14].

2.2 Multi-Modal Sensing u-Healthcare System (MSUS)

As depicted in Fig. 1, our MSUS system consists of four major components: (1) sensor nodes for health monitoring, activity monitoring and patient tracking, (2) a cellular phone functioning as a local processing unit or a monitoring tool, (3) a central server and (4) a terminal PC or PDA. This system has several features and capabilities that are present in already existing u-healthcare systems. However, unlike other healthcare systems, MSUS was developed mainly for elderly persons or patients with chronic diseases living at home. It measures patient activities, defined as sleeping, working, running and falling, together with indoor tracking signals. This context information helps to provide further insight into the natural cause and progression of the patient's condition and enhances the accuracy of early symptom detection. For example, when monitoring arrhythmic heart disease, the underlying cause of altered ECG signals can be attributed to a number of factors other than an intrinsic cardiac condition, including physical and mental stress.

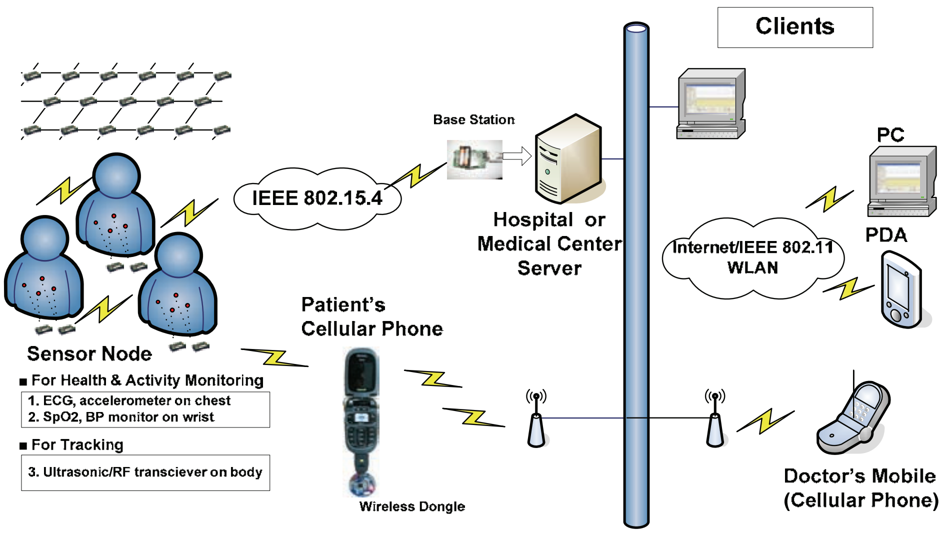

Fig. 1. System architecture of the Multi-Modal Sensing u-Healthcare System (MSUS).

MSUS employs wearable physiological biosensors, such as ECG, SpO_2 and blood pressure sensors, which are used in conjunction with other context awareness sensors, such as accelerometer sensors. Moreover, ultrasonic/RF transceivers can also be fitted together with sensor nodes to characterize the patient's activity and position.

2.3 Design issues and challenges in wireless healthcare

In ubiquitous healthcare applications, the most significant limitations of wireless networks are the slow data transfer rate and lack of a single connectivity standard that enables devices to communicate with one another and to exchange data [10]. Other limitations include wireless devices, which are still in their infancy stages and therefore slower in speed than desktop computers, high initial costs involved in setting up wireless systems and lack of real-time connectivity due to device mobility.

In order to achieve efficiency gains in the healthcare setting, three major issues in wireless development need to be addressed:

1. Appropriate development methodology must be developed to enable proper integration of new solutions with existing wireless solutions.
2. Data access, communication and synchronization issues between mobile devices and existing databases must be resolved.
3. Suitable user interfaces must be designed in order to capture and access data accurately and timely.

While many prototypes of healthcare solutions have been found to be successful, they have also suffered from limitations with regard to code, integration with existing applications, user interfaces and data transmission [15]. To allow flexibility, code is often written as generic as possible and parameters are kept as variables. During real-time testing, some of these parameters have caused run time errors, as the compiled code has not been able to resolve certain data types prior to the run. This has created the necessity to re-visit the code and examine every instance of the run in order to fix the problem. Also integration with existing applications has caused concern, as the healthcare industry lacks uniform standards.

Different types of healthcare sensors require different sampling rates and reliability requirements. Linear, or waveform-independent, healthcare data, such as body temperature, blood pressure and oxygen content, require a lower sampling rate and lower reliability than waveform-like, that is, waveform-dependent data, such as ECG or EKG. Since waveform-like data do not need continuous data transfer, data transfer can be initiated only when desired by the monitoring side or in periods of finite duration. On the other hand, in critical and emergency situations, waveform-like data require long-term data transfer. As a result, data-centric approaches are better for waveform-like data, where a query or command from the base-station initiates data transfer. Linear data can use either the data-centric approach or the event-driven approach, where data are transferred when an event is sensed. It is generally observed that linear data change gradually without any periodic sequences. So, sometimes only a change in amplitude is required to detect an abnormal event. Consequently, a threshold limit can be set to limit the amount of data transferred, and data transfer is initiated only if the value of sampled data exceeds the threshold. For waveform-like data, any packet loss can be a serious problem, as it may lead to loss of useful information or may give a false impression of abnormality. Unlike typical wireless sensor environments, where many sensors are used to sense the same event simultaneously, each sensor in a healthcare application senses a different event. This characteristic has the practical consequence that the query model for a healthcare system can be simpler in design that that for an industrial system.

3 Query-driven architecture in a ubiquitous healthcare system

Wireless healthcare monitoring in a sensor network has different requirements and priorities than environmental, agricultural and industrial monitoring. This section discusses some of the software design issues that must be addressed when implementing query-driven healthcare monitoring, as well as the effects that the varying sampling rates and packet sizes required by different medical sensors have on network performance. Some existing MAC and network layer protocols are modified to enhance their compatibility and flexibility for use in healthcare systems.

3.1 Architecture of a ubiquitous healthcare system

3.1.1 System architecture

Generally speaking, the primary objective of a wireless sensor network is to maximize the node/network lifetime, while performance metrics are secondary objectives. On the other hand, the main aim of a wireless healthcare system should be reliable data transfer with minimum delay, as described in the original papers III and IV.

Some prominent reasons for energy wastage in wireless networks include retransmission after packet loss by collusion, overhearing, idle listening and over-emitting. In a healthcare application, however, recovery of lost packets through retransmission is not necessary, because health data have to be real time. Any lost packet must be replaced by the most recent update in the next transmission. Retransmission of packets also requires more storage memory at the motes, which is generally limited in size. For most cases, the data field in each packet is between 8 bytes and 40 bytes and the sampling rate is between 100/sec and 360/sec, and the data size is 2 bytes in ECG measurement in our study. Thus one packet lost means 4 or 20 sampling data lost form ECG signal.

As mentioned earlier, the type of data to be transferred also plays an important role. Waveform-independent healthcare data do not require continuous data transfer. Consequently, data transfer can be initiated only when the data are desired by the monitoring side or in periods of finite duration. Waveform-dependent data, on the other hand, require continuous data transfer for long periods of time, particularly in critical and emergency situations. As a result, data-centric approaches are more suitable for waveform-like data, where a query or command from the base station initiates the data transfer. Linear data can use either the data-centric approach or the event-driven approach, where data are transferred when an event is sensed. Generally, waveform-independent data change gradually without any periodic sequences.

In a healthcare network, different sensors acquire and transmit data at different sampling rates, subject to different quality of service constraints. Due to this multiple data delivery model, traditional methods of data aggregation cannot be applied to healthcare networks. Nor are energy-saving techniques that use data compression. This type of heterogeneous environment makes data routing more of a challenge. Also scalability is a major issue, because single gateway architecture is not scaleable for a large set of sensors.

For a simple routing test, we chose a data set that includes one form of waveform-dependent data and one form of waveform-independent data. ECG was chosen to represent waveform-dependent data, as it still remains one of the most commonly monitored vital signs in clinical and trauma care. Body temperature was selected to represent waveform-independent data, because it is easily sensed and requires a low sampling rate and less frequent monitoring. However, any other sensor from the two categories could have been selected for the purpose.

Fig. 2 presents the architecture proposed for the ubiquitous healthcare system based on a wireless sensor network. Wireless data communication is bidirectional radio frequency communication with ad-hoc routing, which enables every mote attached to patients to send data to a base-station, even if they are not within its direct radio range. The base-station comprises an IFUS-1 (Integrated fusion sensor node, ver.1) node for receiving and broadcasting packets via its USB serial port, set to 57600 bits per second.

ECG signals from the electrodes of the 3-lead system are first amplified with a low-noise instrument amplifier, and then passed through a 0.1Hz high-pass filter (HPF) and a 35 Hz low-pass filter (LPF). The signals are then digitized and placed in packets for transmission. Patients are identified by a unique id assigned to each mote. In view of the issues discussed in the previous section, energy savings are accomplished by implementing an on-command ‘sleep’ and ‘wake’ feature, which enables the motes to transfer data only when desired and sleep for the rest of the time [16]. These ‘sleep’ and ‘wake’ commands can be issued from the terminal PC. It is important to note that sensing and the associated data transfer is stopped in the ‘sleep’ mode, although the node’s radio is still active to receive, listen and route data or a query from the network. Through the simple query feature it is possible to access specific health parameters of any patient. In addition, the system comprises a low battery alarm function, which sends an alarm message to the base-station when a mote's battery voltage runs low.

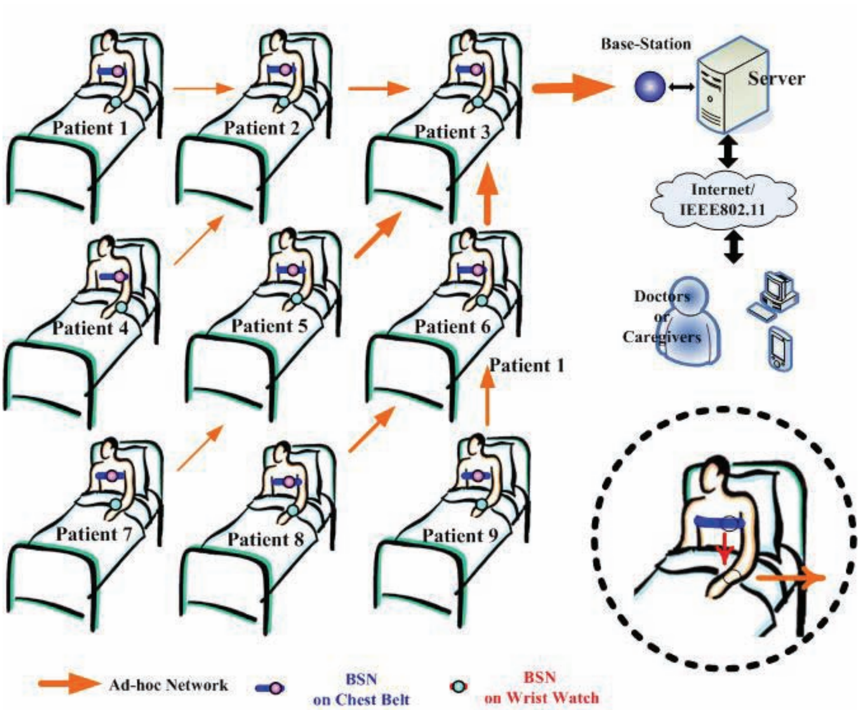

Fig. 2. Architecture example of a healthcare system based on a wireless sensor network.

Of various existing routing protocols, a simple variant of the Destination Sequence Distance Vector (DSDV) algorithm with a single destination node (the base-station) and active two-way link estimation is presently used for routing and transmission. Periodic identity signals transmitted by the base-station at 20 second intervals are used by the receiving nodes to update the routing information table. After discovering the base-station, the motes then rebroadcast the routing update to any other nodes within their range. Thus, a hierarchy of nodes is formed with the base-station at the top, and all nodes target their data to nodes that are just above them. Any change in topology is conveyed to the parent nodes, which update their tables. The MAC layer is designed using cross-layer communication features similar to those of BMAC. Interacting with BMAC, the application layer listens whether the packet transfer is successful or not. Each mote in the network acts simultaneously as a transmitter, receiver and router.

The base-station receives all data packets from all the motes in the network and directs them to the attached server PC. On the server side, the user can view a GUI-based window showing waveform ECG and other parameters. The same GUI can also be used to send commands and queries to the motes in the network, allowing medical professionals to monitor their patients' health status remotely in a mobile real-time environment. All health parameters can be stored for later reference. By combining these data with real-time health parameters, doctors and caregivers can provide useful medical assistance to their patients. This is a particularly valuable feature in emergency situations, as it enables the provision of better medical assistance with least inconvenience.

3.1.2 Hardware design

Fig. 3 shows the architecture of the designed IFUS-1 node platform while Fig. 4 presents the corresponding block diagram. Measuring 40 mm in diameter, the IFUS-1 platform is round in shape so that it can be placed on the patient's body. In addition, the stackable structure of the IFUS-1 circuit facilitates the integration of different sensors with multi-floor structure. At the core of the USN node is an ultra-low power Texas Instruments MSP430F1611 microcontroller, whose main features include 10 kB RAM, 48 kB Flash, 128 B of information storage and an 8-channel 12-bit A/D converter. With its low current consumption (less than 1mA in active mode and ~1 μA in standby mode), the node is capable of running for long periods of time. An IEEE 802.15.4 compliant CC2420 (Texas Instruments Inc.) is used as a radio chip for wireless communication. Providing PHY and some MAC layer functions, the radio chip is controlled by the microcontroller through the SPI port and a series of digital I/O lines. The M25P80 is a 4 Mb (512 x 8) Serial Flash memory with a write-protection mechanism, accessible from the SPI bus.

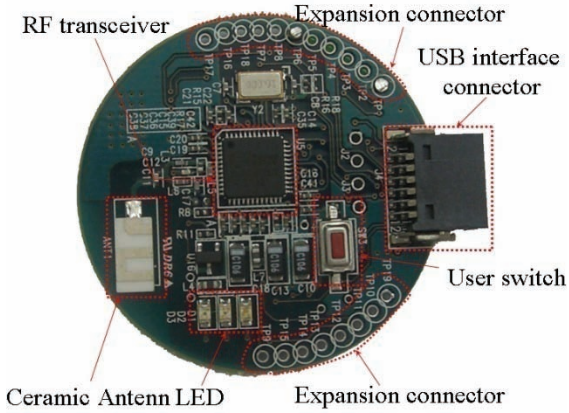

(a)

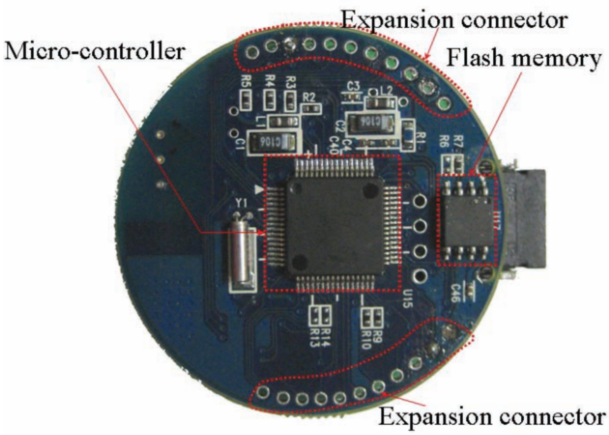

(b)

Fig. 3. Developed IFUS-1 platform (a) front side (b) back side.

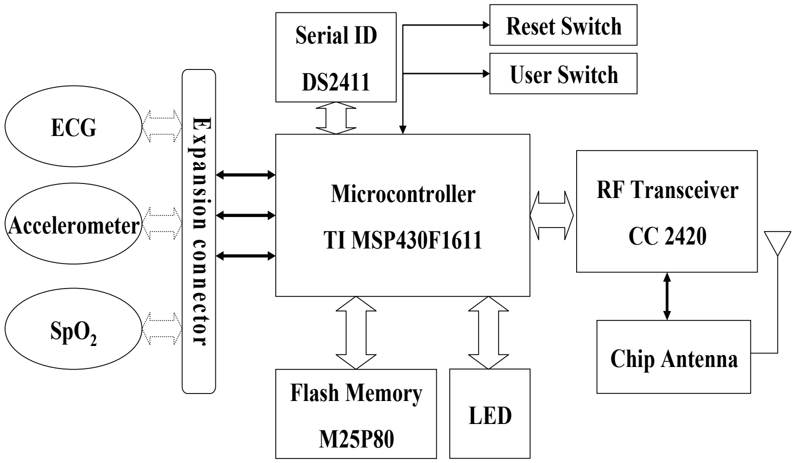

Fig. 4. Block diagram of the IFUS-1 platform (IV, modified by author with permission of Springer).

3.1.3 Software architecture

Software architecture for the WSN-based healthcare system can be classified into three categories depending on their role. Thus, the network programming model deals with the software architecture of the motes used in the network, the query model is associated with the software architecture for issuing commands and queries from the server to the motes and the monitoring model tracks packet losses and delays in packet arrival.

Network programming model

Software running on the wireless sensor nodes performs sampling, query processing and routing. This software is written in the nesC language [17], which runs on TinyOS [18]. The component-based architecture and event-driven execution model of TinyOS enables fine-grained power management while minimizing code size, as required by the memory constraints imposed on the sensor network. Our software architecture is based on the Active Message communication model [19]. Figure 5 shows an application component graph of the network programming model. As seen, one component provides an asynchronous interface to each sensor and another implements networking on the radio. Providing phase and rate control, the Lower Layer transmits or receives bytes over the radio, while the packet level component spools incoming bytes and delivers the packet receive event. The sampling component is periodically interrupted by the clock, and the data sampled from the sensors is put into packets and transmitted toward the base-station via a multi-hop network. Every packet contains a field for storing a count of packets transmitted, which is used by the monitoring program on the remote PC.

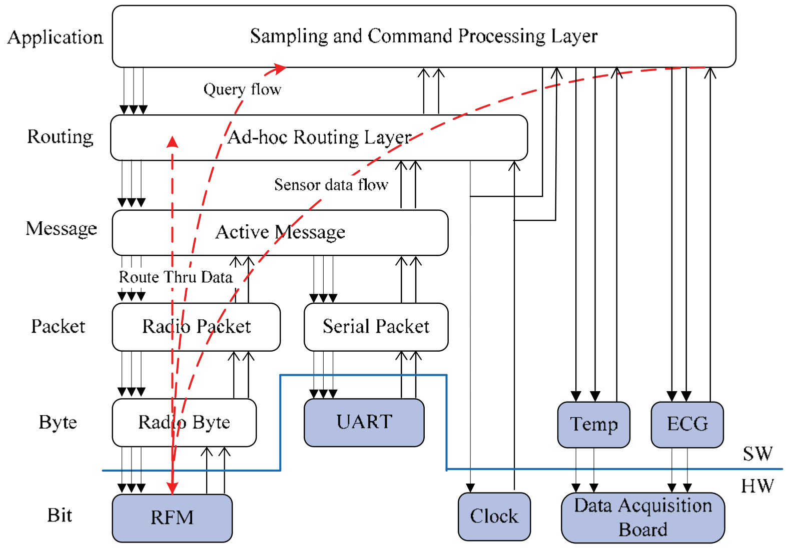

Fig. 5. Application component graph of the network programming model.

Query/command processing of the motes is also implemented at the application level. Application level components have handlers connected directly to hardware interrupts, which can be external interrupts, timer events or counter events. Also transmission rate control is implemented in the application component. If a packet is requested when the radio is busy (i.e., either transmitting or receiving), the request cannot be permitted, and the packet is lost. Once a packet component accepts a packet for transmission, it acquires the channel and transmits the packet.

Query model

The query sending system is implemented in Java and runs on the PC connected to the base-station. To keep the design simple, we use only short one-time snap data acquisition queries [20] instead of long-running (or continuous) queries. As the nodes' data channels work independently of each other, aggregation of queries [21] has to be avoided. To this end, the query system has four associated actions or commands to collect data specified by a query from the nodes and to send the data to the base-station. First, the user needs to issue the 'select_channel' query, before assigning a target node to ensure that the data will be obtained from a specific sensor in a specified target node. The sampling rate can be altered by the 'set_rate' command. To conserve energy, the motes can be sent to the sleep state either individually or all at once by issuing the 'sleep' command. Any particular mote can be wakened by the 'wake_up' command.

Figure 6 shows the query model implemented on a node. In this model, received commands are processed by a Command Interpreter, after which Control activates Sampler. If this node has been chosen, all parameters are modified accordingly to control data access from the Sensor Driver. But if the command is intended for some other node, it is broadcast by the radio transmitter.

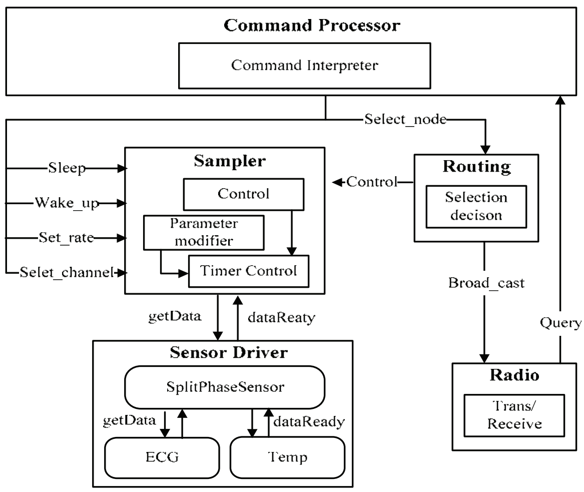

Fig. 6. Query processing model of a node.

Monitoring model

Also the packet monitoring program is implemented in the Java programming language. This program keeps track of packets arriving at the base-station, and when a new packet arrives, it obtains different types of information from the packet fields. Thus, the two-byte “Packet_count” field contains a count of packets transmitted from the motes. Every new packet from a specific mote increases its count by one from the previous packet. Any breakage in the “Packet_count” sequence denotes loss of packet from that specific mote. Since the byte size of this field is two, the number of packets counted is in the range of 0~68095.

After reaching its maximum value, the count field is reset to zero. Fig. 7 shows the algorithm designed to detect this condition. Moreover, to assist the processing of any delays in packet arrival, the arrival time of each packet is recorded.

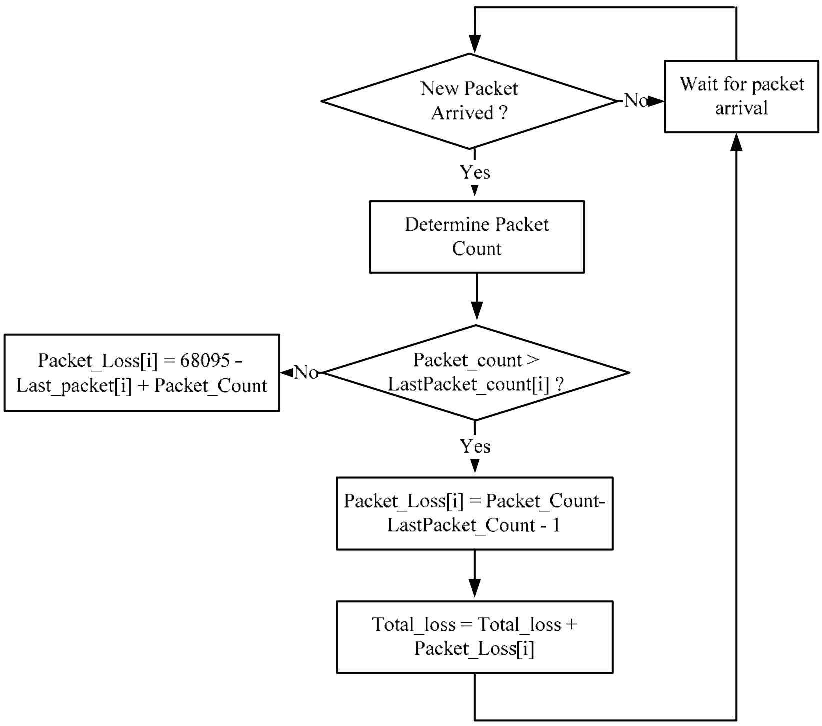

Fig. 7. Flow chart for Packet Loss Counting.

3.2 Performance analysis and verification

3.2.1 Setup and methodology for reliability measurement

In general, the performance of wireless sensor networks is evaluated on the basis of data transfer reliability (that is, packet loss) and energy use among the nodes during operation. Such evaluations should be based on real testing rather than simulations, but this is not always possible. Software for the wireless nodes was developed in the nesC programming language using TinyOS, and the real-time packet loss monitoring software was developed in the Java programming language.

Real-time performance evaluation of the system involved conducting a range of tests on the designed hardware and software. An attempt was made to create an environment that resembles the real situation in home care or hospital care, where patients may be stationary or moving either in a room or outdoors within direct or indirect range of the base-station. The experimental setup was located in our laboratory in the U-IT building at Dongseo University, and experiments were performed at various sampling frequencies, representing different sensors that could be used in a healthcare system comprising 5 motes. Low sampling frequencies were used to obtain waveform-independent data for performance evaluation, while high sampling frequencies helped to visualize the performance of wave-dependent data. Also the number of nodes helped to simulate the real-time situation, when data from many patients have to be accessed at the same time.

The setup environment is shown in Fig. 8, and every node in the scenario is summarized in Table 1. In Fig. 8, the solid arrows show the fixed path taken by data sent from the stationary nodes, while the dotted arrows represent the fluctuating path of data originating from the mobile nodes. In this context, mobile nodes refer to nodes moving in random directions at a speed equal to normal walking speed, at a distance of about 3~6 m from the stationary nodes. Being sometimes close to the stationary nodes and sometimes further away from them, the communication link varies between strong and weak. Node-1 (1.5 m from the base-station) and Node-3 (3 m from the base-station) are stationary nodes within the communication range of the base-station (fixed to a maximum of 5 m). Node-2, on the other hand, is a mobile node moving in the vicinity of the base-station in such a way that sometimes it is within direct range of the base-station, while at other times a communication route has to be established via Node-1. Node-4 is a stationary (2 m from Node 3) and Node-5 a mobile node located outdoors. In each experiment, a “virtual” sensor on each node is used to generate data at a constant rate to depict the scenario of different sensors being attached to a patient’s body.

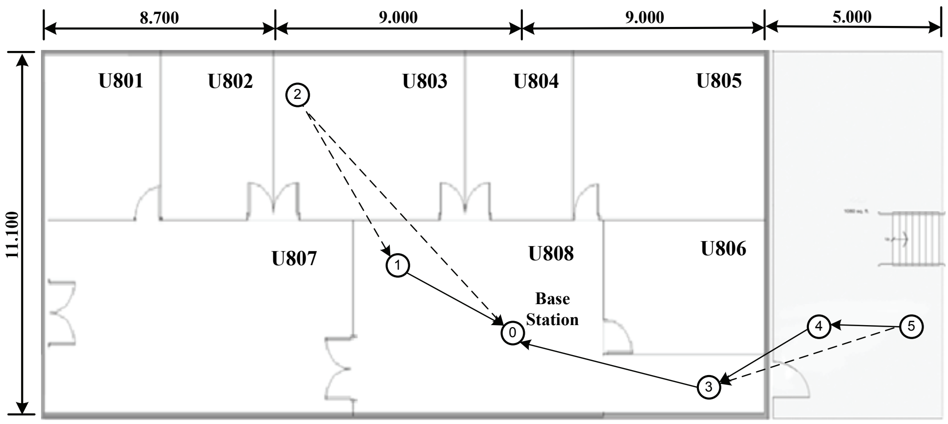

Fig. 8. Experimental setup for testing.

Table 1. Description of node positions and mobility during the tests

Node Name	Number of Hops	Mobility	Position
1	1	Stationary	Indoor
2	1~2	Moving	Indoor
3	1	Stationary	Indoor
4	2	Moving	Outdoor
5	2~3	Stationary	Outdoor

3.2.2 Energy analysis using simulator

Since power consumption is a critical factor for sensor networks or any wireless system operating on limited power reserves, network designers must obtain accurate and dependable power consumption figures for the sensor nodes before deployment. Apart from aggregate power consumption over time, the power load pattern must also be considered, as it affects the power source’s ability to deliver adequate energy over time. It is often advantageous to use simulators to predict energy consumption, because measuring the energy consumption of an individual mode in a network can be rather laborious, when it is running and mobile. Such platform-specific simulators as PowerTOSSIM [22], AVRORA [23] and Atemu

[24] can emulate the real-time behaviour of hardware based on real, experimentally acquired and accurate energy models. Although PowerTOSSIM and AVRORA use the same approach, we used AVRORA due to the simulation convenience even it's simulation speed is slower than the PowerTOSSIM [23].

3.2.3 Packet loss measurement

Only packets that successfully reach the base-station can be counted there. The percentage of packet loss in a network is calculated by the following equation, which depends on packets lost in the network and packets received at the base-station.

$$\%Packet_{Loss} = \frac{Packet_{Loss\_in\_Network}}{Packet_{Loss\_in\_Network} + Packet_{Received}} \, . \tag{1}$$

For all cases, the data field in each packet is 8 bytes, and the update time for packet routing is 80 s. Routing update time is defined as the time within which the nodes exchange topological information. Figure 9 shows the variation in packet loss as a function of sampling frequency and number of operating nodes. As seen, this loss can be as high as 12% at a low sampling frequency, which is a fairly high figure for a healthcare application. This can be explained by the fact that packet formation and communication are slow, due to the slow extraction rate of routing information updates from each packet header. Minimum loss is achieved at 10 Hz using 8-byte data. At higher frequencies, packet loss starts to build up again. This increase may be caused by packet collisions or by losses occurring at the MAC layer of the receiving node in high traffic. Figure 10 shows how average packet loss in each node varies with changes in sampling frequency. Node-1 and Node-3 are one hop away from the base-station and thus show minimum packet loss. In contrast, Node-2 and Node-4 are two hops away, so they experience somewhat higher packet loss. It should be noted here that, being mobile, Node-2 shows a higher packet loss rate than Node-4. Of all the stationary nodes, Node-5, which is 3 hops away and thus furthest away from the base-station, has the highest packet loss rate. The slightly random nature of the plot may be due to the real-time testing conditions and may be attributed to any unnoticed source of noise present in the environment at the time of the experiment.

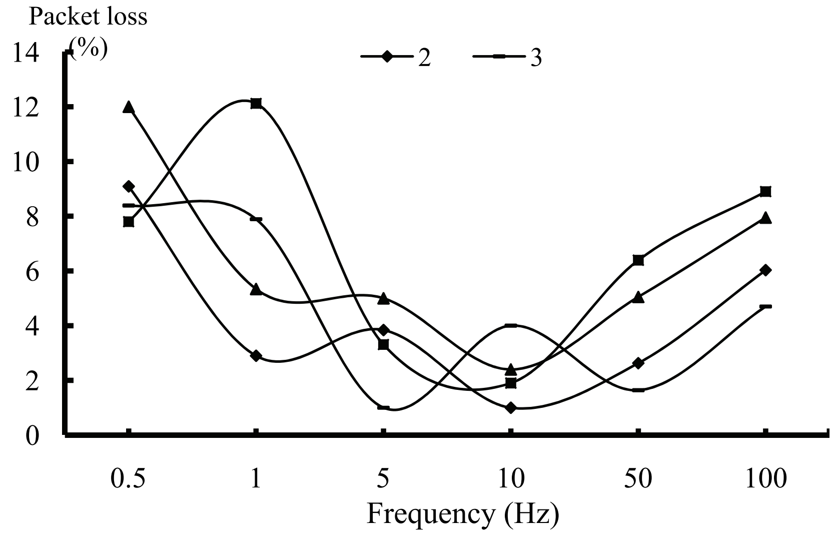

Fig. 9. Packet loss variation as a function of node number.

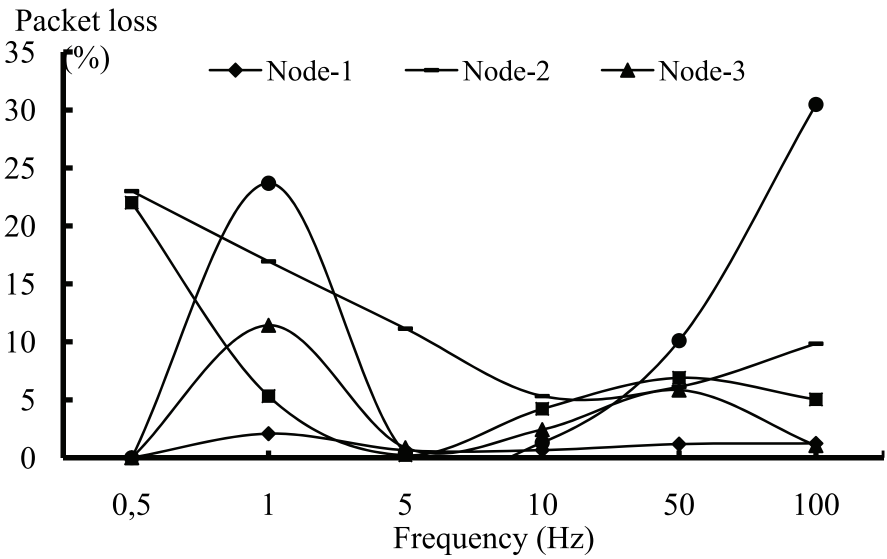

Fig. 10. Packet loss variation in individual nodes.

To study the response of the network to changes in topology caused by the migration of nodes, it is important to establish the effect that routing update time has on packet loss. Experimental results indicate that decreasing the routing update time may lead to fast updates and reduce packet loss that occurs when nodes lose track of their parent nodes after a change in topology. Figure 11 shows the observed packet loss reduction, when the routing update time is reduced by 10 times, from 80 s to 8 s. In this figure, the white bar represents a routing time of 80 s, and the oblique bar adjacent to it, a routing time of 8 s. So, the general conclusion that can be drawn from this result is that updates should be fast so as to minimize packet loss during periods of uncertainty caused by link breakage.

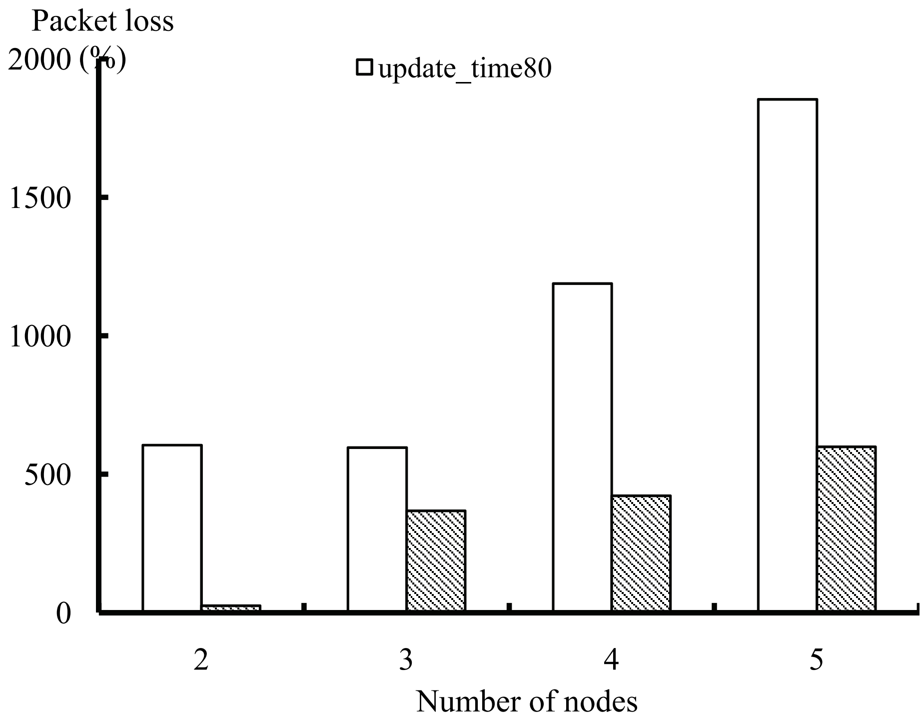

Fig. 11. Effect of decreasing routing update time on packet loss.

Through comparative graphs, Figure 12 summarizes the effects of packet size and packet update time on the packet loss rate. By making the effects more clearly visible, this figure enables analytical comparisons to be made. As seen, a longer data field in a packet decreases the number of packets received. It seems that the longer the packet request, the longer the packet formation time. However, as long as the same amount of information is transmitted, the resulting reduction in traffic is actually beneficial for the network. On the other hand, a decrease in update time increases the number of packets received, as less packet loss occurs during the time when the nodes do not know their parent nodes. Several explanations can be offered for the observed packet loss rate. For example, our laboratory environment contained a large number of glass walls and windows, forming many kinds of RF reflections, which may have caused some of the packet loss. Moreover, since the frequency spectrum of IEEE 802.15.4 lies close to that of commercial Wi-Fi systems, possible interference from these systems cannot be ruled out, and may also have contributed to the recorded packet loss rate. Also the design of the MAC layer may have introduced some limitations.

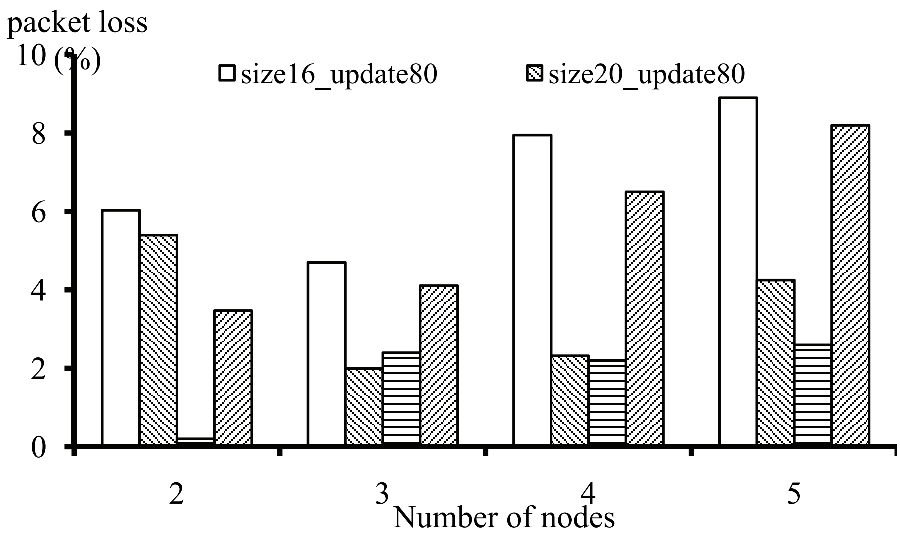

Fig. 12. Packet loss percentage for the different cases.

3.2.4 Energy analysis

Energy consumption in a wireless sensor network system is mainly caused by radio communication and the CPUs of the sensor nodes during operation. Since the energy consumed by the CPUs is very low in comparison with the energy used by the radio, most of the energy usage can be attributed to radio communication. Thus, in terms of the energy efficiency of WSN-based systems, one of the most important design considerations is a low-energy RF communication system [25]. One way to save energy involves using longer communication packets with less frequent communication, rather than shorter packets with more frequent communication. To investigate the effect of packet size and routing update time on energy consumption, simulations were carried out using the AVRORA simulator. Results from the simulations are tabulated in Table 2 for runs lasting 30 s, 120 s and 300 s, respectively. The table also summarizes the energy consumption of the CPU, radio and sensor board according to routing update time and data field length.

It can be seen that although routing update time has little effect, changing the data length from 1 byte to 16 bytes reduces energy consumption. Moreover, this change affects radio communication more than CPU operation, since most of the energy consumed by the sensor nodes goes to radio communication. To put it simply, a longer packet length leads to a shorter running time which, in turn, decreases energy consumption. Our simulation results also show that these variables have no effect on the amount of energy consumed by the sensor board. In addition, the ratio of data bytes per packet demonstrates that the number of bytes received per packet increased as a function of increasing packet size and reducing update time. This value is highest for a data field length of 20 bytes and update time of 80 seconds. Duty time, i.e., the time when the CPU is either in Active and Idle state, is expressed as a percentage and indicates how busy the CPU is when it runs the source code. It is worth noting here that the simulation runs on a single node and may not include the effect of packets received and MAC load, due to transmission from neighbouring nodes. Nevertheless, the table shows trends which can be used to predict the effects of update time and packet size on node performance.

Table 2. Energy consumption predicted by a simulation run of 120 s.

Parameters	Data field 1 byte		Data field 16 bytes		Data field 20 bytes	
	Routing update time 80 s	Routing update time 8 s	Routing update time 80 s	Routing update time 8 s	Routing update time 80 s	Routing update time 8 s
Energy used by CPU (J)	1.490	1.491	1.381	1.382	1.381	1.383
Energy used by radio (J)	3.758	3.759	3.579	3.583	3.590	3.593
Energy used by sensor board (J)	0.252	0.252	0.252	0.252	0.252	0.252
Bytes sent	159677	160300	62984	64755	67888	69659
Packets sent	4683	4705	1236	1291	1236	1291
Bytes/packet	34.09	34.07	50.96	50.16	54.92	53.96
Active state (%)	18.88	18.92	11.68	11.78	11.72	11.82
Idle state (%)	81.11	81.07	88.31	88.21	88.27	88.17

As seen, energy consumption increases slightly with longer routing update times. Increasing the length of the data field in a packet helps to reduce the energy consumed by the CPU and the radio, while the amount of energy used by the sensor board remains constant. Some readers may argue that the improvement is insignificant, but that is only because the simulation was run for a short time. We are confident that a longer run, lasting from a few hours to a few days, would make the difference more apparent.

Increasing packet length also improves the number of bytes sent per packet. It should be noted that the bytes/packet ratio has a fractional value, because the routing update times and data packets are of different sizes and the simulator counts separately the number of packets transmitted and bytes sent. Increasing packet length also improves the percentage of time that the CPU spends in the ‘Idle’ state. Changes in routing update time do not affect performance parameters for a fixed packet length.

4 ECG analysis on a server PC or a sensor node

Heart diseases can be detected by means of analyzing electrocardiograms (ECG) [26]. However, heart rate can be affected by such activities as walking, running and falling, which makes it very important for continuous health status monitoring to record patient activities along with the ECG data. Fusion signal monitoring combines a health parameter and a physical condition [27] to enhance the accuracy of health or cardiac event monitoring. Thus, ECG and activity data are continuously recorded and simultaneously analyzed in a wireless sensor network environment with a built-in automatic alarm system for giving early alarm signals to the treating physician or other caregivers. This section is based on original papers V and VI.

4.1 ECG and accelerometer analysis algorithm

An ECG is a plot of the time-dependence of charging potential differences between electrodes on the body surface. Fig. 13 and Table 3 show a typical ECG with the duration of waves and intervals in a normal adult human heart. Classification of ECG signals rests on a reliable extraction of ECG parameters.

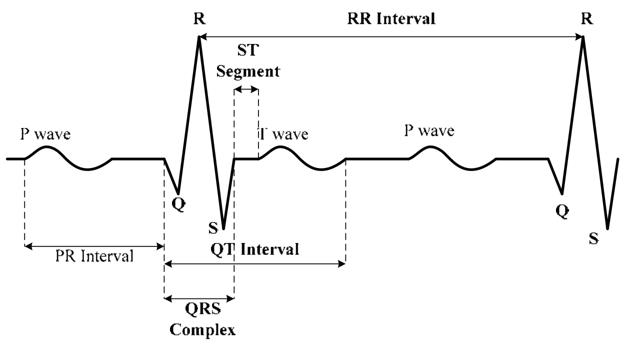

Fig. 13. Typical ECG signal recorded from body surface.

Table 3. Duration of waves and intervals in a normal adult human heart (VI, published by permission of IEEE).

Parameter	Duration (sec)
Intervals	
P-R	0.12 ~ 0.20
Q-T	0.3 ~ 0.40
Waves	
P	0.08 ~ 0.10
QRS	0.06 ~ 0.10

In the system described here, ECG and accelerometer sensors are attached to the human body, and the recorded data are first transmitted to the base-station and then to the server for analysis. This analysis involves determining heart rate and other ECG parameters together with the norm and orientation of acceleration data. If abnormal ECG signals are detected or the acceleration data indicate falling, an alarm is sent to the attending physician's PDA. A flow chart of ECG and accelerometer signal analysis is shown in Fig. 14.

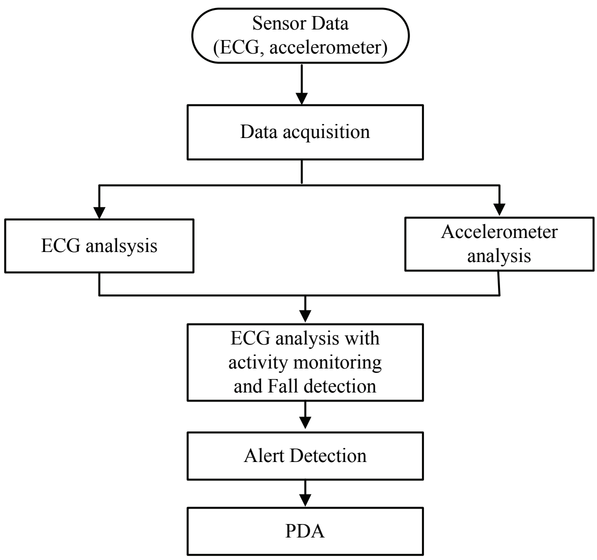

Fig. 14. Flow chart for ECG and accelerometer data acquisition and analysis (V, published by permission of IEEE).

4.1.1 QRS detection

The ECG provides a record of electrical events occurring within the heart and is obtained from electrodes placed on the surface of the body. A typical ECG tracing of a normal heartbeat (or cardiac cycle) consists of a P-wave, a QRS complex and a T-wave.

One commonly used QRS detection algorithm was developed by Pan and Tompkins [28] in assembly language for implementation on a Z80 microprocessor and was later improved and ported to C by Hamilton and Tompkins [29].

Based on the Pan-Tomkins algorithm, the ECG analysis software running on the server PC was developed by our research group. The software is composed of two parts, with the first being dedicated to QRS detection and the other to T-wave and P-wave detection as a complement of QRS detection using C# based on a .NET compiler on the server. Originally designed to operate at 200 Hz, the variant QRS detector uses a single ECG channel. The developed QRS detection algorithm has the advantage of being efficient and easily modifiable for different sampling rates.

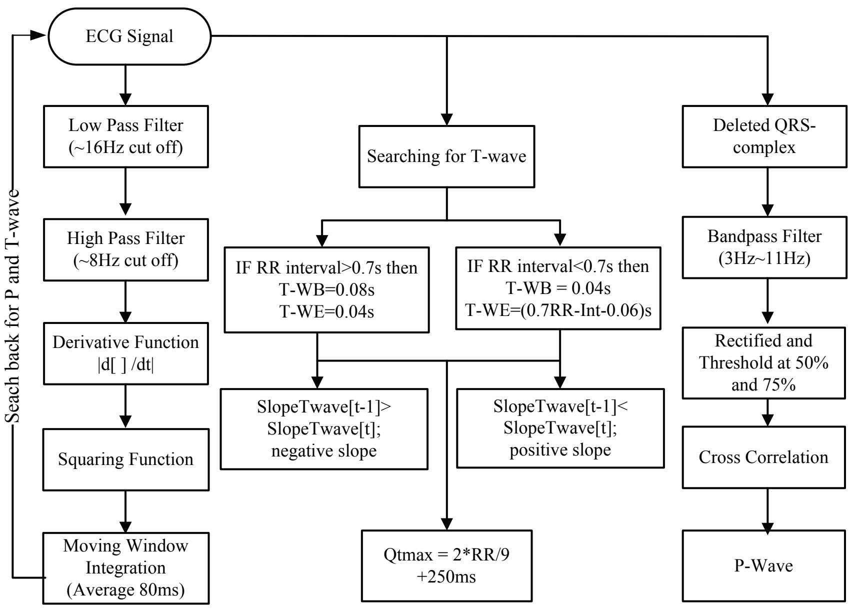

Fig. 15. QRS-complex, P-wave and T-wave detection algorithm.

QRS detection is based on analyzing the slope, amplitude and width of QRS complexes. It includes a series of filters and methods that perform low pass, high pass, derivative, squaring and integration procedures. Filtering reduces false detection caused by various types of interference present in the ECG signal. This filtering permits the use of low thresholds, thereby increasing detection sensitivity. Adapting to changes in QRS morphology and heart rate, the algorithm adjusts the thresholds automatically while other parameters are adjusted periodically. Fig. 15 presents a flow chart of the QRS-complex, P-wave and T-wave detection algorithm. It calculates R-R intervals, QRS complex width and heart rate variability using a moving window integration process. Heart rate is computed by measuring the length of the R-R interval, or a full period of the waveform. These parameters are used to detect abnormal conditions in patients.

4.1.2 P-wave and T-wave detection algorithm

Representing atrial depolarization, the first deflection of the ECG is the P-wave, while repolarization of the ventricles generates the T-wave. The detection algorithm searches for the T-wave first after a QRS complex has been detected, and the wave is expected within a specific time window. The start and end points of the analysis window are set depending on the R-R interval as follows:

If R-R interval > 0.7 s:
  T-wave window beginning = 0.08 s after QRS end
  T-wave window end = T-wave window beginning + 0.04 s

If R-R interval ≤ 0.7 s:
  T wave window beginning = 0.04 s after QRS end
  T wave window end = T wave window beginning + (0.7 R-R interval - 0.06) s

Within this window, the minimum, maximum and slope order of the derived function are important for detecting the T-wave. Also bi-phase T-waves can be identified in the same way. Changes of slope as well as the end point of the T-wave are detected by defined threshold values. The slope is either positive or negative in value, and the minimum detectable slope magnitude resolution for a T-wave is defined as 0.006 mV/s. The algorithm keeps searching for this combination, until the beginning of a new QRS complex is detected. $\mathrm{SlopeTwave}[t-1] > \mathrm{SlopeTwave}[t]$ means that the slope is negative. Five consecutive slope values are checked, before a final decision is made whether the slope is positive or negative. In these calculations, t is the slope encounter number and SlopeTwave is the calculated slope. Initially, the values are set as follows: $t = 1$ and SlopeTwave[0] = 0, respectively.

A P-wave is assumed when a positive slope is followed by a negative slope within a T-wave time window, and the magnitudes of the slopes are greater than 0.004 mV/s. This combination is searched for until the algorithm detects the beginning of a new QRS complex, whereafter it is deleted and replaced with a new baseline. The baseline is determined by analyzing a few samples preceding the QRS complex. The resulting signal is bandpass filtered with −3 dB points at 3 Hz and 11 Hz, and the search interval is defined as QTmax = 2R − R/9 + 250 ms, where R-R is the interval between two successive QRS complexes. The signal is then rectified and divided by three signal levels with thresholds at 50% and 75% of the maximum. After cross-correlating the results of these three calculations, a representative set of P-waves are measured. The peak in the cross-correlation corresponds to the location of the original ECG, and the estimated P-R interval should be less than 0.02 s for normal ECG, which extends from the beginning of the P-wave to the first deflection of the QRS complex.

4.1.3 Acceleration norm and orientation calculus

A human activity monitoring and fall detection system is designed in the form of a wrist-worn device using a single three-axis accelerometer unit on a wireless sensor node. The prototype sensor also includes a data acquisition board for accelerometer data. This system uses Micaz (Crossobw Inc., USA) motes as a platform for processing and radio communication [30]. Each Micaz mote, powered by two AA batteries, has an Atmel Atmega 128L microcontroller, 4 KB of RAM and a CC2420 2.4 GHz ISM band radio capable of transferring data at 250 kb/s. This radio module has a physical layer channel designed in accordance with the IEEE 802.15.4 standard and its communication range is 20 to 75 meters (depending on potential obstacles).

To collect acceleration data, the motes use an MDA300CA data acquisition board, equipped with an ADS7828 IC functioning as a 12-bit ADC MUX. The MMA7260Q accelerometer sensor has a range of up to 6 g and a sensitivity of 200 mV/g. Consisting of two surface micro-machined capacitive sensing cells (g-cells) and a signal conditioning ASIC (A Universal Sensor Signal Conditioning) contained in a single integrated circuit package, the device outputs a voltage signal which is linear within the supply range of 2.2 to 3.6 volts.

Data collected by sensor unit are transmitted wirelessly to the base-station mote, which then sends the data packets to the PC through UART. On the PC, these data are processed for activity monitoring purposes.

If X_i, Y_i and Z_i are the acceleration values at a particular time instant, the acceleration norm A_n is given as

$$A_n = \sqrt{X_i^2 + Y_i^2 + Z_i^2},$$

while orientation is calculated using the magnitude of the vertical axes divided by the norm

$$Cos\Theta = Z_i / A_n.$$

The data collected at the base-station attached to the PC are the sampled values from 0 to 4096 digital levels (2^{12}) of the voltage signal obtained from the sensor unit. These sample data are calculated and checked to ascertain whether this voltage level represents positive or negative acceleration. The formula used for calculating the exact acceleration voltage is given as

$$V.L. = \frac{[VDD(mV) \times (SampleLevel) / 4096 - 1500(mV)]}{200(mV)},$$

where 1500 mV is the reference voltage level of the accelerometer. Values above this level are considered as positive and those below it as negative. 200 mV/g is the sensitivity of the accelerometer.

Basically, fall detection is decided by an algorithm which utilizes acceleration data. When people fall, their acceleration changes rapidly. Thus, a fall can be detected by measuring acceleration values that exceed a set threshold and are horizontal in orientation within a time interval. As shown in Fig. 16, the rationale behind this method is to observe a significant change in the user's orientation angle, and to look for a large acceleration within the same time interval. If the resultant value is continuously greater than the acceleration threshold value for 15 seconds, the orientation angle is analyzed. If this angle is horizontal with ground (90 degrees), the event is classified as a fall. Following a wait of 15 seconds, the algorithm determines whether the orientation angle is still horizontal with ground or tilted towards it. If the orientation angle remains unchanged, a fall is detected.

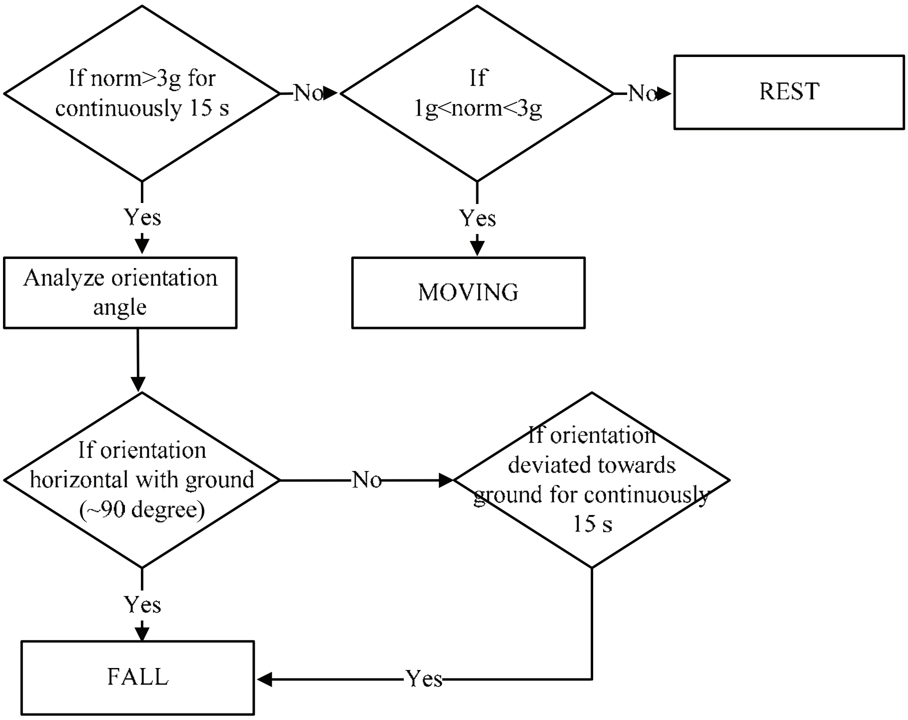

Fig. 16. Activity and fall monitoring algorithm.

4.1.4 Fusion analysis algorithm

After all parameters of the obtained ECG signals are calculated, the results are combined with acceleration data to provide high accuracy monitoring information. For example, a rest heart rate greater than 100 bpm indicates sinus tachycardia, whereas a rate less than 60 bpm denotes sinus bradycardia. A heart rate between 60 and 100 bpm represents normal sinus rhythm. However, these figures do not apply to moving patients, as shown in Fig. 17. Moving activities, such as walking and running, are recorded when the acceleration norm is below 3 g (where g = 9.8 m/s^2).

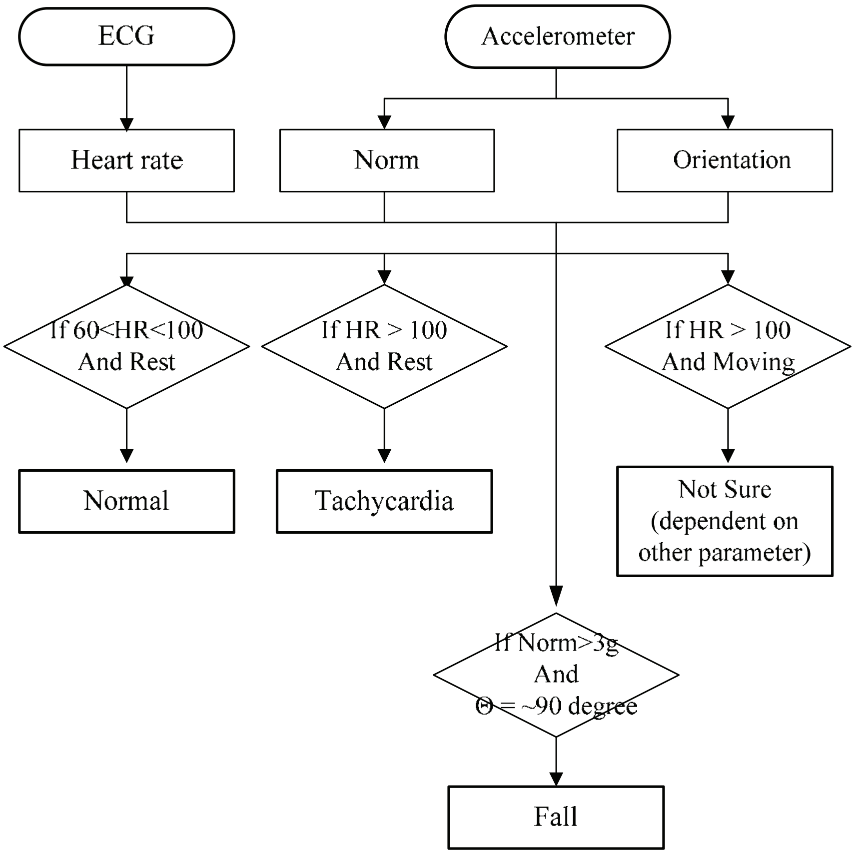

Fig. 17. ECG analysis with activity monitoring.

4.2 Diagnosis

To test the developed fusion signal processing algorithm, two kinds of ECG signals are used. One is directly obtained from the human body and the other from the MIT-BIH arrhythmia database [31]. Firstly, an ECG wave is transmitted from the human body to the base-station and then to the server for the analysis of ECG and accelerometer data. If any abnormalities are detected, an alarm is sent to the PDA of the treating physician for a more detailed diagnosis. Normal ECG data is acquired from a person's body using the MIB510 data acquisition board of a Micaz mote.

Abnormal ECG is obtained from the MIT-BIH arrhythmia database, created in cooperation between the Massachusetts Institute of Technology and Beth Israel Hospital for the development and evaluation of real-time ECG rhythm analysis.

Figure 18 shows step-by-step results of the ECG analysis. In P-wave detection, ECG signals are processed by a bandpass filter, differentiator, squaring, moving window, deleted QRS complex and bandpass filter, as illustrated by Fig. 19. Bandpass filtering can effectively suppress power-line interference at the cut-off frequency of 5 Hz ~ 11 Hz, if such interference is present in the signal. Then, an ideal differential operator employs a five-point derivative function to suppress the low-frequency components of P and T-waves and to provide a large gain of up to 30 Hz to the high-frequency components arising from the high slopes of the QRS complex. Next, a squaring function is applied to make the result positive and to emphasize large differences resulting from QRS complexes, whilst suppressing small differences arising from P and T-waves. QRS complex-related high-frequency components in the signal are further enhanced at this stage. A MWI then smooths the output of the derivative-based operation exhibiting multiple peaks within the duration of a single QRS complex. A window width of N = 30 was found to be suitable for the 200 Hz frequency. Finally, having detected a QRS complex, the algorithm deletes it and replaces it with the base-line, determined by analyzing a few samples preceding the QRS complex.

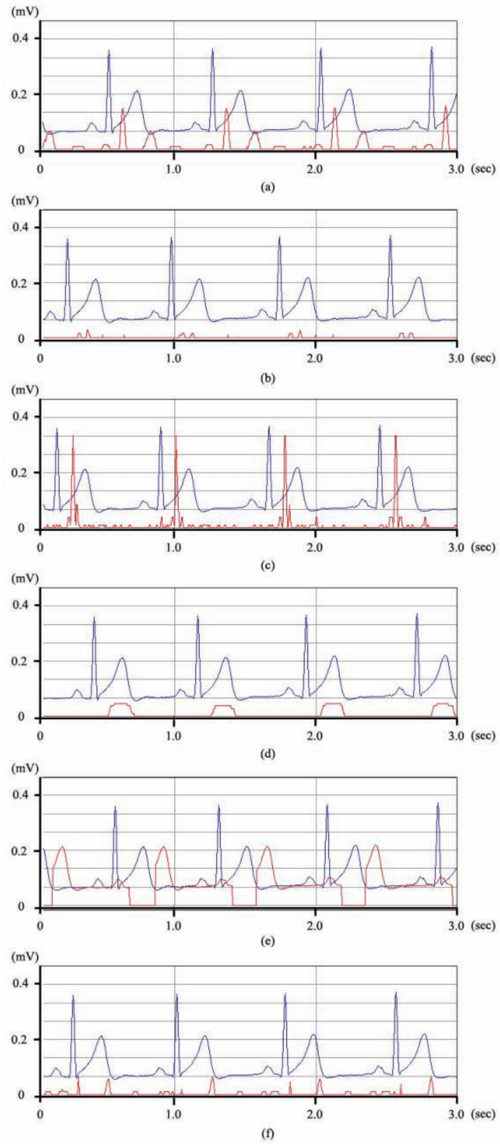

Fig. 18. Step-by-step results of ECG analysis on the server; (a) Output of bandpass filter: 5 Hz and 11 Hz, (b) Output of differentiator: five-point derivatives derived nearly linear between 0 and 30, (c) Output of squaring function, (d) Output of moving window integration: window length is 30 for 200 samples per sec, (e) Output of deleted QRS complex from the, (f) Output of bandpass filter: 3 Hz and 11 Hz.

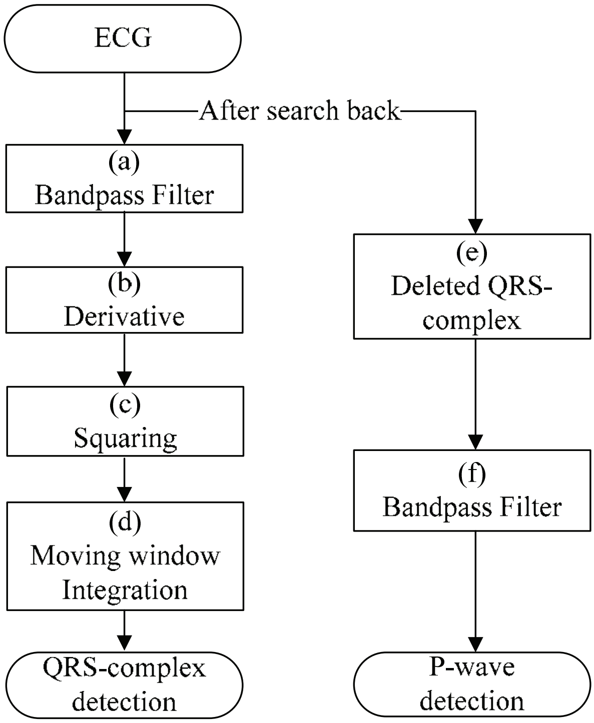

Fig. 19. Flowchart of QRS complex and P-wave detection in the ECG signal.

Accelerometer data are received by the sensor unit, consisting of a 3-axis accelerometer and data acquisition board (AD5893, 12 bit ADC-MUX) connected to Micaz motes (Crossbow Technology Inc.).

Table 4. Description of block numbers in Fig. 19.

Block Number	Description
1	ECG commands: to check the buffer, to increase or decrease the speed of the ECG graph
2	Various parameters of ECG, detected from ECG
3	Serial communication command: to adjust the port number for communication
4	Heart rate variability graph
5	ECG graph
6	Heart rate from ECG analysis
7	ECG status: normal or abnormal
8	Disease status: possible disease detected
9	Alarm condition : if normal, then OFF, and if abnormal, then ON and send necessary information to the doctor’s PDA

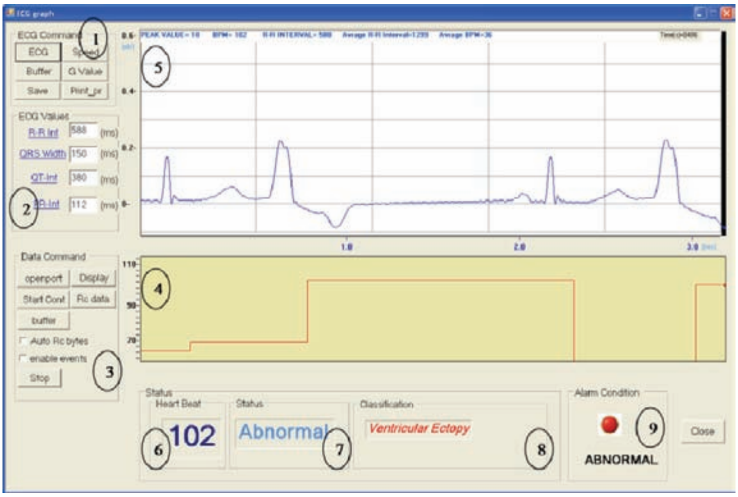

Fig. 20. ECG interface with abnormal status and heart rate variability graph on the server: R-R interval= 588 ms, QRS width = 150 ms, QT interval= 380 ms, PR interval= 112 ms and HR = 102. These data are taken from file no. 119 of the MIT-BIH arrhythmia database (VI, published by permission of IEEE).

Fig. 20 shows ECG analysis data indicating abnormal status; the disease that has possibly been detected is ventricle ectopy. When ECG analysis implies an abnormal condition, an alarm is sent to the treating physician's PDA, indicated by a red button icon. Fig. 21, on the other hand, presents the monitoring interface for fusion data combining ECG and accelerometer sensor data. The data suggest abnormal ECG status caused by tachycardia, but also the fact that the person is running. Taking this into consideration, an analysis combining both ECG and accelerometer data does not indicate abnormality, because normal heart rate may well rise to over 100 bpm during running. Therefore, no alarm is sent to the doctor's PDA, even though the measured heart rate is abnormally high. Fig. 22 presents the ECG interface with the parameter values.

Table 5. Description of block numbers in Fig. 20.

Block Number	Description
1	Tri-axial accelerometer graphs: Channel0 (x-axis) – Blue, Channel1 (y-axis) – Red, Channel2 (z-axis) – Green
2	ECG graph
3	Serial data received by the server in packet format
4	Serial data received by the server
5	ECG parameter values
6	Accelerometer parameter values
7	Heart rate
8	Possible disease detected and patient status(moving, resting or falling)
9	Alarm condition: if normal then OFF, and if abnormal then ON and send necessary information to the doctor's PDA
10	ECG and accelerometer commands

Fig. 21. ECG and accelerometer interface on the server showing abnormal status: R-R interval= 408 ms, QRS width = 68 ms, QT interval= 406 ms, PR interval = 112 ms, Resultant = 1.276345, Angle (degree) = 12.47328 and HR = 147. These ECG data come from the MIT-BIH arrhythmia database, while the accelerometer data are received by a sensor node attached to the body (V, published by permission of IEEE).

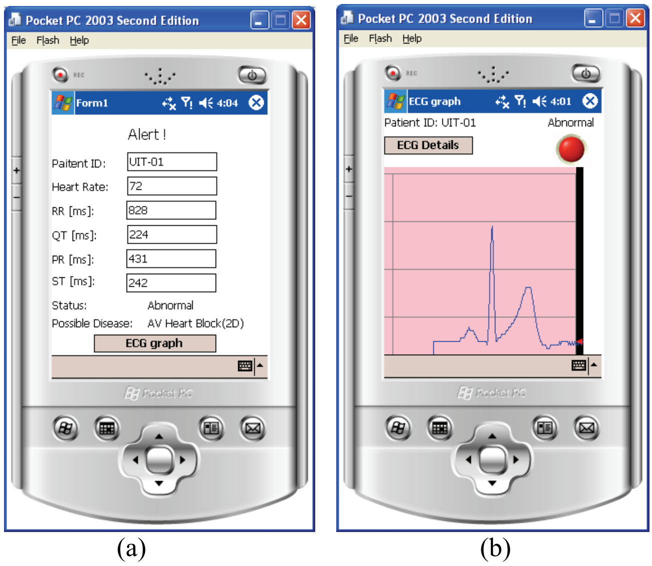

Fig. 22. ECG and patient status as shown on a PDA.

4.3 ECG analysis on a sensor node

4.3.1 Concept of ECG signal analysis on a sensor node

In this system, wireless sensor nodes attached on the body, are used to continuously transmit health parameters, such as electrocardiogram (ECG) data, via a wireless sensor network. This may result in heavy communication traffic between the sensor nodes and the gateways, particularly when dealing with such wavelike health signals as ECG. One attempt to reduce this traffic includes allowing the sensor nodes to perform real-time analysis of ECG signals, thereby eliminating the need to continuously transmit ECG data to the server. Only when a sensor node detects abnormal ECG signals, it is required to transfer these data for further analysis. Although this system can be used to reduce data packet overload and to save power, it can also increase server performance.

4.3.2 Architecture of ECG monitoring and analysis on a sensor node and the server

Figure 23 shows the architecture of ECG monitoring and analysis on a sensor node. The system also incorporates an application for recording activities, events and potentially important medical symptoms with the capacity to transfer data to the server for further analysis. System hardware allows these data to be transmitted wirelessly, together with analysis results, from an on-body sensor to the base-station and then further to a PC/PDA.

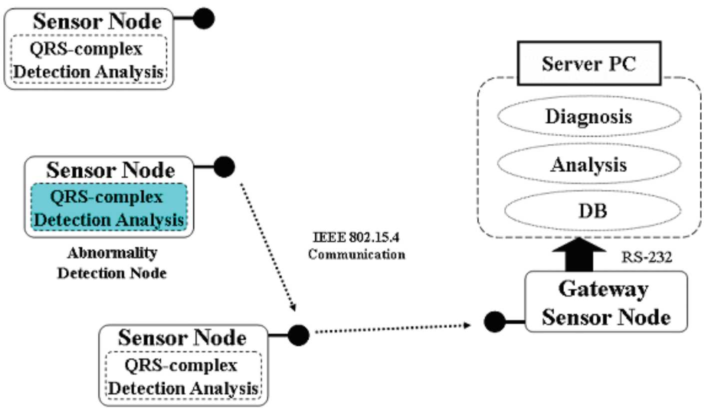

Fig. 23. Architecture of ECG monitoring and analysis on a sensor node and the server.

ECG analysis on a sensor node uses a variant of the Pan-Tompkins algorithm [28] for signal processing. This algorithm has been modified to better comply with our analysis requirements, and programming is done in the nesC programming language. Based on analyzing the slope, amplitude and width of QRS complexes, this Pan-Tompkins algorithm enables real-time QRS detection. Figure 24 explains the QRS complex detection method on a sensor node. It includes a series of filters and methods to perform low pass, high pass, derivative, squaring and integration procedures. Filtering reduces false detection caused by various types of interference present in ECG signals. Moreover, it increases detection sensitivity by permitting the use of low thresholds. Adapting to changes in QRS morphology, the algorithm automatically adjusts these thresholds, while other parameters are adjusted periodically. After detecting abnormal QRS complexes in ECG signals, it transmits the ECG data to the server for further analysis.

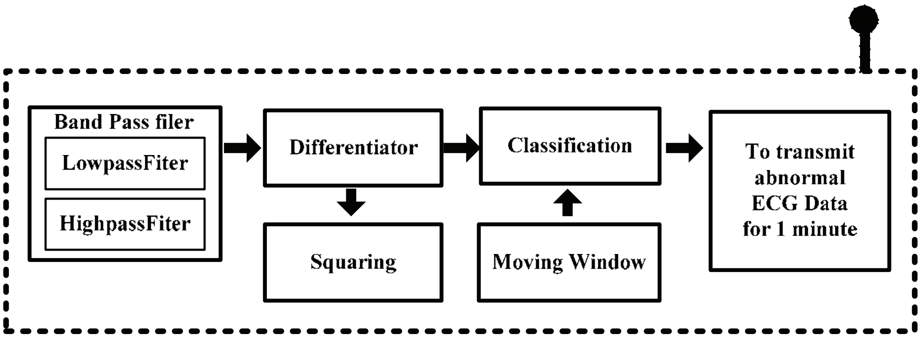

Fig. 24. QRS complex detection on a sensor node (VI, modified by author with permission of IEEE).

Low-pass filter

The recursive low-pass filter used in the algorithm has integral coefficients to reduce computational complexity, with the transfer function defined as

$$H(z) = \left(1 - z^{-6}\right)^2 / \left(1 - z^{-1}\right)^2, \tag{1}$$

$$y[n] = 2y[n-1] - y[n-2] + x[n] - 2x[n-6] + x[n-12]. \tag{2}$$

With the sampling rate being 200Hz, the filter has a rather low cutoff frequency, 11 Hz, and introduces a delay of 5 samples, or 25 milliseconds. At 60 Hz, the filter provides attenuation greater than 35 dB and effectively suppresses power-line interference, if present. Then, the final equation is given by:

$$y[n] = 2y[n-1] - y[n-2] + \left(x[n] - 2x[n-6] + x[n-12]\right)/36. \tag{3}$$

High-pass filter

The transfer function for the high-pass filter with a gain of 32 is:

$$H(z) = Y(z)/X(z) = \left(1 + 32z^{-16} + z^{-32}\right)/\left(1 + z^{-1}\right). \tag{4}$$

All x terms are divided by 32 to diminish the gain. The final equation is:

$$y[n] = x[n-16] - \left(y[n-1] + \left(x[n] - x[n-32]\right)/32\right). \tag{5}$$

Differentiator

After filtering, the signal is differentiated to provide information on the slope of the QRS complex, using a five-point derivative with the transfer function:

$$H(z) = 0.1\left(2 + z^{-1} - z^{-3} - 2z^{-4}\right). \tag{6}$$

The final equation is given by:

$$y[n] = 0.1\left(2x[n] + x[n-1] - x[n-3] - 2x[n-4]\right). \tag{7}$$

This derivative is nearly linear between 0 and 30. The derivative procedure suppresses the low-frequency components of the P and T-waves and provides a large gain to the high-frequency components arising from the high slopes of the QRS complex.

Squaring function

After differentiation, the signal is squared point-by-point in accordance with the equation:

$$y[n] = \left(x[n]\right)^2. \tag{8}$$

Making the result positive, the squaring operation emphasizes large differences resulting from QRS complexes, while small differences arising from P and T−waves are suppressed. The high-frequency components in the signal related to the QRS complex are further enhanced.

Moving-window integration (MWI)

Moving-window integration extracts more information from signals, thereby facilitating the detection of QRS events. This is accomplished by averaging a certain number of samples per window. To achieve the intended purpose, the size of the window must equal the widest possible QRS complex, and its length must also be carefully selected. In our implementation, window length is 30 for 200 samples per sec. As observed in the previous subsection, the output of a derivative-based operation will exhibit multiple peaks within the duration of a single QRS complex. The used algorithm smoothes the output of preceding operations through a moving-window integration filter as

$$y[n] = \left(x\left[n-(N-1)\right] + x\left[n-(N-2)\right] + ... + x[n]\right)/N, \tag{9}$$

where N =30.

Use of the moving-window integration process allows calculating the following variables: R-peaks, R-R intervals, QRS complex width and heart rate variability. Heart rate is computed by measuring the length of the R-R interval, or a full period of the waveform. These parameters are used to detect abnormal ECG signals, i.e., signals, whose width exceeds the moving-window threshold by over 0.195s and whose R-to-R interval is less than 0.6s and over 1.2s. On detecting an abnormal condition, the sensor node will store a 30-second ECG recording and calculate heart rate, variation in RR-interval and width of QRS complexes. The moving window threshold value is 12% of the R-peak.

To detect abnormalities in ECG data, wireless sensor nodes run detection software, developed using the nesC programming language on TinyOS. In keeping with the memory constraints in a sensor network, the component-based architecture and event-driven execution model of TinyOS enable fine-grained power management, while minimizing code size.

Figure 25 shows the component interface for detection of abnormal ECG data on a sensor node. ECGFilterM includes several filters and functions for detecting abnormal ECG. Raw ECG samples are received from UART and processed by ECGFilterM, which also has a real-time ECG detection function. Several filter and classification functions, known as ’Tasks’ are used to detect abnormal ECG. These tasks are used to perform longer processing operations, such as background data processing, and can be preempted by the hardware event handler. If abnormalities are detected in ECG, the data are transferred over the radio using GenericComm.

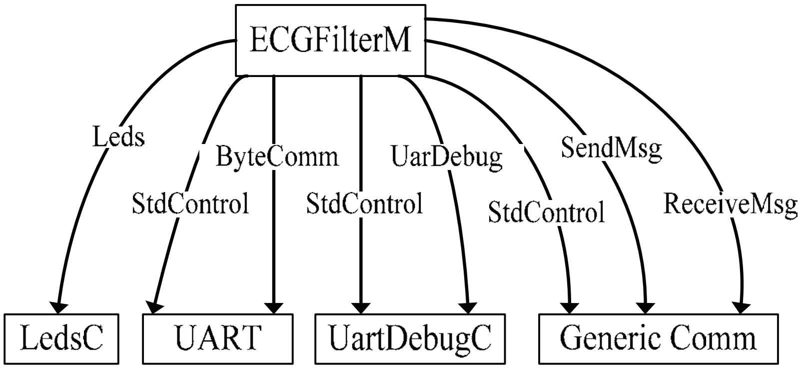

Fig. 25. NesC component interface for an ECG analysis application based on TinyOS (VI, modified by author with permission of IEEE).

Figure 26 shows the QRS detection algorithm on a sensor node. In addition to filtering, this algorithm uses derivative, squaring and moving-window integration methods. On detecting abnormal ECG activities, it transmits the data to the server for further analysis.

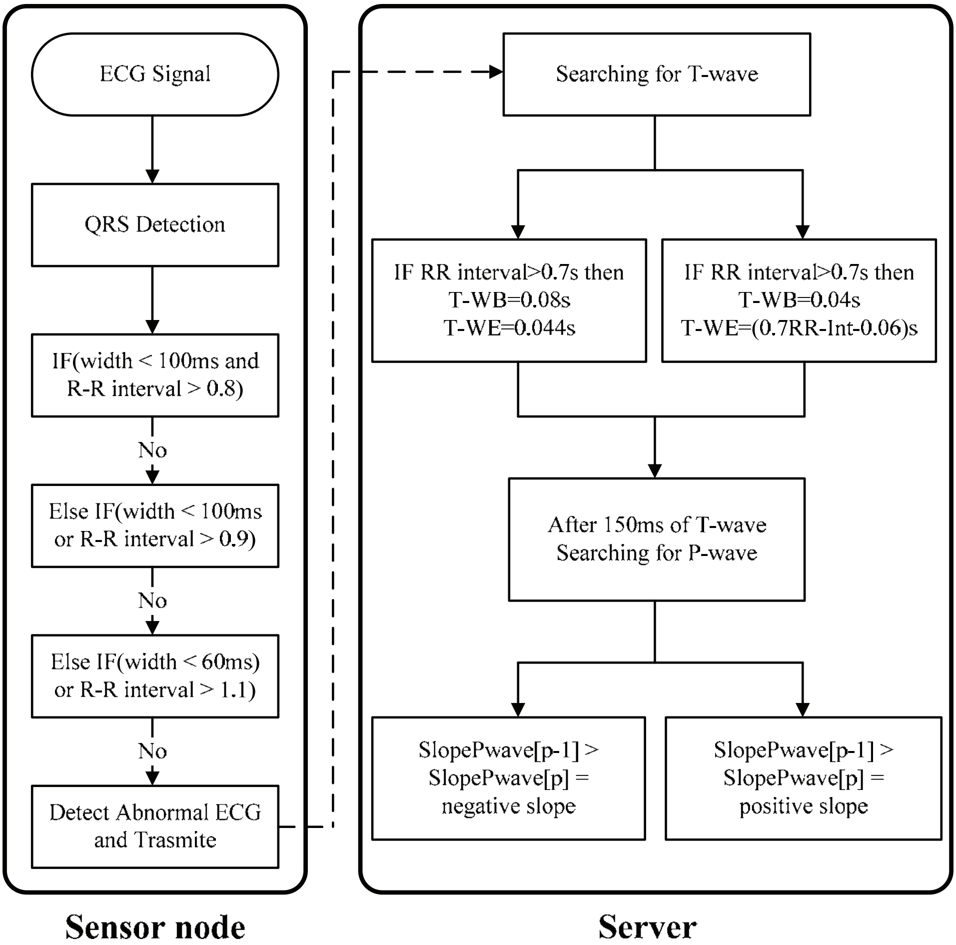

Fig. 26. ECG analysis flowchart on a sensor node and the server (VI, published by permission of IEEE).

Once a QRS complex has been detected by a sensor node, the P-wave and T-wave detection algorithm first searches for the T-wave, as described in 4.1.2 and in the left box of Fig. 26.

After calculating all parameters of the ECG signal, the shape of the signal and the heartbeat rate can be classified. A heart rate greater than 100 bpm indicates sinus tachycardia, whereas a rate less than 60 bpm denotes sinus bradycardia. A heart rate between 60 and 100 bpm represents normal sinus rhythm. Similarly, various types of arrhythmia can be identified on the basis of abnormalities in the QT-interval, PR-interval or heart rate. When abnormal ECG activity is detected, the server transfers the diagnostic results and alarm conditions to the PDA of the attending physician.

4.3.3 Experimental results of ECG analysis on a sensor node

For our experimental set-up, we obtained ECG data from sensors placed on the body and from the MIT-BIH arrhythmia database. Figure 27 shows results from measurements where data pass through the created QRS detection algorithm on a sensor node and the server. Fig. 27(a) displays results for each step of the QRS complex detection process on a sensor node for ECG data from the MIT-BIH arrhythmia database. Similarly, Fig. 27(b) shows the corresponding results for ECG data obtained from the human body.

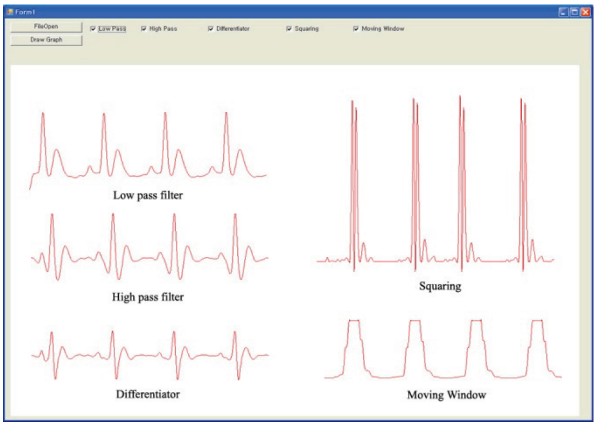

(a)

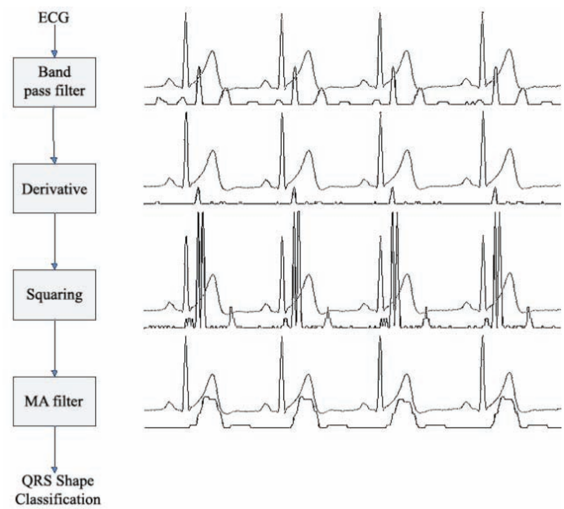

(b)

Fig. 27. Step-by-step results of ECG signal processing; (a) on a sensor node, (b) on the server (VI, published by permission of IEEE).

When abnormal ECG data are detected by a sensor node, it starts sending data packets to the base-station, which takes one minute. Data packet length shows the total data length of the payload of a TOS_Msg. The payload consists of sourceMoteID, lastsampleNum, channel and ECG data, and the value of lastsampleNum in consecutive packets can be used to detect potential packet loss.

The difference in the value of lastsampleNum in consecutive packets is a constant value, which is equal to the number of data readings in a single packet.

Based on data obtained from files 100, 112 and 119 in the MIT-BIH arrhythmia database, Table 6 shows the number of QRS complexes detected by a sensor node. As seen, the node detected 2270, 2537 and 1541 normal QRS complexes and 1, 0 and 444 abnormal QRS complexes in these files. The sensor node is set to send front 300 bytes in buffer memory when it detect abnormal QRS or RR interval, and for continuous 30 sec ECG data is transmitted to server PC in packet form for detail inspection. In total, the sensor node received 32500 data packets from each of the files and sent 1580, 0 and 27750 packets, respectively, to the server. Thus, the difference between packets received and packets sent was 4.9%, 0.0% and 85.4% in each case. In practical situation, abnormal QRS is very few cases, this indicates a huge reduction in data traffic from the sensor node to the server can be obtained.

If a more detailed inspection of the data or signal analysis is required, further analysis is performed on the server. This will only be done, if the sensor node detects abnormalities in the ECG data and forwards the data to the server.

Table 4. Detected QRS complexes on a sensor node.

ECG file name	Normal QRS	Abnormal QRS	Original ECG QRS/Abnormal QRS	Packet (total receiving/sending (for 30 s))	Traffic saving (%)
100	2270	1	2271/1	32500/1580	95.1
112	2537	0	2537/0	32500/0	100.0
119	1541	444	1985/444	32500/27750	14.6

5 Wearable health monitoring system

Recent advances in sensor technology allow continuous, real-time ambulatory monitoring of multiple physiological signals, including ECG, body temperature, respiration rate, blood pressure and acceleration [32–35]. This section presents a wearable wireless node for the ubiquitous monitoring of ECG, activity and SpO_2. Capable of obtaining physiological data from a wearable wireless sensor node, the system then transfers the data wirelessly to a base-station connected to a server PC in an ad-hoc network using IEEE 802.15.4.

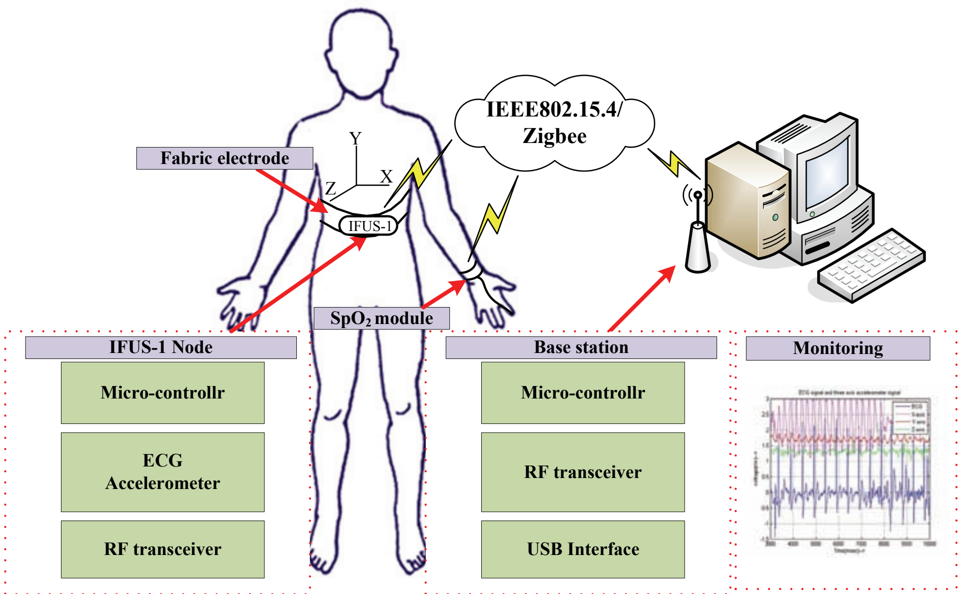

Fig. 28. Architecture of the wearable health monitoring system.

5.1 Wearable sensor node

This chapter describes the developed wearable IFUS (Integrated Fusion Sensor) node containing a conductive fabric electrode (8 cm in width) for ECG measurement and a tri-axial accelerometer sensor (MMA7260Q, Freescale) for measuring acceleration. Figure 29 shows the developed sensor board, which integrates a wireless sensor node, an ECG and accelerometer sensor in an IFUS-1 node (a) and a SpO_2 interface in an IFUS-2 node (b). The wearable IFUS-1 node has a double-layer structure with a wireless sensor node on the top layer and ECG and accelerometer sensor boards on the bottom layer. The IFUS-1 node has one ECG channel with a gain of 300 (24.8db). With a measurement resolution of 12 bits, the sampling frequency of the A/D converter varies between 0.05–123 Hz. Placed firmly on the chest, the bottom layer of the node, containing the accelerometer sensor, is connected to the body by conductive fabric electrodes. Wirelessly connected to the base-station using an IEEE 802.15.4-based radio protocol, the IFUS-1 node measures ECG and accelerometer signals, and transmits them with a sampling rate (fs) of 200 Hz. These ECG signals are later processed using MATLAB 7.4.0 (R2007a). Accelerometer (ACC) signals are used as reference for the adaptive filtering of ECG signals.

Figure 30 shows a wearable shirt with an integrated IFUS-1 node and ECG/accelerometer sensors.

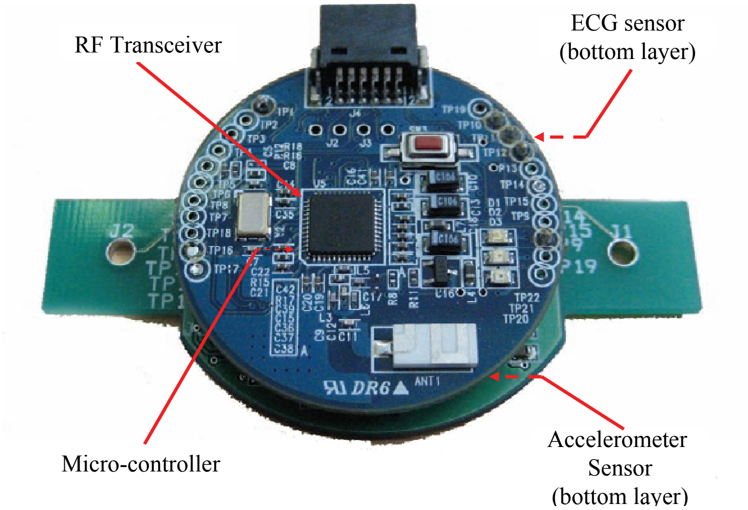

(a)

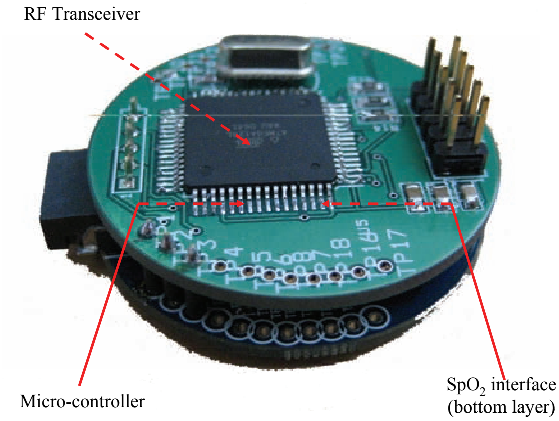

(b)

Fig. 29. Wearable IFUS-1 and IFUS-2 nodes with an ECG and accelerometer sensor (a) a SpO_2 sensor (b).

Fig. 30. Wearable shirt with an integrated IFUS-1 node and ECG/accelerometer sensors.

5.2 Noise cancellation of ECG signals

Cancelling noise present in ECG signals requires different techniques depending on the noise source. Both frequency-domain filtering and adaptive filtering are applicable to the purpose. Here, we choose filters on the basis of suitability for the application, particularly its noise reduction requirement.

5.2.1 Filter selection

Filter selection is governed by a set of principles. Thus, frequency-domain filtering is suitable when the measured signal is statically stationary and noise is a stationary random process that is statically independent of the signal. Power line interference at 60 Hz has these characteristics. To remove this interference, a band-reject filter is used at the cutoff frequency of 60 Hz. Another alternative would be a notch filter, but it may affect adversely the amplitude of the ECG signal.

Adaptive filtering, on the other hand, is a good option when removing motion artifacts and baseline wander noise, because motion artifacts are neither stationary nor necessarily random. Reference input $r(n)$ has little correlation with primary input $x(n)$, because the former comes from the difference between motion-free and motion-added ECG signals, and motion-free ECG sources have little correlation with subject motion. Hence, the adaptive filter proposed in this paper minimizes the error between primary input $x(n)$ and reference input $r(n)$. To improve the signal-to-noise ratio, multi-channels are employed for adaptive filtering.

5.2.2 Filter algorithm

Least mean square algorithm

Due to their computational stability, adaptive filters are usually implemented as finite impulse response (FIR) filters with a finite number of weights m, adjusted by an LMS algorithm [36]. Although its form and implementation is simple, it is capable of delivering high performance during the adaptation process. Controlling the stability and convergence speed of the algorithm, however, requires careful selection of the step-size parameter μ. Weight adjustment of the LMS algorithm is based on the following equation:

$$W(n+1) = W(n) + 2u(n)E(n)X(n)\,, \tag{1}$$

$$Y(n) = W^T(n)R(n)\,, \tag{2}$$

$$E(n) = X(n) - Y(n)\,, \tag{3}$$

where $W(n) \; = \left[w_o(n) \; w_1(n) \; \ldots\ldots w_{M-1}(n) \right]^T$ filter taps at time n. M is the order of adaptive filter, and $R(n)$ is the reference input for adaptive filtering. Primary input for filtering is $X(n) \; = [x(n) \; x(n-1) x(n-2) \; \ldots\ldots\ldots x(n-M+1)]^T$. $Y(n)$ is the output of the FIR filter shown in Fig. 31.

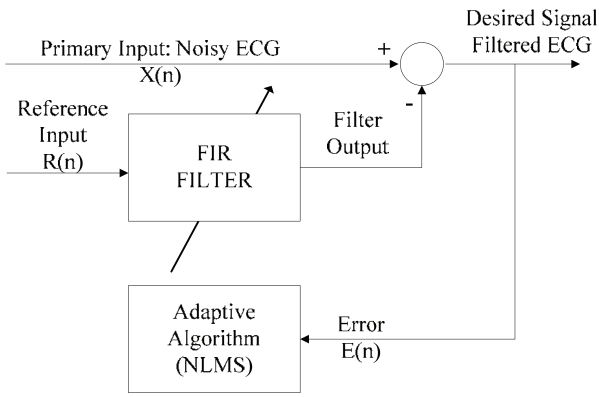

Fig. 31. Adaptive filter structure.

The error signal $e(n)$ is obtained by subtracting the filter output $y(n)$ from the primary input $x(n)$. During signal processing, the filter gradually learns the required correlations between the primary input $r(n)$ and reference signals $r(n)$. It then adjusts the coefficients to cancel these correlations from the output error signal $e(n)$. In cases where the noise is not time varying, the weights converge as the filter learns about the noise. These converged sets of weights can then be used in further processing. With time-varying noise, however, the weights must be updated dynamically and the learning operation becomes continuous.

Normalized least mean square algorithm

In Equation (1), the step-size $\mu(n)$ varies with time. In addition, filter length and signal power influence the stability and convergence of the LMS algorithm. In the normalized least mean square (NLMS) algorithm [37], $\mu(n)$ is defined as

$$u(n) = \frac{1}{2X^T(n)X(n)}, \tag{4}$$

$$W(n+1) = W(n) + E(n)X(n)\frac{u(n)}{\varepsilon + X^T(n)X(n)}. \tag{5}$$

As seen, the NLMS algorithm updates step size and includes the constant ϵ (epsilon). Due to these modifications, this algorithm gives better results than the LMS, thereby improving system performance [38].

Non-adaptive band reject filter

Used to remove frequency bands from ECG signals, the non-adaptive band reject filter is a frequency-domain filter with a cutoff frequency of 60 Hz. Normalized frequency W_o is defined as

$$W_O = 2\pi(\frac{60}{fs}) . \tag{6}$$

And filter gain as

$$G = 1/(2 - 2 * \cos(W_O)) , \tag{7}$$

$$Z1 = \cos(W_O) + j * \sin(W_O) , \tag{8}$$

$$Z2 = \cos(W_O) - j * \sin(W_O) , \tag{9}$$

where *fs* is the system's sampling rate and Z1 and Z2 are the poles of the band reject filter.

5.2.3 Baseline wander reduction

Eliminating baseline wander noise [39] requires removing the 0–0.05 Hz frequency range. Fig. 32 shows a raw (noisy) ECG signal containing baseline wander noise. Adaptive filters to remove baseline wander noise have been described by Nitish V. Thakor and Yi-sheng Zhu [40], for example. We have designed a 4th order adaptive filter with a sampling rate of 200 Hz. Using the NLMS algorithm described above, this filter removes noise by taking a reference signal as the unit step input. Figure 33 shows an ECG signal after the application of the adaptive baseline canceller, which adjusts the step-size dynamically to obtain the desired low-frequency responses.

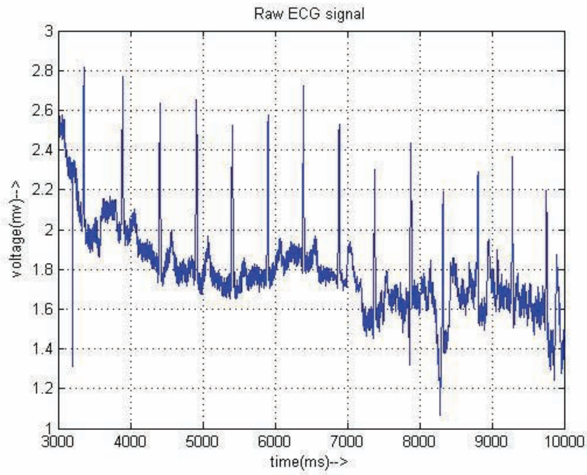

Fig. 32. Raw (noisy) ECG signal with base line wander.

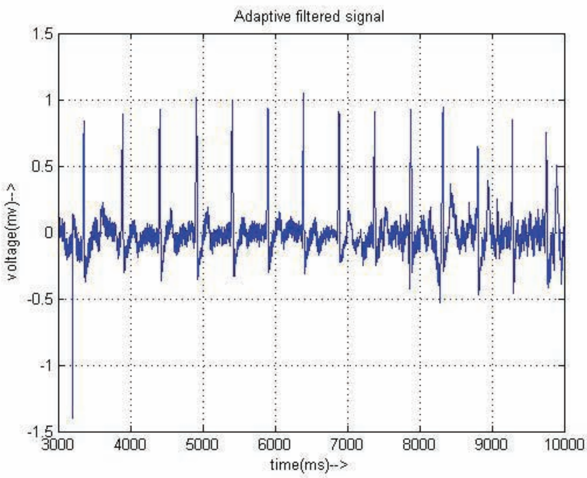

Fig. 33. Filtered ECG without base line wander noise.

5.2.4 Power line interference

Power line interference is typically caused by environmental interference with the ECG device at about 50 Hz or 60 Hz. To remove it, the healthcare monitoring system described here employs a specifically designed band-reject filter. Although it is possible to design an adaptive filter with a 60 Hz sinusoidal reference signal, power line interference is not purely sinusoidal. Figure 34 shows the resultant wave after filtering.

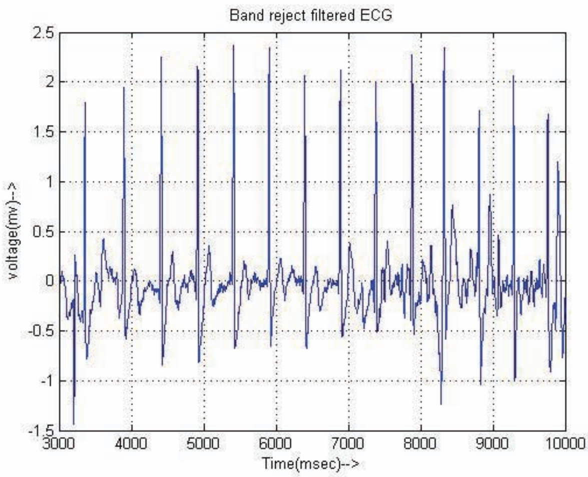

Fig. 34. Band-reject filtered ECG.

5.2.5 Motion artifact

Obtaining a clear ECG signal depends for the large part on the ability to remove noise generated by motion artifacts caused by the patient's movements. Any motion can produce a change in skin potential due to skin stretching or a change in the position of the conductive fabric electrodes.

One approach to reducing motion artifacts involves the use of adaptive filters that extract noise by utilizing a measured reference input which is correlated with the motion artifact. As an adult human has a normal heart rate of 60 bpm, the corresponding R-wave appears at one second intervals. Consequently, when the heart rate changes, the duration between consecutive R-R peaks also changes. However, since the heart rate is influenced by any activity, impulse responses need to be continuously adjusted in accordance with the R-waves. This is not only laborious and inconvenient, but also distorts the shape of the ECG signal.

Adaptive filtering therefore uses accelerometer signals as a reference, because they are correlated to the noise present in noisy ECG signals due to motion artifacts, while being highly uncorrelated with the ECG signals themselves. To this end, we designed a 4th order adaptive filter. In this method, the ECG signal is measured from the chest by a USN sensor node. This signal represents the primary input, while a simultaneously measured accelerometer signal provides a reference for adaptive filtering. Since the accelerometer signal does not vary with time, tap weights converge once the filter becomes aware of the correlation. The converged set of weights can then be used in further processing.

The accelerometer provides reference noise input to the NLMS algorithm. The X, Y, Z axes of the triaxial accelerometer provide three-axis acceleration data of the human body. A triaxial accelerometer is attached on the chest belt of smart shirts. Thus the X-axis here is right-left direction, Y-axis is high-low direction and Z-axis is front-rear direction of the human body. Accelerations generated during movements depend on the type of activity performed, such as resting, walking or running. Fig. 35 presents a three-axis accelerometer signal together with an ECG signal containing motion artifact noise. Normally the Y-axis data of accelerometer is most sensitive when the person is run or walk because high-low movement is biggest than then other two directions during running and walking. As seen in Fig. 35, Y-axis acceleration data is most sensitive to the motion artifact noise contained in the ECG signal, even though X-axis acceleration data varies much more widely in our experiment on treadmill. For this reason, we decided to use the Y-axis acceleration signal as reference input $R(n)$ in adaptive filtering, as shown in Fig. 31. The filtered ECG signal is shown in Fig. 36.

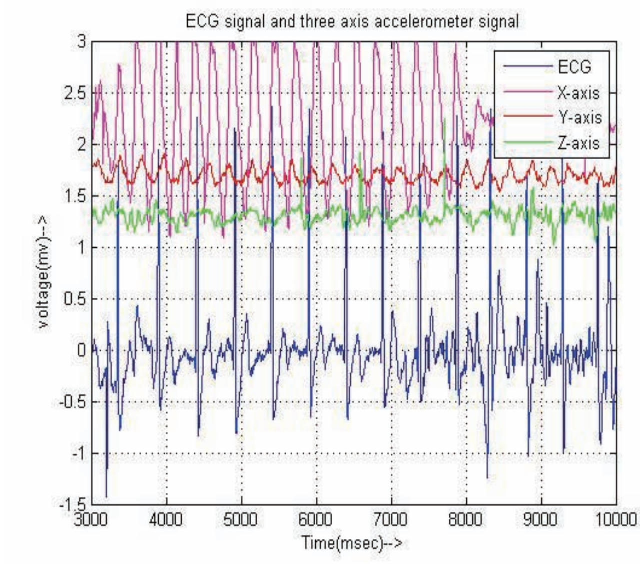

Fig. 35. ECG signal with motion artifacts and three-axis accelerometer signal.

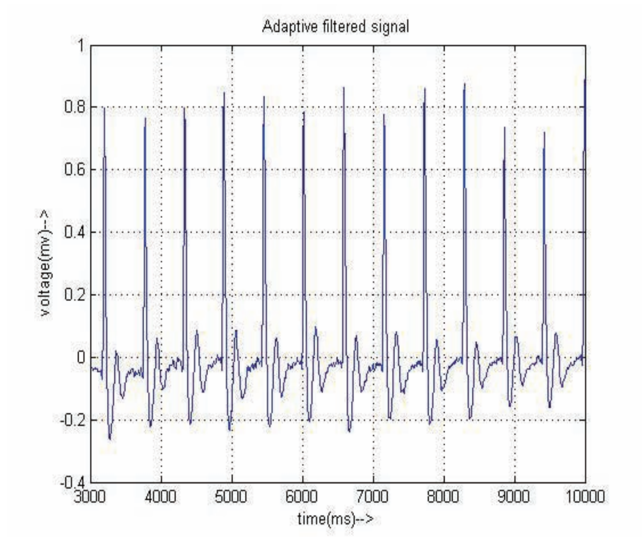

Fig. 36. Filtered ECG signal.

5.3 Wrist type SpO_2 monitoring system

Wireless sensor networks are an essential enabling technology for unobtrusive medical monitoring. Continuous and non-intrusive monitoring of major functions by various sensors measuring ECG, oxygen saturation, temperature and acceleration is critical for the future development of pervasive healthcare systems based on IEEE 802.15.4 Zigbee compatible communication.

The idea of this SpO_2 monitoring system is to place unobtrusive sensors on a person's body to form a wireless network that provides interoperability layers which enable portable sensors to access body signals and route these signals to a monitoring PC. This section describes the architecture of the SpO_2 monitoring system, which comprises measurements, communications and a monitoring system. In addition, the section provides a brief introduction to the hardware devices used in the system and explains the functionality of the applied communication methods in detail.

5.3.1 Portable SpO_2 sensor module

Due to technological advances, medical devices now include tiny wearable sensors worn on the wrist or chest. These tiny sensors and wearable devices are capable of measuring parameters such as ECG, SpO_2, body temperature and blood pressure. Placed on the body, the sensors collect physiological signals and transfer them to a base-station. When portable sensors are installed within a wireless sensor network area, body signals can be monitored even as the person moves about.

The healthcare monitoring system described in this dissertation utilizes a portable sensor to measure SpO_2 values. Built using a Nonin OEM (original equipment manufacturing) pulse oximeter module (Nonin Inc., USA), the sensor measures 53 mm × 20 mm × 15 mm. Its optical components include a red LED, an infrared LED and a photodiode for light transmittance measurement. SpO_2 values can be obtained by calculating the ratio of the two lights, depending on the absorption of light. 5-byte photoplethysmographic (PPG) data sampled at 75 Hz and SpO_2 values are acquired at one second intervals.

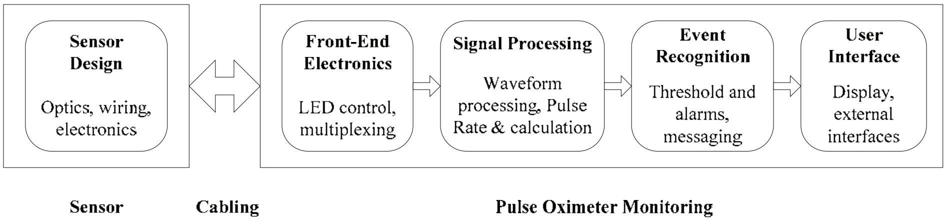

Fig. 37. Procedures in SpO_2 value monitoring.

SpO_2 values are obtained by the portable sensor device in accordance with the process illustrated in Fig. 37. As seen, this module contains three parts: sensor, cabling and pulse oximeter monitoring. The sensor part includes a probe with two LEDs as light sources and a photodiode for photon detection on the wrist. Cabling connects the probe to the SpO_2 module and sends signals received from the body to the device. The module's main processing component is the pulse oximeter monitor. It includes signal processing, LED control, calculation and display. Thus, almost all functionality required to obtain SpO_2 values is managed in this part. To enable communication, the sensor is designed to be attached to an IFUS-1 node.

Figure 38 shows the developed OEM pulse oximeter module connected to a wireless sensor node. Both the sensor module and the probe are designed to be placed on the wrist. To ensure high signal precision, one of the high-gain ADC channels on the IFUS-2 node is used for SpO_2.

Fig. 39 presents the portable SpO_2 sensing system, which is designed to be compatible with homecare systems and comfortable to wear. Its main function is to collect body signals wirelessly from the sensor and then forward the data to the base-station via a wireless sensor network.

Fig. 38. The OEM pulse oximeter module and an IFUS-2 sensor node.

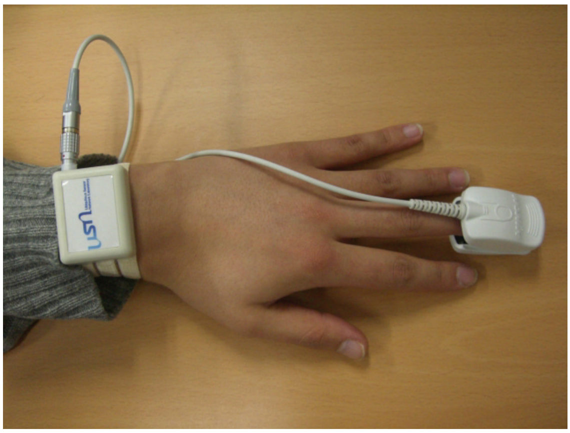

Fig. 39. Portable SpO_2 sensing system.

5.3.2 Communications

In essence, the communications part is a network system dedicated to the efficient transmission of body signals to the server. It acts as an intermediary between the portable sensor and the monitoring system. Drawing on the results of a preliminary performance evaluation test on the sensor, this system is designed for efficient patient monitoring. All data from the portable sensor are transmitted to the base-station, which is connected to the server via a WSN. Ambient sensors, a typical component of stationary WSNs, are integrated into the environment and connected to the server. All measured data can be formed into packets for transmission and sent to the server with a low packet collision rate and low power operation. Shown in Fig. 40, this module performs 1 second 5-byte data acquisition of photoplethysmographic (PPG) data sampled at 75 Hz and SpO_2 values. In addition, we have developed a monitoring program, consisting of a server program and a database for storage purposes.

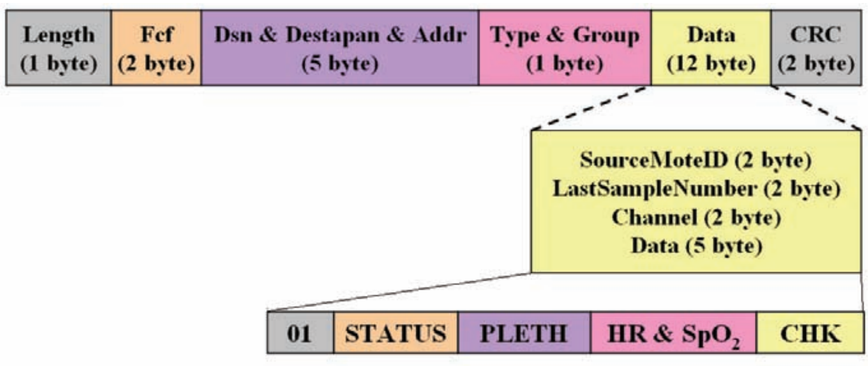

Fig. 40. Packet of SpO_2 value.

5.3.3 SpO_2 monitoring

To manage patient information effectively, a home-care management program had to be developed to enable patients/users and doctors to monitor/modify/update relevant personal details and health information. This monitoring system provides a user-friendly interface for the remote monitoring of SpO_2 parameters, also outside the WSN area. It comprises a real-time system capable of capturing parameter data either continuously or regularly from portable sensors. A local SpO_2 value feature notifies the treating physician of any abnormalities by sending signals from the affected person to an ambient node. In addition, the system allows users to access the hospital center. For evaluation purposes, experiments are performed to ascertain that the portable sensor functions properly and transmits SpO_2, heart rate and photoplethysmographic(PPG) data to the server.

Figure 41 presents a screen capture of the SpO_2 monitoring program. Designed with LabVIEW, it monitors the SpO_2 wave signal by drawing the pulse waveform on the server PC connected to the base-station as soon as it receives the SpO_2 value (%) from the portable sensor.

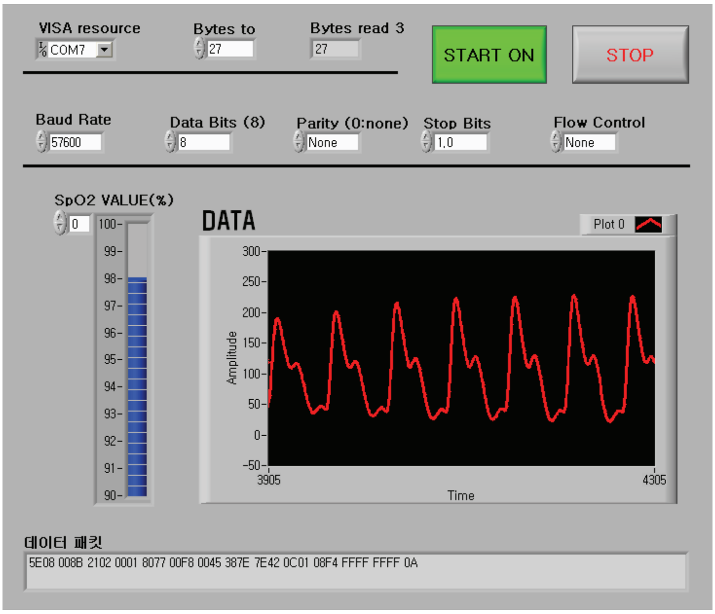

Fig. 41. Monitoring system on the server.

This system acts as a continuous event recorder, which can be used to follow up patients at home, as they live a normal life. Although the SpO_2 value is calculated by the module, measured data are saved on the server. It can reach a correct diagnosis even under situations where the patient is unconscious and in daily activities. To enhance the informative content of the recorded data, this type of real-time measurement of SpO_2 values needs to be combined with action or activity monitoring data.

Having received SpO_2 wave data, the server modifies them using such MATLAB functions as filtering, amplification and compensation. Figure 42 shows a SpO_2 wave complemented with other parameters.

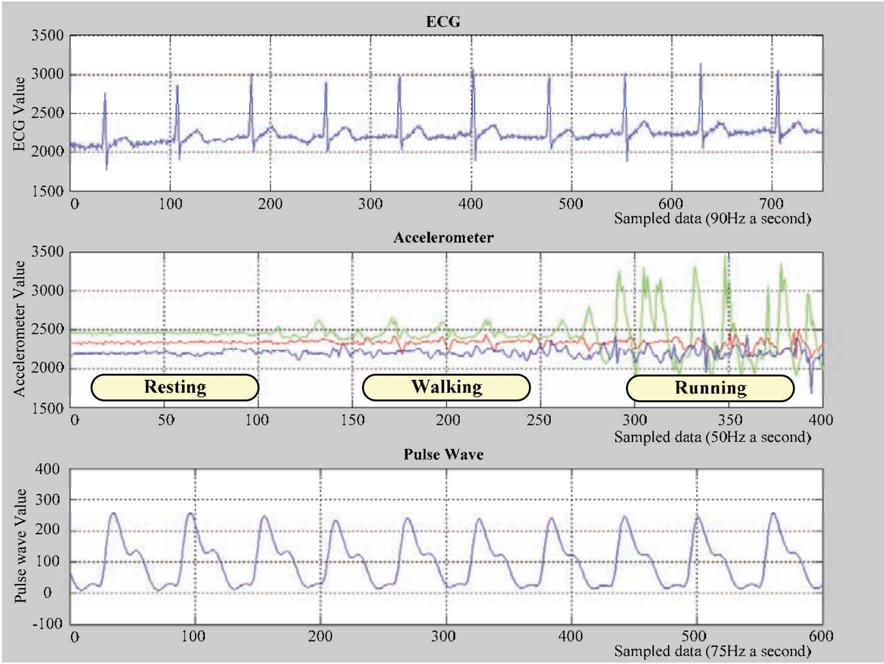

Fig. 42. GUI showing integrated waveforms of ECG, acceleration and SpO_2 signals.

5.4 Experimental results from a treadmill test

ECG and accelerometer signals were continuously monitored and recorded as a test person spent 10 minutes on a treadmill. Figure 43 shows the treadmill exercise in a fitness center, with the test person donning a wearable IFUS-2 node for the simultaneous monitoring of ECG and accelerometer signals. Figures 44 and 45 show the test results for walking and running, while Figure 46 depicts resting data recorded after the exercise. Figure 47 illustrates the results of a standing and sitting test in which the subject changed his position every 10 seconds for a total of 3 minutes. In addition, a squatting and standing test, with the results shown in Fig. 48, was also carried out, in which the subject changed his position every 5 seconds during a 3 minute period, in much the same way as in the standing and sitting test.

Fig. 43. Test of the u-healthcare system during exercise on a treadmill.

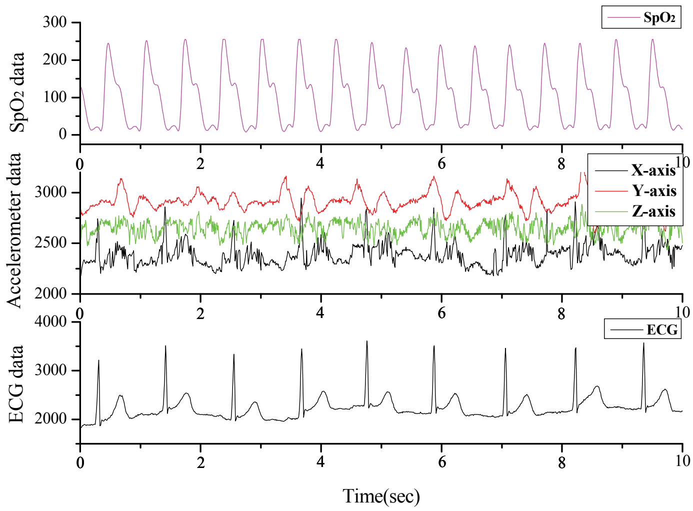

Fig. 44. Walking data on a treadmill.

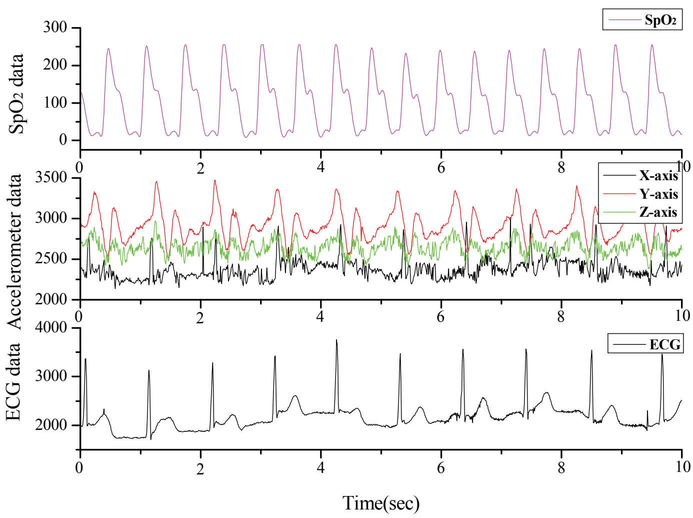

Fig. 45. Running data on a treadmill.

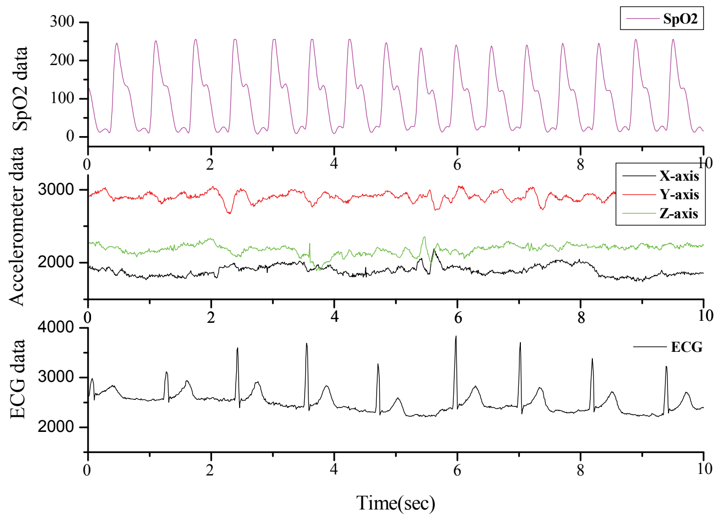

Fig. 46. Resting data.

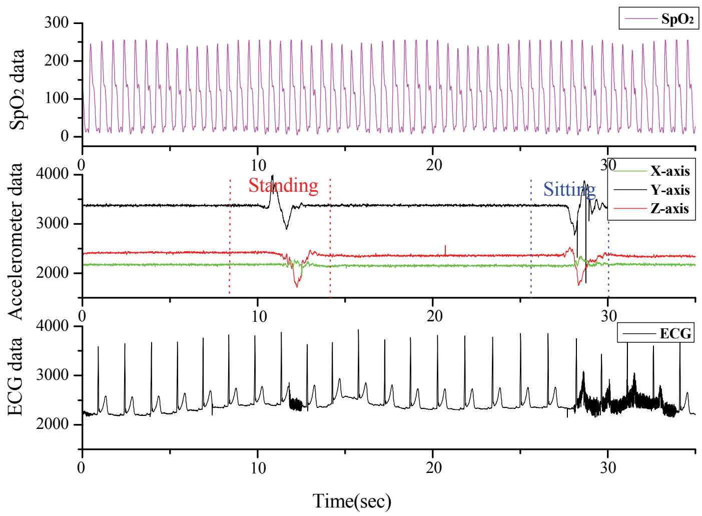

Fig. 47. Standing and sitting data.

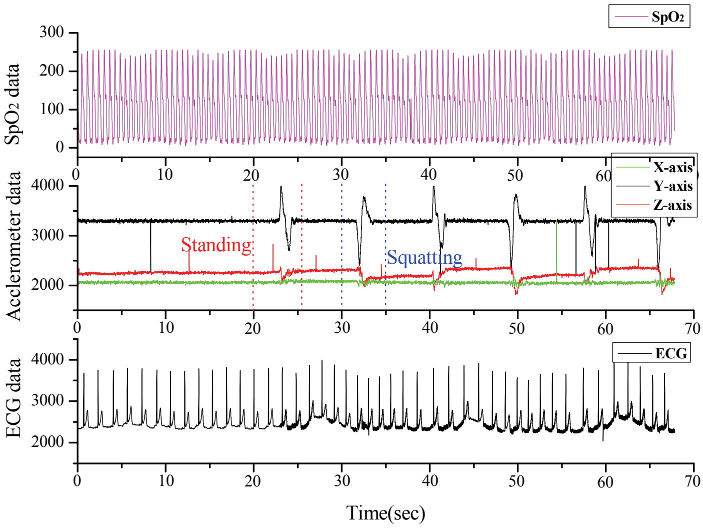

Fig. 48. Squatting and standing data.

6 Indoor location tracking

This section deals with an indoor location system based on wireless sensor network technology. The system aims at helping to evaluate the health status and monitor the activities of elderly persons or chronic patients in the home environment [32, 41, 42]. A location-aware application provides information about the daily activities of elderly persons at home or hospital to caregivers. To locate an object, active, ceiling-mounted reference beacons are placed throughout a building. By periodically publishing location information using RF and ultrasonic signals, these beacons allow a location-aware application running on mobile or static nodes to determine its physical location. Once a passive listener carried by the person being tracked receives the information, it infers its location from the set of reference beacons it hears. This information from sensor nodes is then forwarded to a base-station, where further computation is performed to determine the current position of the listener and several applications are enabled for context awareness.

6.1 System architecture for indoor location tracking

In a wireless sensor network, although the sensors or motes are computationally capable of doing some local data processing and exchange information with their neighbours, aggregating data to more resourceful nodes or base-stations remains a more feasible means of processing the collected data.

Our system comprises a number of nodes that are deployed on the ceiling throughout a building and send location information using RF and ultrasonic signals. This architecture is used to determine the user's position and to provide spatial information at the base-station. To implement the sensor network, the sensor nodes are arranged in the configuration illustrated in Fig. 49. This indoor tracking system uses sensor nodes with an ultrasonic sensor and an MCS410CA (Crossbow Technology Inc., USA) receiver. These sensor nodes are able to process the data, send RF and ultrasonic signals after a predetermined time interval and can be easily configured. Devices installed on the ceiling are known as beacons, while those carried by the user are referred to as listeners. Despite their different names, these nodes are identical in all aspects but the embedded program structure. Beacons work as reference devices and send their location in packets to the listeners, which then forward these signals towards the base-station. At the base station, the location of the target is calculated by a tracking algorithm and context-aware applications are can be activated to use this information. As the users only need to carry a sensor node, very little extra weight is put on them. Perhaps, even the cost of the system is also reduced. Moreover, no external infrastructure is necessary at the base-station to track the user's position, shown on its GUI. All position and context-aware information is distributed from the base-station to various applications via the internet, allowing doctors and other caregivers to access this information through handheld devices.

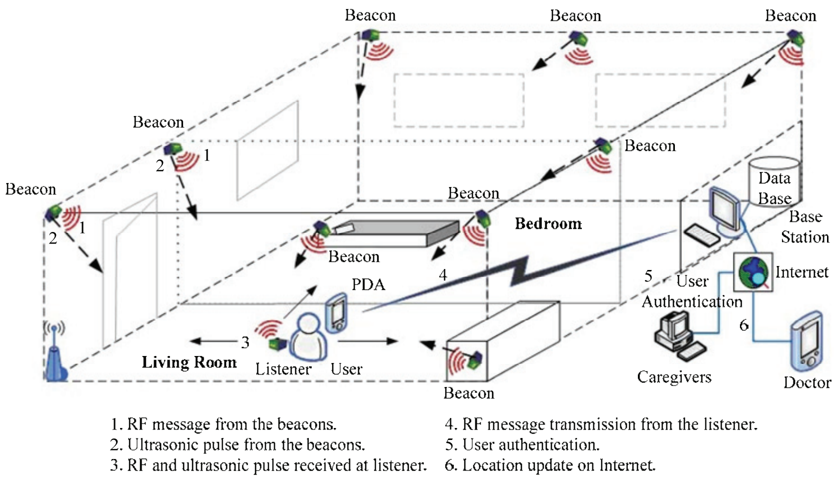

Fig. 49. System architecture of the developed indoor tracking system.

In this system, a combination of RF and ultrasonic hardware is used to enable a listener to determine its distance to beacons, of which the nearest can be identified. Measuring the one-way propagation time of ultrasonic signals emitted by a beacon involves taking advantage of the fact that the speed of light (=3 × 10^8 m/sec) is greater than that of ultrasonic signals (speed of sound) in air. In each transmission, the beacon sends information about the space over RF concurrently with an ultrasonic pulse. When the listener hears the RF signal, it uses the first few bits as training information and turns on its ultrasonic receiver. It then listens for the ultrasonic pulse, which usually arrives a short time later, because it travels at a slower speed than the RF signal. The listener uses the time difference of arrival (TDOA) [43] between the receipt of the first bit of RF information and the ultrasonic signal to determine the distance to the beacon. The distance between a listener and the beacons can be determined by multiplying the speed of sound with the TDOA. Because the speed of the sound varies with temperature, the effect of temperature is also considered in distance determination. The location of the static listener is determined by a triangulation algorithm as follows. Consider a listener located at (*x, y, z*) in the beacon coordinate system and assume that the listener can measure the distance to n beacons $b_1, b_2 \ldots b_n$. Let d_i be the measured distance between b_i and the listener. Beacon b_i has the coordinates (x_i, y_i, z_i). The true distance between the listener and b_i is given by $d_i - €_i$, where $€_i$ is the measurement error. If $n = 3$ and the distance measurement errors are not too large, a reasonable estimate of the listener's position can be obtained by solving three simultaneous equations:

$$d_i^2 = (x_0 - x_i)^2 + (y_0 - y_i)^2 + (z_0 - z_i)^2 \qquad for \quad i = 1, 2, 3 .$$

Two possible solutions are calculated for these three equations. In the first one, the listener is located above the plane containing the three beacons, and in the other, the listener is placed below this plane. Because the beacons are deployed on the ceiling, we can assume that the listener is always located below the plane containing the beacons. When $n \geq 4$, the following non-linear optimization is used to compute the listener's coordinates. We assign some initial coordinates (x_0, y_0, z_0) to the listener. For each beacon b_i, residual $e(i)$ is defined as follows

$$e(i) = \sqrt{((x_0 - x_i)^2 + (y_0 - y_i)^2 + (z_0 - z_i)^2) - d_i} \ .$$

The sum squared error E_{ss} is defined as

$$E_{ss} = \sum_{n}^{i=1} e(i)^2 \ .$$

The optimization problem is to find the listener coordinates (x_0, y_0, z_0) that minimize E_{ss}. As the number of beacons giving location information to the listener increases, the accuracy of localization becomes higher. When the listener is mobile, distances to multiple beacons are received at different instances of time, with the listener in different positions. However, it is still possible to compute a representative position for the listener on the basis of these distance samples. Moreover, the same technique can be used for mobile users, the only difference being that the error now has two components: measurement error and error caused by the listener being at different positions when the different distance samples are obtained. However, these errors can be reduced by using the Kalman filter approach [44], which also considers the effect of temperature on the velocity of sound.

6.2 Software design

Software for the u-healthcare system can be divided into two parts: sensor node software and server application software. Both parts will be discussed in the following presentation.

6.2.1 Sensor node software design

Sensor nodes were programmed using nesC (network embedded C) on the TinyOS platform. Fig. 50 presents component graphs for two application programs. The first one, running on the beacons and the listeners, is shown in Fig. 50(a), which illustrates the connections between different program components. A modification of the cricket code from MIT [45], it contains several additional components to forward the beacon message from the listener towards the base-station. Through the addition of these components, each sensor node is capable of receiving and forwarding beacon signals. Using only sensor nodes without any external network infrastructure leads to a significant reduction in system costs.

Various components are added to this application. Of these, ‘BeacManage’ is used for beacon transmission, ‘UltrasoundM‘ is responsible for ultrasonic signals and ‘RadioCRCPacket’ is responsible for sending data through the ‘BareSendMsg’ interface. Further, the ‘ForwardM’ component is used to forward beacon messages towards the base-station using the ‘GenericComm’ component via the ‘SendMsg’ interface. However, the speed of ultrasonic signals plays an important role in distance calculation, because the speed of sound is affected by temperature variations. To remove the effect of temperature, we have added a component called ‘OnBoardTemp’, which is used to read the temperature from an onboard temperature sensor and provide the reading to the distance calculation algorithm. Components in the second application are used to receive messages from the RF channel and transfer them through UART. The UART interface is used to accept signals from sensor nodes and transfer them towards the server, while the Led interface is used to glow the led on the sensor nodes for interactive and debugging features. As shown in Fig. 50(b), the ‘GenericComm’ component is used for receiving messages through the ‘ReceiveMsg’ interface, and the ‘SerialM’ component sends messages from the main component to ‘HPLUARTC’ using the ‘HPLUART’ interface, and so on.

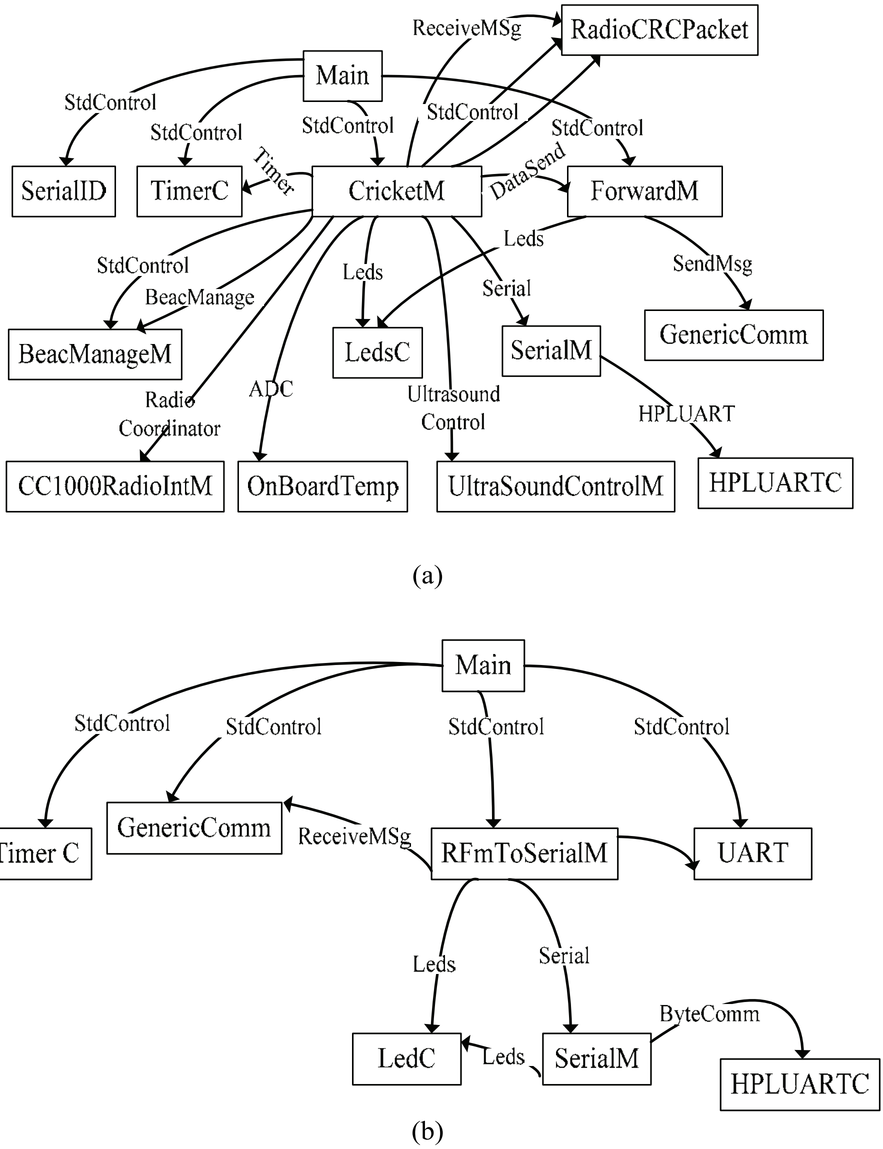

Fig. 50. Component graph for beacon and listener software (a) and base-station software (b).

6.2.2 Software architecture for the base-station

Application programs on the server are implemented using Java 1.6 API. As shown in Fig. 51, the software is divided into several components. The server application receives RF signals from the listener via the RS232 port and, based on the previously described technique, calculates the position of the user. RF signals contain a variety of information in packet form, including the space ID of the beacon, distance from the listener and atmospheric temperature. These fields are separated from the packets by the server, which then uses the tracking algorithm to calculate the position and closest space ID of the listener. This position information is then provided to the server's broker component, whose function is to accept third party connections and provide them with location information. Using TCP/IP sockets, it has the capacity to handle several connections at the same time.

Providing location information to third parties entails the possibility that this information might be accessed by unauthorized persons and misused, thereby violating the privacy of the user. To ensure privacy, our system uses the Geopriv approach [46], which requires authentication before giving out information. Once a connection is established, the user has to authenticate himself by providing a user name and a password. If the user is not authorized to access this information, he will not be connected to the server program. As shown by Fig. 50, a number of applications are connected through TCP/IP sockets. These applications will be described in the next section.

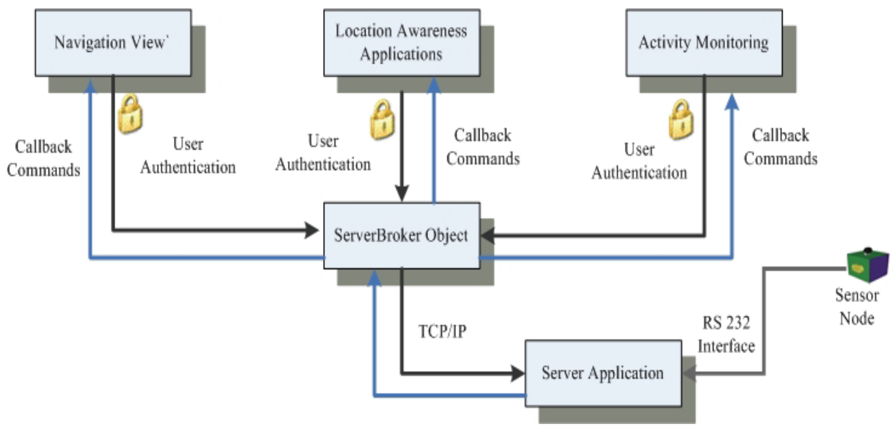

Fig. 51. Authentication software architecture for the base-station (VIII, published by permission of IEEE).

6.3 Experimental deployment

For an experimental evaluation of the developed system, its location determination capability was tested by deploying beacons on the ceiling and measuring the obtained coordinate and space information at the base-station. Testing was carried out by installing beacons in a home in two different arrangements. In the first one, illustrated by Fig. 52, one sensor was placed in each room, while in the second arrangement, sensors were only installed in two rooms. In the first arrangement, the activities of the test person were determined by three variables: the room visited, frequency of visits per room and time spent in each room. In the second arrangement, on the other hand, the main parameters under observation were the path travelled by the person and the measurement accuracy of the tracking system.

The beacons were assigned coordinates in accordance with a reference coordinate system. Once the reference coordinates were assigned to the beacons, the location information obtained from the system was compared to real coordinate values. For user convenience, all spaces were also given an individual ID, so that the location of the test person could be understood simply by reference to the closest space ID. As the user moved around this test environment, spatial information and 2D coordinates were calculated at the base-station on the basis of beacon signals and displayed on the GUI. The accuracy of the location in the form of user space is dependent on many variable parameters such as the deployed topology of the beacons that are attached to the ceiling of a building, and the interference avoidance and detection algorithms. Achieving a position estimation accuracy between 7~15 cm, the developed system is very efficient compared to other approaches such as radar, active bat and active Badge, whose tracking accuracy is several meters [47]. In addition, this accuracy can be further improved by placing the beacons closer to each other on the ceiling. One lesson to be drawn from these experiments is the need to accurately describe the quality of the sensed information. For example, granularity and freshness of location information are quality attributes. Providing this information to relevant applications, and possibly to the user, allows people to understand the limits of this technology, and use it with care.

6.4 Application to ubiquitous healthcare

Location-awareness can be used to trigger specific information to users, permitting more informed decision-making. Applying this concept to ubiquitous healthcare offers a potentially promising approach to extending its quality and reach. This tracking system, for example, enables several applications to provide a useful service. One of these applications is activity monitoring, which provides information about the state or action of an active target. Several other potential application scenarios are also being discussed.

6.4.1 Activity monitoring

Activity is a term used to describe the state, quality and action of an active object, such as elderly person at home or patients in a hospital. Their physical state and the activities they perform [48] have a close relationship with their health and wellness. By utilizing location awareness, we can easily monitor the state and actions of persons in their daily life. This type of information includes frequency of visits to each room, time spent in a particular room and the latest motion events. Sensors deployed in a space will be able to sense the activities of its occupants and learn about their routines. Several applications have been tested, but in this experiment, the emphasis was on recording the frequency of visits to each room, time spent in each room and the distance travelled during the observation time. One application which has been developed stores the motion history of the person in terms of space and time.

As shown in Table 5, the activities of a test subject were observed from afternoon to evening by sensor nodes placed in every room. The time spent by the person in each room is also shown, and the duration of the time spent in each room is added to the previous value to establish the total time spent in that room or space in a day or week. An activity is defined as normal, when the user visits the relevant room or space as part of a daily routine. However, if the user spends a lot of time in any room, say, the toilet, then the activity is labelled abnormal. Privacy is of course a serious issue when applications, and those who have access to them, such as colleagues, start tracking people's locations. As a method of securing privacy, this application requires all users to authenticate themselves, and only shows the desired information, if the authentication process concludes with success. Space information is only used to increase the granularity of the deployment of the sensor nodes. Location information is updated as soon as the user moves to a different room, which allows calculating the duration of time the user spends in each particular room.

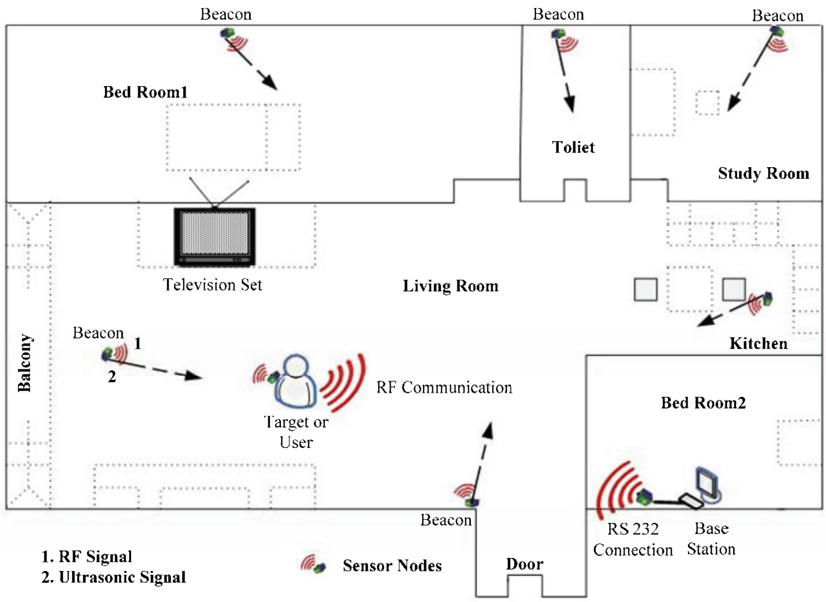

Fig. 52. Deployment of sensor nodes for activity monitoring in a traditional home environment.

Table 5. Activity monitoring of the user from afternoon to evening in traditional home environment.

Room Visited	Start time	End time	Total time spent	Activity
Living Room	11:37 P.M.	11:45 P.M.	8 minutes	Normal
Toilet	11:46 P.M.	11:49 P.M.	3 minutes	Normal
Kitchen	11:50 P.M.	12:06 P.M.	16 minutes	Normal
Bed Room	12:07 P.M.	13:00 P.M.	53 minutes	Normal
Living Room	13:03 P.M.	13:30 P.M.	27 minutes	Normal
Bed Room	13:31 P.M.	14:40 P.M.	59 minutes	Normal
Toilet	14:41 P.M.	14:55 P.M.	14 minutes	Normal
Study Room	14:56 P.M.	16:20 P.M.	84 minutes	Normal

6.4.2 Estimation of moving path

By processing the data obtained from the listener, we can track the movements of the user over short (minutes or seconds) or long time periods (hours and days). Each type of moving path provides important cues for understanding what is going on. Recognition of short-time activities can be used to determine the current status of the user, while long-term activities can be regarded as routines, from which deviations can be measured.

To determine measurement accuracy and track the moving path of the user, sensor nodes were placed as shown in Figs. 53 and. 54. Since the previous experiments indicated that the user spent most of his time in the living room and the bedroom, sensor nodes were deployed there. Fig. 53 shows a comparison between the observed and the actual path travelled by the user. As seen, the obtained accuracy was between 7 to 15 cm. In the second scenario, the main focus was to visualize the user's travel path, using the same sensor arrangement as before. These movement paths are plotted on the graph shown in Fig. 53. The path travelled shows the movement of the person inside the experimental test bed. Fig. 55, on the other hand, displays the distances travelled per hour and enables us to estimate the activity of the person at the time of observation. This type of activity information can be very useful for remote monitoring. For better visualization and understanding, we have tried to plot the experimental test bed on the plot by measuring its length and width. Measurement accuracy and the path observed are mapped on this plot, as shown in the figures. These results provide information for the experimental evaluation of this system and for the various application scenarios that can be developed using the system.

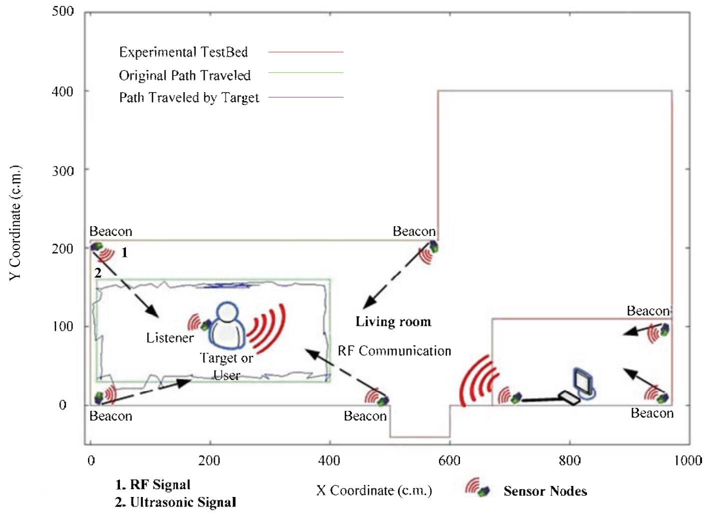

Fig. 53. Deployment of sensor nodes for accuracy measurement in traditional home environment.

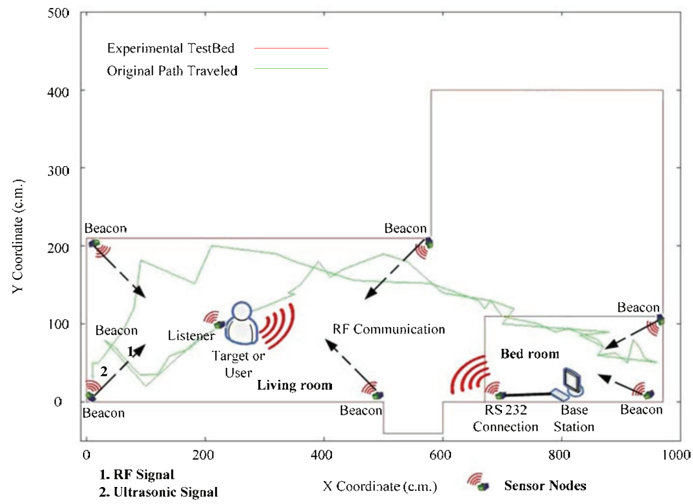

Fig. 54. Deployment of sensor nodes for evaluation of moving paths in traditional home environment.

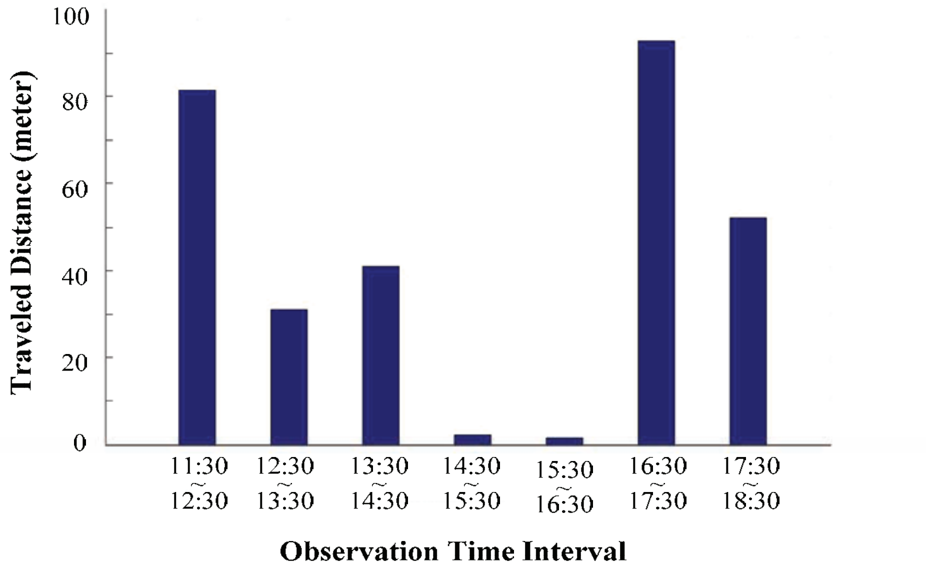

Fig. 55. Activity monitoring based on distance information.

6.5 Location-aware visualization of VRML models

6.5.1 Location-aware visualization

In most navigation systems, the current location of the user is indicated and marked on a map. To provide such a service, the adopted solution usually employs some form of graphical representation that is familiar to the user, such as a flat 2D map. This rather conservative form of presenting spatial information requires that the user has some experience in interpreting the information. It contrasts with the use of 3D representation of indoor environments, which is a more intuitive and effective way of presenting spatial information, even though previous 3D models are very difficult to find.

Construction of a 3D indoor environment can be divided into three distinct stages. The first stage involves acquiring data of the building and indoor environment to be constructed. In terms of efficiency, 3D world generation is greatly dependent on the data required by the next stage, and the use of detailed constructions will definitely complicate the task, as more data is required. Also the locations of objects within the environment must be determined at this stage. All in all, the manual input required to produce the desirable data relies on the level of detail required by the 3D world.

To construct an indoor environment from the data gathered at the second stage, floors as well as other objects inside a building must be modelled and placed in the 3D world. Careful consideration must be given to the amount of details, since this factor not only affects the complexity of the construction process, but greatly complicates the process of obtaining the data required.

The final part is to export data in a format that can be rendered and then render the data. Every object inside every building must be placed in an accurate position, which requires additional input data. This is because each building and object requires its own parameters to describe the movement to the correct position in the world. As a result, the amount of input data increases and further complicates the process.

6.5.2 3D modelling by VRML

Virtual reality is an emerging technology that promises significant advances in the area of user interfaces applicable to various application domains. It is a powerful means to increase the cognitive effectiveness of virtual indoor environments, virtual buildings or virtual campuses for naive end-users. The recent expansion of such technology has been made possible by the introduction of VRML.

In our implementation, the building of our laboratory, that is, the U-IT building of Dongseo University comprises the modelled environment. CAD data shown in Fig. 56(a) only provided a layout of the basement of the building, while other dimensions, especially the walls and objects inside the rooms, had to be measured manually. VRML-constructed rooms of the building are presented in Figs. 56(b)–(d).

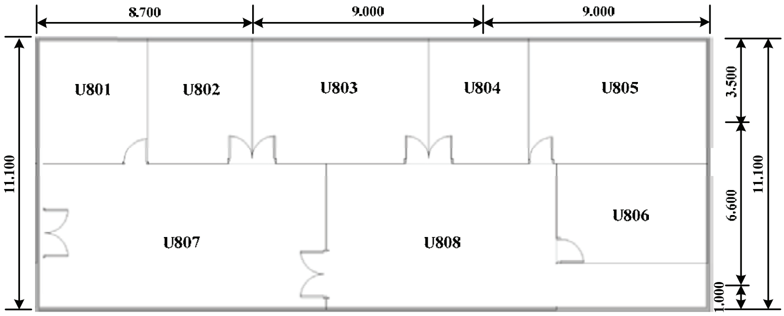
8.700
9.000
9.000
U801
U802
U803
U804
U805
U806
U807
U808
11.100
3.500
6.600
11.100
1.000

(a)

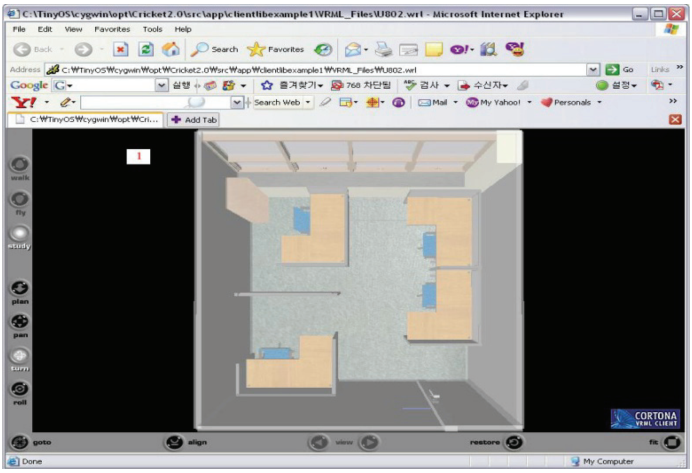

(b)

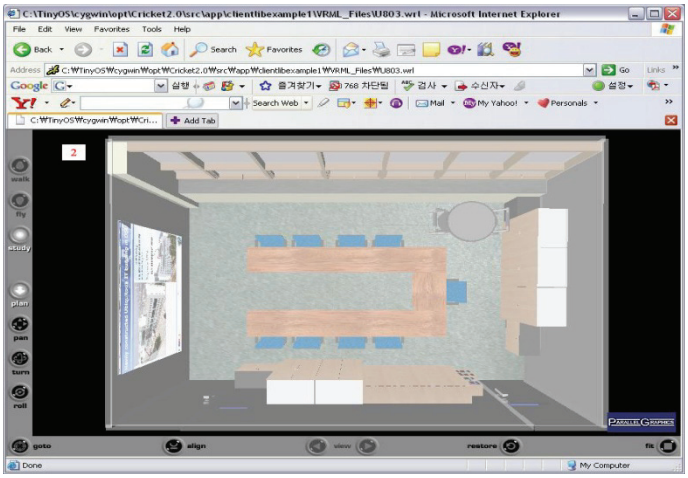

(c)

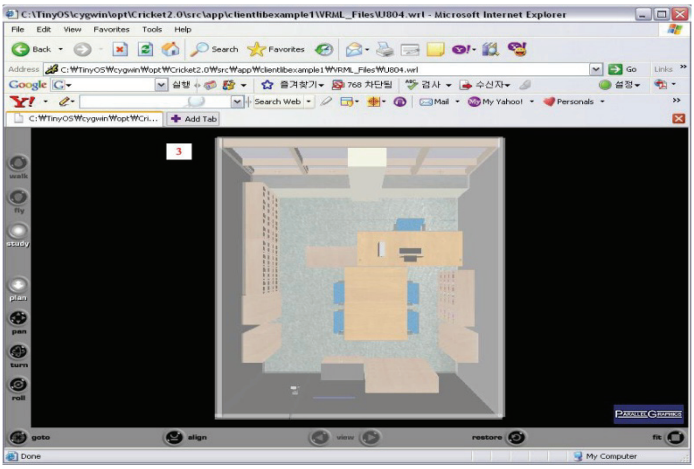

(d)

Fig. 56. 3D indoor environment modelling; (a) CAD floor map of the modelled building, 8th floor of the U-IT building of Dongseo University, (b)-(d) Constructed indoor environment for each room.

Figure 57 highlights the quality of the constructed 3D indoor environment, verifying the realism of the world and that the features of the environment are accurately modelled. To convey the naturalness of the real world, image texture was used to improve the realistic appearance of the environment. Although it was drawn manually, we believe that, in the near future, the modelling process will be automated.

(a)

(b)

Fig. 57. Realistic VRML-constructed indoor environment and the corresponding physical environment; (a) Actual room U808, (b) Virtual room, constructed using VRML.

6.5.3 VRML plug-ins / viewers / browsers

VRML files can be viewed using a variety of plug-ins freely available on the market [49], such as Cortona VRML Client, SGI CosmoPlayer, WorldView, etc. Aside from the nature of plug-ins, there are several other inconsistencies over platforms – the quality of Java Virtual Machine (JVM) as well as the feature sets of each browser. Our implementation was done using Internet Explorer 6.0 with the Cortona VRML Client plug-in [50] on Microsoft Windows XP Professional, Version 2002. Use of Microsoft Virtual Machine (MVM) instead of JVM or Java applets is not feasible.

6.5.4 3D object manipulation via external authoring interface (EAI)

VRML ushered in a new era in computer graphics by providing the first international standard 3D format for the Web. Unfortunately, in many cases, VRML applications have to be extended to include features that it lacks, such as a sophisticated user interface and interactivity, database access, multi-user support, security and system integration support. These important aspects of modern systems were added via a programming interface known as External Authoring Interface. EAI emerged out of the need to communicate with VRML scenes from the outside. Thus, the VRML scene is no longer at the center of the architecture, but is more of a resource on which the primary program can act and to which it can respond. This facility is used extensively in our work to update the user's viewpoint and position within the VRML file through a Java applet. In order for Java to be able to manipulate VRML using EAI, the easiest approach is to define the node to be manipulated using the keyword DEF. The Java applet includes EAI packages that are included in any VRML plug-in and communicates with the VRML world by first obtaining an instance of the Browser class. This class is the Java encapsulation of the VRML world. It contains the entire Browser Script Interface as well as the getNode() method, which returns a node given a DEF name string. Only nodes defined by DEF keyword in the VRML file are accessible. Once the node instance is obtained from the getNode() method of the Browser class, its EventIns and EventOuts can be accessed. In VRML, EventIns and EventOuts are objects which handle specific events for a particular node. If a node generates a particular action, an EventOut is used. To affect a particular node, the EventIn of the node must be manipulated. The node can be accessed using the getNode() method. Events of the node can be triggered to generate actions via EventIns and EventOuts. As shown in Fig. 58, once a node in a VRML scene is engaged, the translation field in the “object" node can be set through the object.getEventIn (“translation") getEventIn() function. Thus, the object is then translated to its new location in the 3D world.

```
import java.applet.*;
import vrml.external.*;
import vrml.external.field.*;

public class system extends Applet {

  Browser browser=null;
  Node object;

  protected static EventInSFVec3f set_translation;

  public void start() {

     browser = (Browser)vrml.external.Browser.getBrowser(this, null, 0);

     if (browser  != null) {
         // get the handle for the object
         object = browser .getNode("object");

         // get the reference to the set_translation event
         set_translation = (EventInSFVec3f) object.getEventIn("translation");
     }

     set_translation.setValue(coordinateToVRML);

  }
}
```

Fig. 58. Integration between VRML and Java through EAI.

6.5.5 Handling of VRML scenes

Through EAI, all forms of direct communication between VRML and a scripting language like Java are possible. In our implementation, only two out of four types of access provided are used: accessing the functionality of the Browser Script Interface and sending events to EventIns of nodes inside the VRML world, as depicted in Fig. 59.

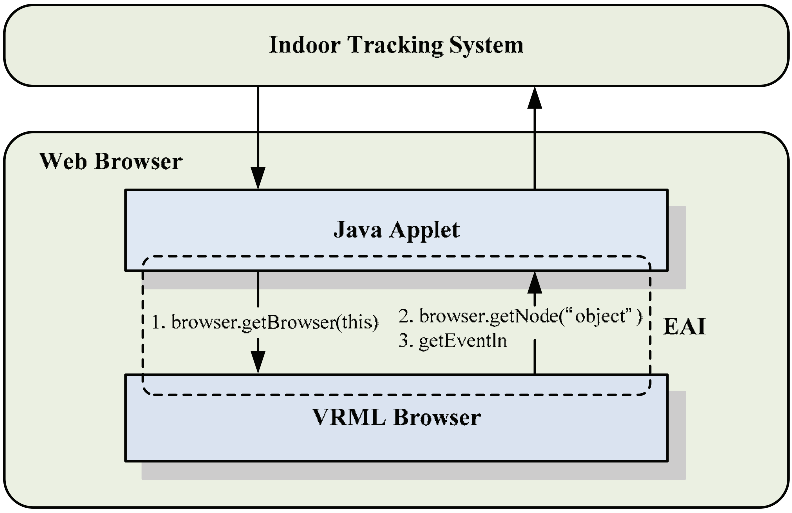

Fig. 59. Handling of a VRML scene through EAI.

6.5.6 3D Navigation view

Together, Java and VRML offer the promise of functionality on the Web that is truly interactive and more useable than the current Web. Although the technology that bridges VRML and Java is still quite erratic, with the advances in Java technology it is possible that, in a few years, VRML may be the mainstay of the Web. A VRML file is always created beforehand, containing all the 3D objects in the environment. An additional approach to relieve the navigation limitations of the VRML browser is the hybrid user interface that has been designed to support users with additional features through Java applets.

In our implementation, the Java applet can be divided into two functional parts – awt part and EAI part. These two parts work on different activities on specific fields and exchange data between each other. The awt part is the only visible part. Its objective is to display a user interface for showing the acquired results. From a functional viewpoint, this part is responsible for user-computer communication using awt classes, which are included in standard Java installations. It is dependent on the spatial information retrieved and extracted from the indoor location tracking system. EAI, on the other hand, handles communication between the applet and the VRML world located on the same

Web page. Using EAI, this part of the applet just sends the processed data into the VRML world for 3D visualization. The main disadvantage of EAI is that the virtual world and the applet have to be on the same Web page. Fig. 60 illustrates the 3D-style interface of the prototype system developed. Three main parts can be easily identified: an upper area where the actual 3D world is visualized with the user's current viewpoint and a lower left area indicating the user's location within the virtual world and a lower right area providing status information about the user's current position.

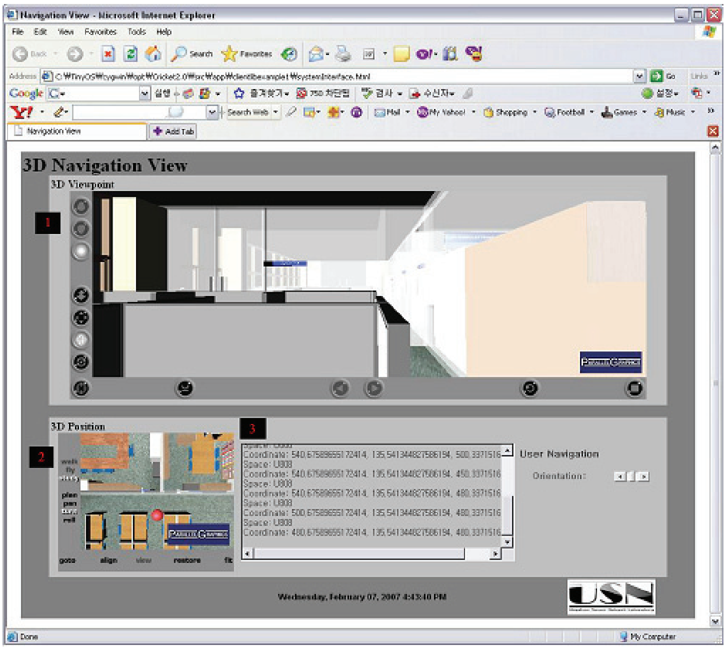

Fig. 60. 3D-style interface for indoor location tracking system.

A combination of traditional user interface items (Java) and the VRML interface was used to provide a richer choice of interactions. The main aim was to offer users a structured and easy-to-manage interface, instead of overwhelming them with a huge amount of windows and options.

A fundamental test was carried out to observe the accuracy of user location positioning in a 3D indoor environment using the indoor location tracking system. To conduct the experiment, previously configured beacons were mounted on the ceiling of our laboratory. The user's travel path, shown in Fig. 61, from U802 to U803 through U807 was decided before the test. In addition, the quality of the constructed world was evaluated to ensure its realism. A secondary aim of the experiment involved testing the usability of the 3D graphics, to establish whether the graphics enhance the indoor location tracking system in terms of visualization, navigation and performance.

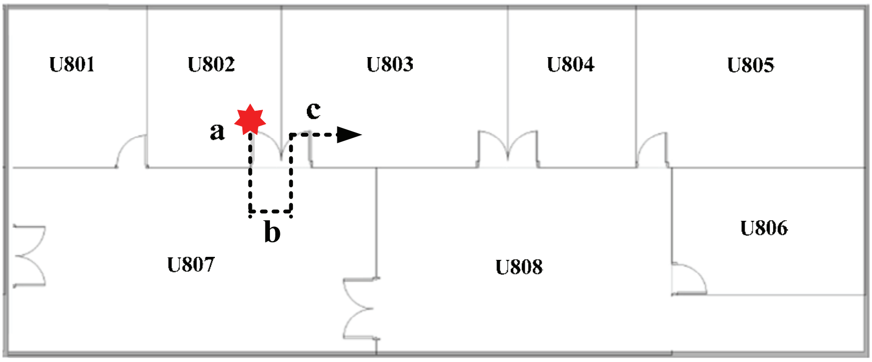

Fig. 61. Travel path set for experimental purposes.

The construction and display quality of VRML scenes is greatly dependent on the client machine's processing power. Moreover, this performance varies slightly in the different VRML plug-ins. To accelerate both display and rendering speed, it is necessary to use additional 3D graphics hardware. As predicted, a usability study confirmed that users have no difficulty matching objects in the physical world with their 3D representations, because the 3D models are more recognizable to them than flat 2D representations. With the proposed user positioning scheme, 3D Navigation View reads and extracts useful spatial information from the indoor location tracking system and, based on the latest information, updates the user's viewpoint and location in the VRML world. Location mapping in a 3D environment depends largely on the accuracy of the location determination capability of the location tracking system. Desired accuracy can be achieved only if the spatial information provided by it is sufficiently fine-grained and precise. Figure 62 depicts the result of 3D Navigation View updating the user's position and viewpoint in the virtual 3D indoor environment as the user moves freely in the physical world. As the user moves from U802 to U803 through U807, the Java applet reads and extracts spatial information from the indoor location tracking system and subsequently updates the user's location and viewpoint in the 3D world through EAI.

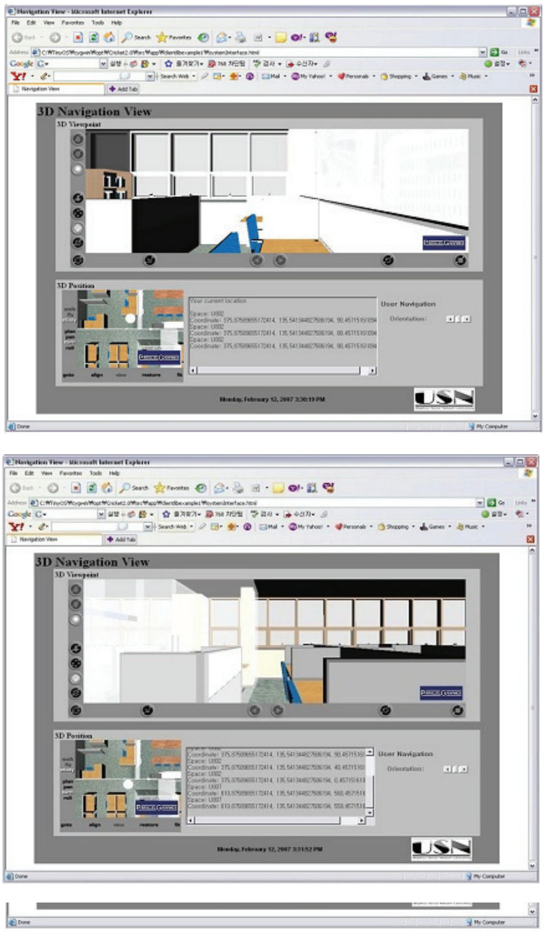

Fig. 62. 3D navigation view with the capability to update the user's position and viewpoint periodically in the 3D indoor environment when the user travels from U802 to U803 through U807.

7 IEEE 802.15.4-based personal mobile healthcare diagnosis system

A robust wireless CDMA-based healthcare diagnosis system is designed and implemented to transmit physiological signals between IEEE 802.15.4 wireless networks and CDMA cellular networks, allowing seamless roaming between hospital and home environments. Until now most of mobile healthcare system send the health data from the cellular phone to the internet connected to the server PC. These mobile healthcare systems are connected continuously to the internet and have to pay expensive data fee.

To solve the high cost problem, a software solution is developed in this study. Instead of sending vital data for monitoring and diagnostic analysis to a server over a cellular network, this system comprises an external standalone electrocardiogram (ECG) diagnosis system in cellular phone, which checks the abnormality of ECG first in cellular phone inside and send the data to the server for detail inspection when it find abnormality in the signal.

The mobile healthcare system enable patients to measure their health parameters anytime, and allows caregivers to continue the real-time monitoring of physiological signs using cellular phones. When an unknown or suspect pattern of signals is detected, the cellular phone immediately forwards them to the server and sends an alert to medical caregivers. This not only helps to decrease traffic congestion caused by inessential overhead/data over the cellular network, but also reduces the relapse rate, together with overall hospitalization cost and length of stay.

7.1 Architecture of the cellular phone-based healthcare system

This system is constructed with the aim of developing concepts and tools for wireless mobile healthcare services. Since such services allow constant, remote access to clinical applications at patient point-of-care, they help to improve the quality of care. Moreover, by eliminating handwriting and paper records, the use of wireless technology may also lead to a reduction in the number of medical errors. Continuous local self-monitoring and diagnosing of physiological signals is likely to drive down relapse rates and thereby overall hospitalization costs and length of stay.

The developed system utilizes mobile computing technology in a merged infrastructure consisting of IEEE802.15.4 networks and CDMA networks. It employs

IEEE802.15.4-enabled medical devices to empower caregivers to access vital information and provide quality patient care in a cost-effective manner.

Figure 63 depicts the architecture design of the system, composed of three main parts: sensing units, communication infrastructures and healthcare management. Sensing units include tiny, wearable IEEE802.15.4-enabled devices, such as body sensor nodes or chest belts, which aggregate and transmit collected vital signs to a server outside the hospital or to a wireless dongle prototype. These data are then relayed to the hospital by a cellular phone. Thus, the major communication protocols in this system are the IEEE 802.15.4 wireless network protocol and the CDMA network protocol. The third part of the system, i.e., healthcare management, includes a web server, used to handle received data and to respond to requests to and from cellular phones, and a server monitoring program [51, 52], which provides real-time monitoring, analyzes the acquired data and formulates a diagnosis in case of abnormal data. However, due to the memory limitations of cellular phones and the cost of data communication, a simple ECG diagnosis algorithm is constructed, permitting the mobile application to continuously analyze the signals it receives. It only forwards unknown or suspicious signals.

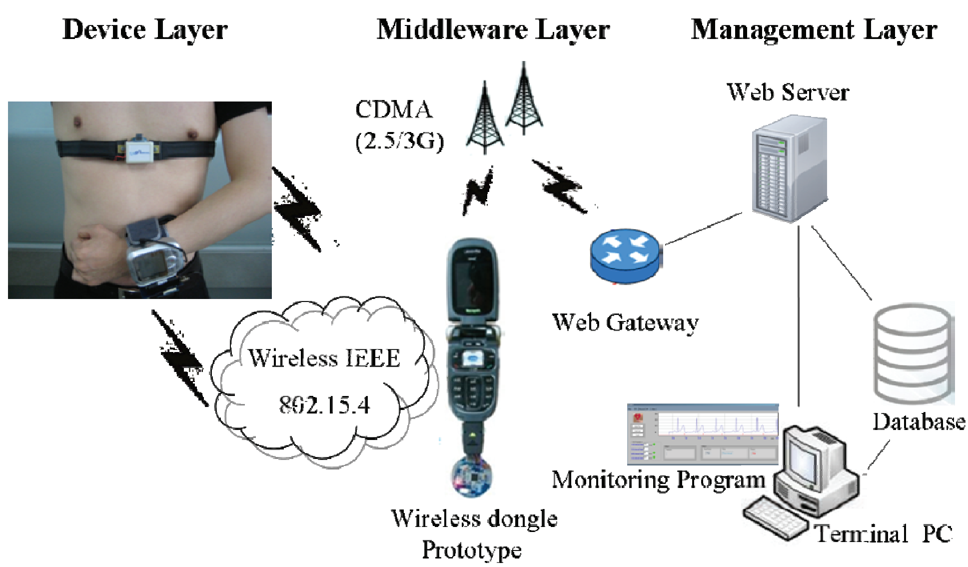

Fig. 63. System architecture of the mobile healthcare system.

7.1.1 Sensing units

Medical sensors, a fixed base-station and a wireless dongle prototype are the three main hardware devices in our system. Built on the IEEE 802.15.4 standard, these devices are compatible with each other and capable of providing interoperability. Figure 64 presents the sensor node and the wireless dongle prototype, measuring $4 \times 4 \times 0.2$ cm^3, based on the hardware specifications shown in Table 8.

The MSP430F1611 microcontroller (MCU) by Texas Instruments is a 16-bit ultra-low power MCU with 48kBytes Program Flash, 256Bytes data Flash and 10kBytes RAM. Providing a low-supply-voltage range from 1.8V to 3.6 V, it enables sensor nodes to continue data acquisition and transmission by only consuming 330 A at 1 MHz in the active mode, 1.1 A in the standby mode and 0.2 A in the off mode (RAM Retention). Other features include 12-bit ADC, Dual DAC, 2 USARTs, I2C, HW, MULT and DMA to allow the wireless dongle prototype to collect, store, process and transmit digital ADC output received from the sensor interface using the serial port interface (RS232) through SPI/UART or I2C. The developed wireless dongle prototype is pluggable to cellular phones and acts as an intermediary device (base-station) for data acquisition from IEEE802.15.4-enabled medical devices and interacts with CDMA networks to relay the data to the server.

Table 6. Hardware specifications.

MCU	MSP430F1611
RF transceiver	CC2420
Bandwidth	2.4 GHz
RF range	≈ 100 m
Power	2.5~4.0 V (battery or cellular phone)

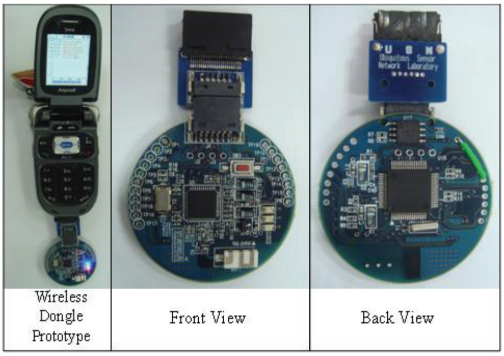

(a)

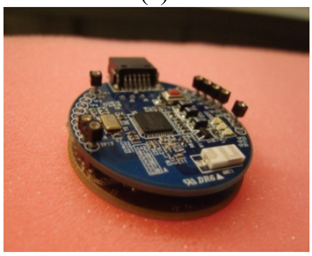

(b)

(c)

Fig. 64. Cellular phone with a wireless dongle (a), sensor node together with ECG interface board (b) and wrist blood pressure monitor with wireless sensor node (c).

7.1.2 Communication infrastructure

To extend the range of the developed healthcare solution from the hospital to outside environments, where CDMA networks are available, the system integrates wireless sensor networks with CDMA networks. The original IEEE 802.11 standard offered a radio networking scheme with data rates of 1 or 2 Mbit/s, while the IEEE 802.11b standard introduced higher-speed operation (up to 11 Mbit/s), with the slower rates being employed as an automatic fall-back in the event of poor reception. However, there are many wireless networking application that do not require the speed and complexity of the IEEE 802.11, so the IEEE 802.15.4 specification for a 'Low-rate Wireless Personal Area Network' (LR-WAN) was created to operate in the 868/915 MHz or 2.4GHz bands. An ad-hoc network is a peer-to peer system, where each node can transmit and direct communication between nodes on the network.

Access points which act as gateways allow transparent communication between wired and wireless nodes, thus enabling the existing network software to be used on a wireless sensor network with no changes. During a wireless network assessment, the developed IEEE 802.15.4-enabled medical devices can perform a quick scan to detect any wireless devices operating in the vicinity, to discover access points (APs) in the area and to determine the path for routing the vital information between CDMA and IEEE802.15.4 networks.

The purpose of installing the monitoring program on the server is to directly monitor and interpret the data received from the medical devices in the network. This arrangement helps to reduce the burden of medical caregivers, as it reduces the need to measure vital parameters individually.

To continue the provision of care even outside the hospital, the system employs a cellular network to establish a link between doctors and patients regardless of their physical location. Cellular networks based on the TCP/IP protocol enable mobile users to connect to the internet. A web server was developed to upload data received from IEEE802.15.4 devices to a cellular network and then to the server. However, continuous transmission of data over a cellular network is costly and imposes a heavy burden on network traffic. Most current cell phone models have the capability to support mobile applications, which require high resolution and large memory resources. As a result, we have developed a mobile monitoring application that includes a simple ECG diagnosis algorithm for the local monitoring of vital parameters on a cellular phone and only transmits abnormal or unknown data to the monitoring program on the server for further analysis.

7.2 Mobile application

7.2.1 Software design

When the Korean Wireless Internet Standardization Forum (KWISF) announced WIPI as the standard mobile network platform, three major operators agreed to jointly develop and commercialize the next version of WIPI in 2003. WIPI has adopted C++, Java 2 Platform and Micro Edition (J2ME platform) as integral parts of Korea's wireless standard to enable consumers to personalize their handsets with applications such as games, infotainment and location-based services. Our system uses the Samsung Anycall SCH-V670 cell phone.

The mobile application, developed for our system using the J2ME platform, provides such functions as remote access to medical information, updating and requesting health records, as well as local monitoring of vital parameters. Figure 65 presents a flow chart of the developed mobile healthcare application. Using the application, users can trigger the wireless dongle to measure and aggregate vital parameters and to continuously monitor and analyze ECG signals until any abnormalities are detected. Abnormal data are then relayed to the monitoring program on the server for a more detailed analysis. The ECG diagnosis module consists of two submodules: QRS detection and status decision rule.

7.2.2 QRS detection module

A number of QRS detection algorithms are available on the internet to assist application developers to build healthcare applications. Among these, the classical Pan-Tompkins QRS detection [28] algorithm is the most famous with a proven sensitivity of 99.69 percent and a positive prediction of 99.77 percent, when evaluated against the MIT/BIH arrhythmia database. We implemented the Pan-Tompkin algorithm in our ECG diagnosis module. As shown in Figure 65, it has four filtering stages: band-pass, derivative, squaring and moving-window integration.

The band-pass filter includes a cascaded filter containing a low-pass filter (1) with the cut-off at 12 Hz and a high-pass filter (2) with the cut-off at 5 Hz. The gain of the low-pass filter is 36 with a filtering process delay of 6 samples, while the gain of the high-pass filter is 32 with a 16 sample filtering processing delay. To differentiate electrical signals obtained from the band-pass filtering stage, the derivative stage (3) provides information on the slope of the QRS complex. The filtered signal is then squared, rather than rectified, at the squaring stage (4), which causes the QRS detector to be somewhat gain sensitive, intensifies the slope of the frequency respond curve of the derivative and helps to restrict false positives caused by T-waves with a higher spectral energy. At the last stage, an averaging window is chosen which is roughly equal to the width of the R-wave to obtain waveform information in addition to the slope of the R-wave.

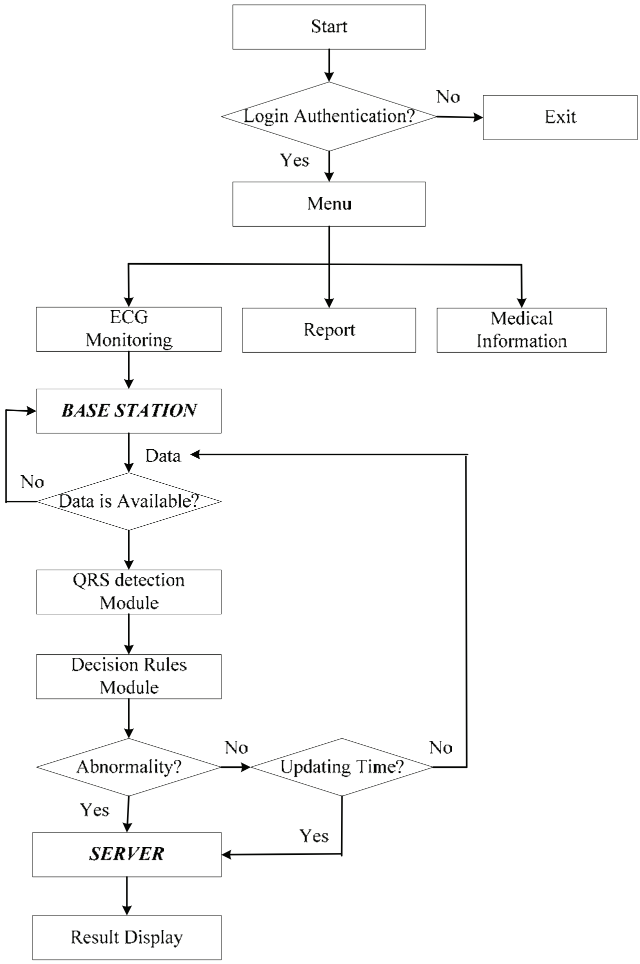

Fig. 65. Flow chart for the developed mobile healthcare application.

$$y[nT] = 2y[nT - T] - y[nT - 2T] - 2x[nT - 6T] + x[nT - 12nT] \quad (1)$$

$$y[nT] = y[nT - T] - x[nT] - x[nT - 32T] \quad (2)$$

$$y[nT] = \frac{2x[nT] + x[nT - T] - x[nT - 3T] - 2x[nT - 4T]}{8} \quad (3)$$

$$y[nT] = [x(nT)]^2 \quad (4)$$

$$y[nT] = \frac{1}{N}[x(nT - (N-1)T) + x(nT - (N-2) + ... + x(nT)]^2 \quad (5)$$

T: Sampling interval

N: Width of window

After filtering, the algorithm uses two sets of thresholds to detect and select candidate QRS complexes. Periodically, each threshold is automatically adjusted on the basis of signal peak values. The QRS threshold is readjusted and RR interval updated for each heartbeat. A local peak can be regarded either as a QRS complex or noise, or it is saved for later classification. To classify peaks, the algorithm uses peak height, peak location and maximum derivative.

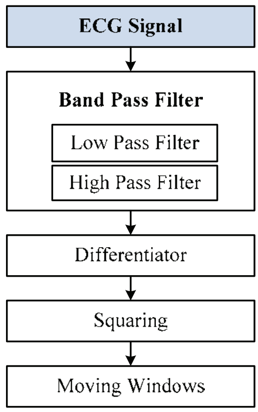

Fig. 66. QRS detection stages.

7.2.3 Status decision rule model

There are basically three main conditions for judging and determining the normality of ECG signals. Figure 67 shows the status decision rule for ECG signals, based on features/information obtained from the QRS detection module, including width, amplitude and R-to-R interval. Normal waveform signals are those whose width is less than 100 ms and whose R-to-R interval is between 0.8s and 0.9s, or whose width is less than 60ms and R-to-R interval exceeds 1.1s. Unknown waveforms are sent to the monitoring program on the server for further analysis.

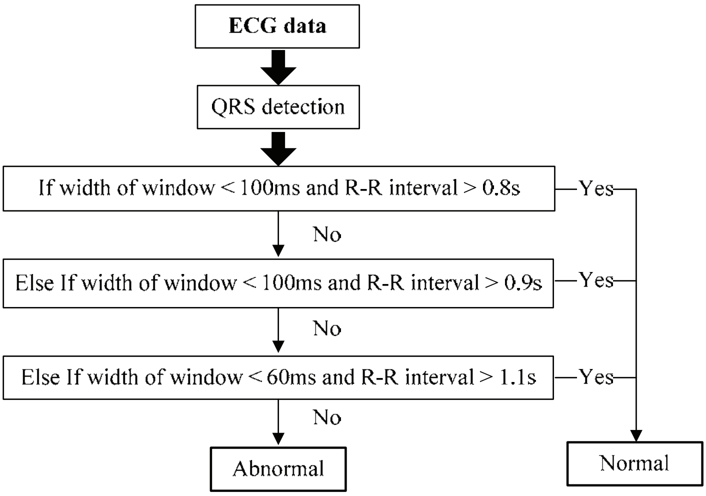

Fig. 67. Set of disease classification rules (XI, published by permission of IEEE).

7.3 System evaluation

This module is responsible for visualizing data and displaying measurement results. In addition to providing a user-friendly interface for viewing ECG waveforms, it has the capacity to monitor ECG waves by detecting QRS complexes and determining the normality of vital signs. On detecting abnormal signs, the module transmits the data to the monitoring program on the server for further evaluation.

Figure 68 shows a snapshot of the ECG monitoring screen, together with additional information such as status, suspected disease, RR interval peak, RR interval time, QRS interval time and ECG value (a). Also shown is a blood pressure monitoring screen together with a summary report screen, showing systolic and diastolic blood pressure as well as pulse and status information after a measurement (b). Patients can save their blood pressure records on their own cellular phones for tracking and monitoring purposes, as shown in Fig. 47(c). This feature enables them to retrieve and view their past medical history anytime, and may also serve to remind them of their health condition. As a result, patients have a clear picture of their own health status, and preventive action can be taken earlier on the basis of the information provided by this monitoring program.

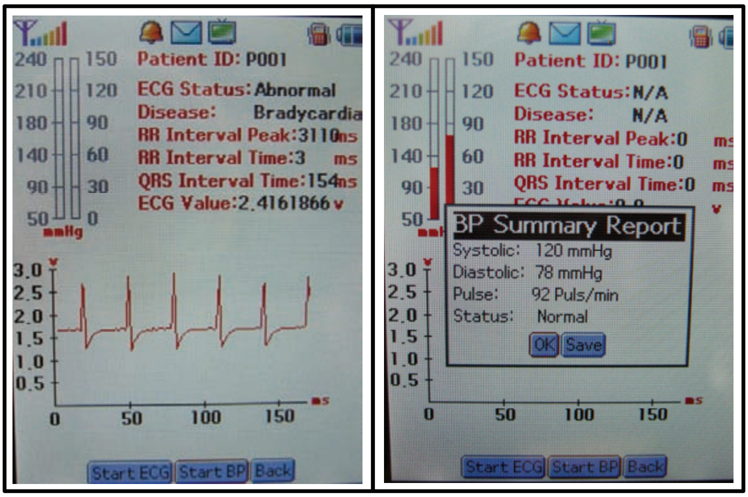

(a) (b)

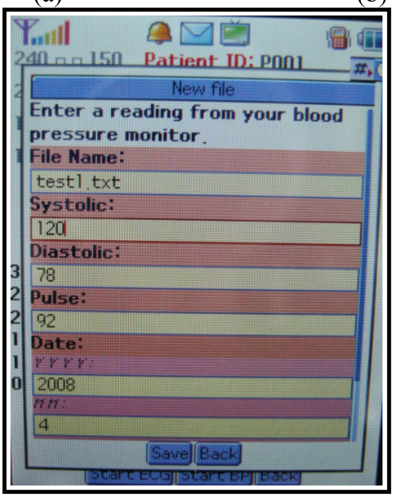

(c)

Fig. 68. Screen capture of the ECG and blood pressure diagnosis program on a cellular phone (a, b), and medical records saved locally on a cellular phone (c).

8 Summary

The emerging field of wireless sensor networks combines sensing, computation, and communication into a single tiny device. The power of wireless sensor networks lies in their ability to deploy large numbers of tiny nodes that assemble and configure themselves. One of the major challenges in wireless sensor network applications is remote continuous monitoring of patients or elderly persons staying at home or in hospital even though our system was developed in small size wireless sensor network environment for the elderly or patients with chronic disease who live with a few number of persons without caregivers or doctor’s attention in house or small nursing home.

Because healthcare applications typically deal with several types of waveform data, the use of wireless sensor network technology to u-healthcare is much more demanding than the use of WSNs for other real-time monitoring tasks, including temperature, humidity, acoustics, light and pollution measurements.

This thesis summarizes the research around the “Multi-modal Sensing U-healthcare System (MSUS) project”, which has been carried out as an international cooperative venture by the USN Laboratory, Dongseo University and Pukyong National University, Korea and the Optoelectronic and Measurement Techniques Laboratory, University of Oulu, Finland. MSUS employs wearable physiological biosensors, such as ECG, SpO_2 and body temperature sensors, in conjunction with other context-awareness sensors, such as accelerometer sensors and ultrasonic/RF transceivers, to recognize the activity and position of the users.

Several outstanding research efforts have been made in the field of continuous remote health monitoring. For example, the CodeBlue project extended WSNs to a range of medical applications, including disaster response. The European Community’s MobiHealth System, on the other hand, demonstrated the use of Body Area Networks (BAN) in remote health monitoring, while UbiMon addresses issues related to using wearable or implantable sensors for distributed mobile monitoring. CardioNet employs PDAs to collect data from ECG sensors to detect potential abnormalities, which are then sent over to a service center for analysis.

Compared to these projects, our research has several distinctive characteristics:

1. Our system is fully based on the wireless sensor network environment, that is, users' health parameters, including ECG and body temperature and context-awareness information, such as activity and position as well as tracking data, are acquired in wireless sensor network at home or small rest home environment.
2. Special characteristics of healthcare data, including waveform data from sensors, were considered when the system architecture was designed. Also the effect of packet size and routing update time on the reliability of wireless data transfer has been carefully researched.
3. Context-aware information, such as user activity, location and tracking, is also collected to enhance the reliability of health parameter analysis.
4. Waveform health parameters may place a heavy burden on wireless communication between sensor nodes. To reduce wireless traffic between sensor nodes and the gateway node, ECG analysis on sensor nodes is proposed, together with query architecture.
5. A three-dimensional viewer using VRML is developed for monitoring the user's moving path and localization in a WSN-based patient tracking system.
6. Two communication technologies, the 802.15.4 wireless sensor network and CDMA cellular network, are used to gather medical data from sensors on a patient's body to a server PC at the hospital. Choice of network technology depends on whether the sensor is within or outside the wireless sensor network area.

Integrating these different approaches, which reflect the special characteristics of u-healthcare applications, the developed MSUS system offers very good performance. The design and performance of wireless sensor networks always depend on application requirements, hardware and software limitations. Keeping these considerations in mind, we attempted to develop a healthcare system for the hospital and home environment. This system integrates all individual applications developed during the work leading up to this thesis. Future efforts include practical field testing in the home and hospital environment. Results obtained from these tests can then be used in further design to improve the performance of the u-healthcare system.

References

1. Report of an expert group meeting population aging and development (2001) Social, health and gender issues with a focus on the poor in old age 29–31. Valletta, Malta.
2. Konstantas D (2004) The Mobihealth Project. IST Project, IST-2001-36006, European Commission: Deliverable 2.6. URI: http://www.mobihealth.org.
3. Shnayder V, Chen B-R, Lorincz K, Fulford-Jones TRF & Welsh M (2005) Sensor Networks for Medical Care. Harvard University Technical Report TR-08-05.
4. Lim L & Yee B (2002) Coach's Companion – Athlete's Health Monitoring System. Berkeley, University of California. URI: http://coach.limlloyd.com.
5. Ross PE (2004) Managing Care through the Air. IEEE Spectrum: 14–19.
6. Hill J, Szewczyk R, Woo A, Hollar S, Culler D & Pister K (2000) System Architecture Directions for Networked Sensors. ACM SIGPLAN Notices 35(11): 93–104.
7. Zhao F & Guibas LJ (2004) Wireless Sensor Networks: An Information Processing Approach. Elsevier: 291–306.
8. Znati T (2005) On the challenges and opportunities of pervasive and ubiquitous computing in health care. Proceedings of the IEEE International Conference on Pervasive Computing and Communications – PerCom 2005, Kauai Island HI, USA: 396.
9. Yang G-Z (ed) (2006) Body Sensor Networks. Springer-Verlag London Limited.
10. Golmie N, Cypher D & Rebala O (2005) Performance Analysis of Low Rate Wireless Technologies for Medical Applications, Computer Communications 28(10).
11. Chigan C & Oberoi V (2006) Providing QoS in Ubiquitous Telemedicine Networks. Proceedings of the Fourth Annual IEEE International Conference on Pervasive Computing and Communications Workshops (PERCOMW'06).
12. Lee J-M, Lee J-H & Chung T-M (2008) Experimental QoS Test of Medical Data over Wired and Wireless Networks. Proceedings of ICACT 2008: 142–146.
13. Fensli R, Gunnarson E & Gundersen T (2005) A Wearable ECG-recording System for Continuous Arrhythmia Monitoring in a Wireless Tele-Home-Care Situation. Proceedings of 18th International Symposium on Computer-Based Medical Systems, Dublin, Ireland.
14. Park C, Chou PH, Bai Y, Matthews R & Hibbs A (2006) An Ultra-Wearable, Wireless, Low Power ECG Monitoring System, In Proceedings of Biomedical Circuits and Systems Conference (BioCAS 2006): 241–244.
15. Gururajan R & Vuori T (2003) Experience in Wireless Application Development in a Healthcare Setting. Perth, Australia: Web Center, Edith Cowan University: 1–7.
16. Schurgers C & Shrivastava MB (2001) Energy Efficient Routing in Wireless Sensor Network. MILCOM.
17. Gay D, Levis P, Culler D &Brewer E (2003) nesC 1.1 Language Reference Manual.
18. TinyOS URI: http://www.tinyos.net.
19. Buonadonna P, Hill J & Culler D (2001) Active Message Communication for Tiny Networked Sensor. Proceedings of the 20th Annual Joint Conference of the IEEE.

20. Bonnet P, Gaehrke J & Seshadri P(2000) Querying the Physical World. IEEE Personal Communications 7: 5.
21. Considine J, Li F, Kollios G & Byers J (2004) Approximate Aggregation Techniques for Sensor Databases. Proceeding of the 20th International Conference on Data Engineering, ICDE: 449–460.
22. Shnayder V, Hempstead M, Chen B-r, Allen GF & Welsh M (2004) Simulating the Power Consumption of Large-Scale Sensor Network Applications. Proceedings of Second ACM Conference on Embedded Networked Sensor Systems (ACM SenSys), Baltimore, MD. ACM Press:188–200.
23. Titzer BL, Lee DK & Palsberg J (2005) Avrora: Scalable Sensor Network Simulation with Precise Timing. Proceeding of IPSN'05, Fourth International Conference on Information Processing in Sensor Network: 477–482.
24. Polley J *et al.* (2004) ATEMU: A Fine-Grained Sensor Network Simulator. Proceeding of SECON 04, First IEEE Communication Society Conference on Sensor and Ad-hoc Communication and Network: 145–152.
25. Hempstead M, Tripathi N, Mauro P, Wei G-Y & Brooks D (2005) An Ultra Low Power System Architecture for Sensor Network Applications. SIGARCH Compt Archit News 33(2): 208–219.
26. Bedcos C, Harris M, Bover R, Schmidt R & Perez-Villacastin J (2007) Decision Support System for the Practical Implementation of the Chronic Heart Failure Guidelines: The MyHeart Approach. Computers in Cardiology 34: 57–60.
27. Chen J, Kwong K, Chang D, Luk J & Bajcsy R (2005) Wearable Sensors for Reliable Fall Detection. Proceedings of Engineering in Medicine and Biology IEEE: 27.
28. Pan J & Tompkins WJ (1985) A real-time QRS detection algorithm, IEEE Trans Biomed Eng 32: 230–236.
29. Hamilton PS & Tompkins WJ (1986) Quantitative investigation of QRS detection rules using the MIT/BIH arrhythmia database. IEEE Trans. Biomed Eng. 33: 1157–65.
30. Hill J & Culler D (2002) Mica: a wireless platform for deeply embedded networks. IEEE Micro 22: 12–24.
31. MIT-BIH Arrhythmia Database CD-ROM (1992) Available from the Harvard-MIT Division of Health Science and Technology.
32. Gao T, Greenspan D, Welsh M, Juang RR & Alm A (2005) Vital Signs Monitoring and Patient Tracking Over a Wireless Network. Proceedings of the 2005 IEEE Engineering in Medicine and Biology, Shanghai, China: 102–105.
33. Jovanov E, Milenkovic A, Otto C & de Groen PC (2005) A wireless Body Area Network of Intelligent Motion Sensors for Computer Assisted Physical Rehabilitation. Journal of NeuroEngineering and Rehabilitation 2: 6.
34. Otto C, Milenkovic A, Sanders C & Jovanov E (2006) System Architecture of a Wireless Body Area Sensor Network for Ubiquitous Health Monitoring, Journal of Mobile Multimedia 1(4): 307–326.
35. Milenkovic A, Otto C & Jovanov E (2006) Wireless Sensor Networks for Personal Health Monitoring: Issues and an Implementation, Computer Communications 29(13–14): 2521–2533.

36. Sayed AH & Nascimento VH (2003) Energy Conservation and the Learning Ability of LMS Adaptive Filters. In: Haykin SS & Widrow B (eds) Least-Mean-Square Adaptive Filters. John Wiley & Sons Inc: 79–104.
37. Rangayyan RM (2001) Biomedical Signal Analysis –A Case Approach. IEEE Press Series in Biomedical Engineering, Wiley-IEEE Press.
38. Raya MAD & Sison JG (2002) Adaptive Noise Cancellation of Motion Artifact in Stress ECG Signals using Accelerometer: 1756–1757.
39. Wu Y & Rangayyan RM (2007) An Unbiased Linear Artificial Neural Network with Normalized Adaptive Coefficients for Filtering Noisy ECG Signals. Proceedings of Canadian Conference on Electrical and Computer Engineering 2007 (CCECE 2007): 868–871.
40. Thakor NV & Zhu Y-S (1991) Applications of Adaptive Filtering to ECG Analysis: Noise Cancellation and Arrhythmia Detection, IEEE Trans Biomedical Engineering 38: 785–794.
41. Nagl L, Schmitz R, Warren S, Hildreth TS, Erickson H & Andresen D (2003) Wearable Sensor System for Wireless Sensor System for Wireless State-of-Health Determination in Cattle, In Proceedings of 3rd Joint EMBS-BMES Conference, Cancun, Mexico.
42. Pandey S & Agrawal P(2006) A Survey on Localization Techniques for Wireless Networks, Journal of the Chinese Institute of Engineerings 29(7): 1125–1148.
43. Hightower J & Borriello G (2001) Location Systems for Ubiquitous Computing. Computer 34: 57–66.
44. RE Kalman (1960) A new approach to linear filtering and prediction problems. Trans ASME D 82: 35–45.
45. Priyantha NB, Chakraborty A, Balakrishnan H (2000) The Cricket Location-Support system. Proc. 6th ACM MOBICOM, Boston, MA.
46. Danly M, Mulligan D, Morris J & Peterson J (2003) Threat analysis of the Geopriv Protocol. draft –ietf-geopriv-threat analysis 01.
47. Nissanka BP (2005) The Cricket Indoor Location System, Ph.D. thesis, MIT.
48. Virone G, Wood A, Selavo L, Cao Q, Fang L, Doan T, He Z, Stoleru R, Lin S & Stankovic JA (2006) ALARM-NET: an Assisted Livingcentered and Testbed-oriented In-formation System Based on a Residential Wireless Sensor Network. Distributed Diagnosis and Home Healthcare Transdisciplinary Conference (D2H2), Virginia USA.
49. VRML Plugin and Browser Detector. URI: http://cic.nist.gov/vrml/vbdetect. html/.
50. Cortona VRML Client. URI: http://www.parallelgraphics.com/products/cortona/.
51. Dae-Seok L, Sachin B, Myllylä R, Chung W-Y (2006) A Wireless ECG Monitoring System for Continuous Event Detection and Analysis. Proceeding of International Meeting on Chemical Sensors, Brescia, Italy: 185.
52. Sachin B, Walia G, Myllylä R & Chung W-Y (2006) Query Based ECG Monitoring and Analyzing System via Wireless Sensor Network. 2nd international conference on WCSN, India: 146–153.

Original papers

I Chung W-Y & Myllylä R (2006) Ubiquitous Sensor Network for Chemical Sensors. Rare metal materials and engineering 35(S3): 400–404.

II Lee Y-D, Lee D-S, Chung W-Y & Myllylä R (2006) A Wireless Sensor Network Platform for Elderly Persons at Home. Rare metal materials and engineering 35(S3): 95–99.

III Lee Y-D, Lee D-S, Walia G, Myllylä R & Chung W-Y (2006) Query Based Duplex Vital Signal Monitoring System Using Wireless Sensor Network for Ubiquitous Healthcare. IFMBE Proceedings, World Congress on Medical Physics and Biomedical Engineering 2006. August 27-September 1, Coex, Seoul: 388–391.

IV Chung W-Y, Walia G, Lee Y-D & Myllylä R (2007) Design issues and implementation of query-driven healthcare system using wireless sensor Ad-hoc network. IFMBE Proceedings, International Workshop on Wearable and Implantable Body Sensor Networks (BSN 2007). March 26-28, RWTH Achen University, Germany: 99–104.

V Chung W-Y, Bhardwaj S, Purwar A & Lee D-S (2007) A Fusion Health Monitoring using ECG and Accelerometer Sensors for Elderly Persons at Home. Proceedings of EMBC 2007(29th Annual International Conference of the IEEE Engineering in Medicine and Biology Society), Lyon, France, August 23–26: 3818–3821.

VI Lee D-S, Bhardwaj S, Alasaarela E & Chung W-Y (2007) An ECG Analysis on Sensor Node for Reducing Traffic Overload in u-Healthcare with Wireless Sensor Network. Proceedings of IEEE Sensors Conference, Georgia, USA, October 28–31: 256–259.

VII Singh VK, Lim H, Myllylä R & Chung W-Y (2006) Passive and Cost effective People Location Tracking System for Indoor Environments Using Distributed Wireless Sensor Network. IFMBE Proceedings, World Congress on Medical Physics and Biomedical Engineering. August 27–September 1, Coex, Seoul: 384–387.

VIII Chung W-Y, Singh VK, Myllylä R & Lim H (2006) Security Enhanced Indoor Tracking System for Ubiquitous Home Healthcare. Proceeding of IEEE Sensors Conference, B1L-B2, October 22-25, Daegu, Korea.

IX Purwar A, Myllylä R & Chung W-Y (2008) A Wireless Sensor Network Compatible Triaxial Accelerometer: Application for Detection of Falls in the Elderly. Sensor Letters 6(2): 319–325.

X Chung W-Y & Yang C-S (2008) Dynamic VRML-Based Navigable 3D Map for Indoor Location-Aware Systems. In: Mukhopadhyay SC & Huang RY-M (eds) Sensors: Advancement in Modeling, Design Issues, Fabrication and Practical Applications. LNEE Series. Berlin Heidelberg, Springer-Verlag: 269–284.

XI Chung W-Y, Yau C-L, Shin K-S & Myllylä R (2007) A Cell Phone Based Health Monitoring System with Self Analysis Processor using Wireless Sensor Network Technology. Proceedings of EMBC 2007(29th Annual International Conference of the IEEE Engineering in Medicine and Biology Society), Lyon, France, August 23–26: 3705–3708.

Original publications are not included in the electronic version of the dissertation.

327. Härkönen, Janne (2009) Improving product development process through verification and validation

328. Peiponen, Kai-Erik (2009) Optical spectra analysis of turbid liquids

329. Kettunen, Juha (2009) Essays on strategic management and quality assurance

330. Ahonen, Timo (2009) Face and texture image analysis with quantized filter response statistics

331. Uusipaavalniemi, Sari (2009) Framework for analysing and developing information integration. A study on steel industry maintenance service supply chain

332. Risikko, Tanja (2009) Safety, health and productivity of cold work. A management model, implementation and effects

333. Virtanen, Markku (2009) Mathematical modelling of flow and transport as link to impacts in multidiscipline environments

334. Liimatainen, Henrikki (2009) Interactions between fibres, fines and fillers in papermaking. Influence on dewatering and retention of pulp suspensions

335. Ghaboosi, Kaveh (2009) Intelligent medium access control for the future wireless networks

336. Möttönen, Matti (2009) Requirements engineering. Linking design and manufacturing in ICT companies

337. Leinonen, Jouko (2009) Analysis of OFDMA resource allocation with limited feedback

338. Tick, Timo (2009) Fabrication of advanced LTCC structures for microwave devices

339. Ojansivu, Ville (2009) Blur invariant pattern recognition and registration in the Fourier domain

340. Suikkanen, Pasi (2009) Development and processing of low carbon bainitic steels

341. García, Verónica (2009) Reclamation of VOCs, n-butanol and dichloromethane, from sodium chloride containing mixtures by pervaporation. Towards efficient use of resources in the chemical industry

342. Boutellier, Jani (2009) Quasi-static scheduling for fine-grained embedded multiprocessing

343. Vallius, Tero (2009) An embedded object approach to embedded system development

Book orders:
OULU UNIVERSITY PRESS
P.O. Box 8200, FI-90014
University of Oulu, Finland

Distributed by
OULU UNIVERSITY LIBRARY
P.O. Box 7500, FI-90014
University of Oulu, Finland

UNIVERSITY OF OULU P.O.B. 7500 FI-90014 UNIVERSITY OF OULU FINLAND

ACTA UNIVERSITATIS OULUENSIS

ISBN 978-951-42-9289-7 (Paperback)
ISBN 978-951-42-9290-3 (PDF)
ISSN 0355-3213 (Print)
ISSN 1796-2226 (Online)

UNIVERSITY of OULU
OULUN YLIOPISTO